THE
PHYSICAL REVIEW
A Journal of Experimental and Theoretical Physics Established by E. L. Nichols in 1893

VOL. 50, NO. 8 NOVEMBER 1, 1936 SECOND SERIES

Absorption of Cosmic-Ray Secondaries and Showers

DAROL K. FROMAN, *Macdonald College, McGill University*
AND
J. C. STEARNS, *University of Denver*

(Received July 6, 1936)

A triple Geiger-Müller counter system has been used with the three counters in a vertical line to measure the absorption by lead of single secondary and shower rays produced in lead and emerging in a small solid angle including the vertical. The precision in the estimate of the absorption coefficient with this arrangement of the counters is much less than that with a triangular arrangement, but this method includes the possibility of simultaneous excitation of the three counters by single secondaries. The apparent absorption coefficient obtained is 0.82 ± 0.18 per cm Pb. This value is somewhat higher than values previously found for purely shower rays making a larger angle with the vertical, but the difference is not established definitely. With the triangular arrangement of counters the penetrating power of the shower particles arising in aluminum and emerging at an angle of several degrees with the vertical has been found to be of the same order of magnitude as that for lead showers. Data have been obtained which show, within experimental error, (a) that the optimum thickness of lead scattering block for shower production is not a function of the amount of absorbing material placed above a lower counter; and (b) that the penetrating power of the shower particles is independent of the thickness of the scatterer from 0 to 3 cm of lead.

INTRODUCTION

IN the work described here the usual triple coincidence Geiger-Müller counters and recording circuits were used. The counters were enclosed in a constant-temperature box and the voltage supply to the counter tubes was controlled by a modified Johnson and Street[1] circuit. The apparatus was set up under a thin roof at an altitude of 120 ft.

THE ABSORPTION OF NEARLY VERTICAL SHOWERS

In order to measure the absorption of showers near the vertical the counters were arranged in a vertical line as shown in Fig. 1(a). A lead scattering block 0.952 cm thick was placed alternately in positions *A* and *B* and the lead absorber was placed at *C*. With the scatterer in position *A* coincidences can be produced (i) by primary rays, (ii) by single secondary rays from the scatterer and (iii) by shower particles from the scatterer. With the scatterer in position *B* coincidences can be produced (i) by primary

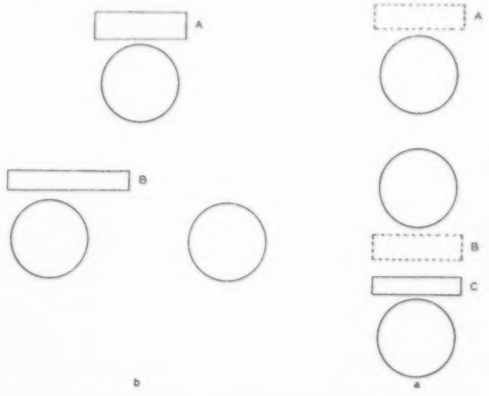

FIG. 1. Arrangements of the Geiger-Müller counters, scatterers and absorbers.

[1] T. H. Johnson and J. C. Street, J. Frank. Inst. **215**, 239 (1933).

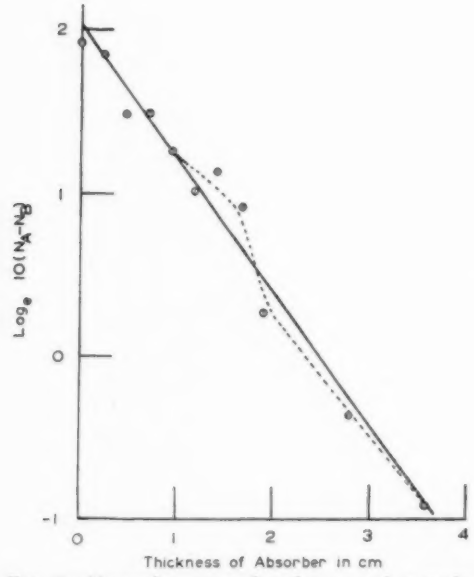

FIG. 2. Absorption curve for shower and secondary particles emitted from lead nearly vertically. $\mu=0.82\pm0.19$ per cm Pb.

rays and (ii) by ionizing primaries which pass through the upper two counters and release, in the scattering block, single or shower particles which actuate the lower counter. The number of coincidences produced by the last-mentioned process depends upon the solid angle subtended by the lowest counter at the scatterer. The counting rate was found to be the same for the scatterer placed either between the upper pair or between the lower pair of counters. It was assumed, then, that the number of coincidences produced by this process was negligible. The number of coincidences produced by primary rays is the same for the scatterer in positions A and B. It follows that the difference in counting rates is, essentially, a measure of the number of secondaries and showers which have penetrated the absorber, C. Differences in these counting rates were taken for several thicknesses of the absorber and the absorption coefficient computed from them. The results for a run of 1700 hours are summarized in Table I. T is the thickness of the absorber, C, and N_A and N_B are the counting rates with the scatterer in positions A and B, respectively.

TABLE I. *Data on absorption of vertical showers.*

T cm of Pb	N_A per min.	N_B per min.	N_A-N_B	$\log_e 10(N_A-N_B)$
0	3.24	2.56	0.68	1.92 ± 0.05
0.238	3.17	2.53	0.63	1.85 ± 0.07
0.476	3.05	2.61	0.44	1.48 ± 0.08
0.714	2.97	2.53	0.44	1.49 ± 0.08
0.952	2.92	2.57	0.35	1.25 ± 0.08
1.19	2.76	2.49	0.27	1.01 ± 0.13
1.43	2.88	2.57	0.31	1.13 ± 0.11
1.67	2.80	2.55	0.25	0.92 ± 0.13
1.90	2.69	2.56	0.13	0.26 ± 0.28
2.79	2.60	2.53	0.07	-0.36 ± 0.7
3.57	2.57	2.53	0.04	-0.92 ± 0.9

In Fig. 2, $\log_e 10(N_A-N_B)$ is plotted. The full line is the straight line fitted by the least-squares method. This gives a value of the apparent absorption coefficient, $\mu=0.82\pm0.18$ per cm of lead. The dotted curve appears to fit the data somewhat better and shows a plateau in the 1.5 cm region. This curve has the same shape as the one previously reported[2] for shower absorption curves taken with the triangular formation of counters. Since this plateau appears at about the thickness of absorber for maximum shower production it seems likely that it is caused by showers arising in the absorber excited by shower particles from the scatterer. The absorption coefficient, 0.82 cm^{-1} Pb, is somewhat higher than that previously obtained,[2] 0.49 cm^{-1} Pb, for showers making a larger angle with the vertical. This may be due to the fact that, with the counters in a vertical line, relatively low energy single secondaries can produce coincidences whereas they cannot do this for the triangular formation of counters. This interpretation is supported by the work of Morgan[3] who has found that the most penetrating shower particles are found most frequently near the vertical. In any case, the difference between these absorption coefficients is only twice the probable error and cannot be considered to be established definitely.

After the first few hundred hours run in a counting experiment the probable error decreases so slowly that, unless there is some definite hypothesis to test, it seems better to measure these absorption coefficients only approximately at first, to determine the marked characteristics, than to spend the very long time required for precise evaluation.

THE ABSORPTION OF SHOWERS PRODUCED IN ALUMINUM

For measuring the absorption of showers from aluminum the counters were arranged in tri-

[2] J. C. Stearns and Darol K. Froman, Phys. Rev. **49**, 473 (1936).
[3] J. E. Morgan, Phys. Rev. **49**, 871 (1936).

angular formation as shown in Fig. 1(b). An aluminum scatterer, 3.18 cm thick, was placed at *A* and counts were taken with various thicknesses of lead in the absorbing position, *B*. The accidental counting rate was determined by taking the count without the aluminum present. It was found that the accidental rate remained constant for all thicknesses of the lead absorber used. This establishes that the number of showers coming from the roof, etc., was negligible and that the showers detected with the aluminum present really arose in the aluminum. As only about one shower in ten minutes was detected from the scatterer, even with no absorber, a long period of observation was necessary to obtain an estimate of the absorption coefficient. A run of 800 hours was made and the results are summarized in Table II. T is the thickness of the lead absorber and N is the counting rate obtained from the observed rate by subtracting the accidentals. The accidental counting rate was 0.136 ± 0.032 per min.

The value of the absorption coefficient obtained by the least-squares method from these data is $\mu=0.54\pm0.19$ per cm of lead. This value is very close to that obtained for showers from lead[2] for the same positions of the counters, *viz.*: 0.49 per cm of lead, but the statistical error is so large that we can conclude only that the two coefficients are of the same order of magnitude.

Production and Absorption of Showers

An experiment was done to determine whether or not the penetration of shower particles is a function of the thickness of the scatterer. If the penetrating power changes with this thickness, then the optimum thickness of scatterer for shower production must vary with the amount of absorber in the path of the showers.

The counters were arranged in the triangular formation shown in Fig. 1(b). With a fixed thickness of the absorber, *B*, the rate of counting was determined for various thicknesses of the lead scatterer. The results are shown graphically in Fig. 3. In these graphs the counting rate is plotted against the thickness of the scatterer for absorber thicknesses of 0, 1.19 and 3.20 cm of lead. Vertical lines represent the probable errors in the plotted points.

Table II. *Data on absorption of showers from aluminum.*

T in cm	N per min.	log, $100N$
0	0.111 ± 0.04	2.41
0.476	0.092 ± 0.04	2.22
0.952	0.069 ± 0.04	1.93
1.43	0.030 ± 0.03	1.10
1.90	0.038 ± 0.04	1.33
2.38	0.014 ± 0.04	0.34
2.86	0.043 ± 0.03	1.46

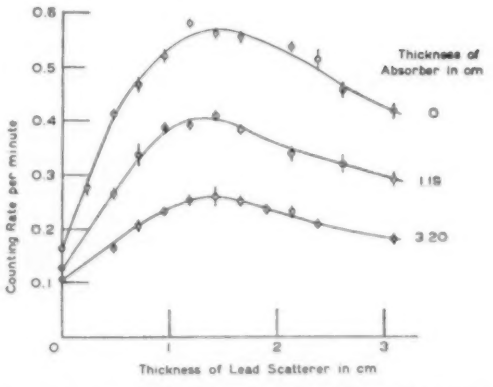

Fig. 3. Shower production curves for different thicknesses of absorber.

It is evident from Fig. 3 that the optimum thickness for shower production is the same for the various absorbers used. Moreover, for a given absorber, the fraction of the showers absorbed at different thicknesses of scatterer is constant within experimental error. Thus the average penetrating power of shower particles is not a function of the thickness of the block in which it is produced, up to a thickness of 3 cm of lead. This is in agreement with the work of Woodward.[4] However, Woodward finds that the penetrating power of the shower particles is not a function of elevation whereas we have found a slight increase in penetrating power with elevation.[2] Measurements are being made now to test this point.

Acknowledgments

We wish to acknowledge financial aid to one of us from the United States National Research Council, The Rumford Committee and the American Association for the Advancement of Science. Also we wish to thank the Garden City Press, Ste. Anne de Bellevue, Quebec, for furnishing laboratory space and power for some of this work.

[4] R. H. Woodward, Phys. Rev. **49**, 711 (1936).

K X-Ray Absorption Spectra of Some Compounds of Bromine, Rubidium and Strontium

S. T. STEPHENSON, *State College of Washington, Pullman, Washington*

(Received August 3, 1936)

The *K* x-ray absorption spectrum of Br in solid AgBr and in each of the vapors CH_3Br, C_2H_5Br and Br_2 is obtained with a double crystal ionization spectrometer. Edge widths and the positions of secondary fine structure are given and discussed. The small widths given were checked by narrow *K* edges obtained for Rb in RbBr and Sr in $SrCl_2$ and are shown to be in agreement with data on emission line widths. The effect of chemical combination on the wavelength position of the main edge is discussed.

INTRODUCTION

THE width and secondary structure of x-ray absorption edges are of importance since the former is related to the widths of x-ray energy levels and emission lines[1] and the latter is determined by the different energy zones in the absorber.[2] It was thought that it would be of interest to investigate the Br edge in AgBr, CH_3Br, and C_2H_5Br because of the use of these compounds in photographic or ionization methods of x-ray detection. (This part of the present investigation was suggested by Professor C. D. Cooksey in correspondence concerning some results which have already been reported.) Br_2 and the edges of Rb in RbBr and Sr in $SrCl_2$ were also studied.

The apparatus was the same as that described previously.[3] The absorbers were placed either between crystals *A* and *B* or immediately in front of the ionization chamber. The AgBr absorber consisted of five dental films. RbBr and $SrCl_2$ screens were made up of several cigarette papers saturated with a solution of the salt and rapidly dried. CH_3Br, C_2H_5Br and Br_2 vapors were used in glass tubes either with Cellophane or thin glass windows.

RESULTS AND DISCUSSION

Figs. 1 and 2 show typical results obtained. Ordinates are ionization currents in mm/sec. due to transmitted energy, and abscissae are wavelengths in X. U. starting from an arbitrary zero. Table I contains a summary of the experimental results.

The distances (in volts) from the center of the main edge of any secondary structure observed are given in the last three columns of Table I. *A* refers to the first minimum, α the first maximum, and *B* the second minimum in the trans-

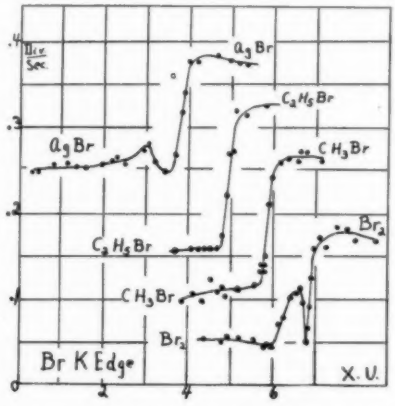

FIG. 1. *K* x-ray absorption spectra of Br in AgBr, C_2H_5Br, CH_3Br and Br_2.

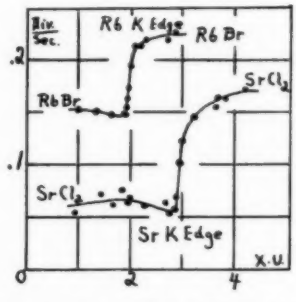

FIG. 2. *K* x-ray absorption edges of Rb in RbBr and Sr in $SrCl_2$.

[1] F. K. Richtmyer, S. K. Barnes and E. Ramberg, Phys. Rev. **46**, 843 (1934).
[2] R. de L. Kronig, Zeits. f. Physik **70**, 317 (1931); **75**, 191 (1932).
[3] S. T. Stephenson, Phys. Rev. **49**, 495 (1936).

TABLE I. *Widths of absorption edges and positions of secondary structure in volts.*

Edge	Compound	Width	*A*	α	*B*
Br	AgBr	9±1.5	6	12	22
Br	C_2H_5Br	5±1.5			
Br	CH_3Br	5±1.5			
Br	Br_2	3.5±1.5	1.5	4.5	10.5
Rb	RbBr	5±2			
Sr	$SrCl_2$	6±2			

mission curve. The secondary structure for AgBr is similar to that for those other bromides of cubic lattice which have previously been studied[3] as would be expected from Kronig's theory. A secondary structure peak about 10 to 13 volts out on the short wave-length side of the edge is apparently quite characteristic of these different compounds. The expected shift of the structure due to the smaller grating space of AgBr (*ca.* 0.8A less than KBr) is not found and is perhaps within experimental error here so close to the main edge. The presence of this secondary structure for AgBr would make difficult the interpretation of results obtained photographically on the structure of the bromine edge in other bromine compounds. Secondary structure in agreement with that reported here has been obtained by Hanawalt[4] and by Sandström and Carlsson,[5] using a photographic method.

The structure for Br_2 is interesting because of its pronounced character and its closeness to the edge. It may be of the Kronig[2] type and due to a forbidden zone in the Br_2 molecule, or of the Kossel[6] type and due to some outer lying level of the Br atom involved. In either case differences in the positions of *A*, α, and *B* between Br_2 and a crystalline bromide containing Br ions are to be expected. No definite evidence was obtained for any pronounced structure in or near the edges of the other Br compounds investigated.

Any shifts in the positions of the main edges due to different chemical combinations are very small. As a special test, readings for absorbers of KBr, CH_3Br, and Br_2 considered typical of cubic crystalline bromides, polyatomic bromides, and molecular bromine, respectively, were obtained during the same run. The transmitted energy for each absorber in turn was measured at each setting of crystal *B* before moving crystal *B* to a new position. This provides a very delicate test for small shifts. No significant difference was found between the edges of KBr and CH_3Br. Both of these were shifted about 1.1±0.5 volts to the short wave-length side of Br_2. The effect of chemical combination on the position of the Br edge would seem to be less than that indicated by Hanawalt's data.[4]

The widths (in volts) of the edges determined by the usual triangle method and not corrected for the effect of the crystals are given in the third column of Table I. The widths of the Br edges differ considerably among themselves. This is not to be attributed to an actual variation due to the element's being in different chemical compounds but rather to a very small shift with time in the verticality or some other adjustment of the crystals caused by slight jarring of the apparatus. The width (9 volts) for Br in AgBr was obtained from runs made shortly after the completion of work previously reported[2] for other bromides and agrees with the results reported then. CH_3Br and C_2H_5Br were run later after a readjustment of the ionization chamber had jarred the apparatus slightly and gave widths of about 5 volts. Still later, after one absorption tube had blown up and sent a blast of air against crystal *B*, the runs for Br_2 were made giving widths of 3.5 volts. To check the fact that the narrower widths were not due to the new compounds tried, KBr and CH_3Br were run again and gave widths of 3.5–4.5 volts, so any actual effect on the width due to chemical combination is small. The uncorrected width of the Br edge is between 3 and 5 volts as determined in this experiment. As a further check on these values, the edges of Rb[7] in RbBr and Sr in $SrCl_2$ were run and were found to have about the same angular width as the bromine edge. The voltage width of course is greater. This is considered evidence for the fact that the widths of the *K* absorption edges for Br and for Rb and Sr in the compounds studied are less than those reported in the literature reviewed, due presumably to a fortuitous adjustment of the crystals in this case.

Richtmyer[1] and others have suggested that the

[4] J. D. Hanawalt, Phys. Rev. **37**, 715 (1931).
[5] A. Sandström and E. Carlsson, Zeits. f. Physik **80**, 597 (1933).
[6] W. Kossel, Zeits. f. Physik **1**, 119 (1920).

[7] The 11-volt value previously given for Rb was obtained at the same time that the 9-volt value was found for Br.

width of an x-ray emission line is the sum of the widths of the initial and final states of the radiating atom. The full width at half maximum of either line in the $K\alpha$ doublet for Ge (32) is about 3.5[8] volts and for Sr (38) is about 5.8[8] volts, so that the sum of the L and K energy level widths for Br, Rb and Sr should lie between 4 and 6 volts and the widths of the K levels alone must be less than this. The widths of the K edges of Table I, determined as they are by the triangle method, are approximately $\pi/2$ times the actual[1] widths of the K levels involved. It would seem, therefore, that the width values given in this paper are not too low but are in agreement with experimental line width data.

[8] S. K. Allison, Phys. Rev. **44**, 63 (1933).

NOVEMBER 1, 1936 PHYSICAL REVIEW VOLUME 50

Geologic Time and Isotopic Constitution of Radiogenic Lead

JOHN L. ROSE AND R. K. STRANATHAN, *Department of Physics, New York University, University Heights, New York City*

(Received August 10, 1936)

The isotopic constitutions of samples of lead from Colorado carnotite, Wilberforce uraninite, and Katanga and Great Bear Lake pitchblendes were found from densitometer measurements of the hyperfine structure of λ5372. The probable geologic ages of these minerals calculated from the Ac D : Ra G ratios agree very well with the ages from Pb : U ratios with the exception of the Great Bear Lake pitchblende in which case leaching or some other method of alteration may have changed the Pb : U ratio.

ACCURATE knowledge of the relative abundance of the lead isotopes, Th D, Ac D, and Ra G (Pb^{208}, Pb^{207}, and Pb^{206}), end products of the thorium, actino-uranium (Ac U), and uranium (U I) families, found in radioactive minerals is very useful in the solutions of certain cosmological problems, especially those of the geologic ages of the minerals[1, 2] and origin of the actinium series.[3–12] Estimates of the isotopic constitutions of radiogenic leads have been made from chemical atomic weights. Mass spectrograph results[11] are available for only a few samples of lead. Both methods of analysis are long and laborious, the mass spectrograph requiring a new discharge tube for each lead examined.

From the hyperfine structure of the lead spectral line λ4245, Rose and Granath[12] were able to observe Ac D in lead from Katanga pitchblende and it was suggested by them that densitometer measurements of certain hyperfine structure patterns might be a very simple and effective method of determining the relative abundance of the isotopes of lead. Recently the present authors,[13] using the structure of λ5372 found this method very satisfactory in obtaining the isotopic constitution of ordinary lead from galena.

Isotopic Analyses of Radiogenic Leads

The spectra of several samples of lead from different uranium bearing minerals have been photographed and variations in the relative

[1] "The Age of the Earth" (National Research Council Bull. 80, 1931).

[2] Annual Report of the National Research Council Committee on the Measurement of Geologic Time (1932, 1933, 1934, 1935).

[3] A. Piccard, Arch. des Sci. **44**, 161 (1917); A. Piccard and E. Stahel, ibid. (5) **3**, 541 (1921).

[4] T. R. Wilkins, Nature **117**, 719 (1926); Phys. Rev. **29**, 352 (1928).

[5] O. Hahn, Zeits. f. anorg. allgem. Chemie **147**, 16 (1925); Zeits. f. angew. Chemie **42**, 927 (1929).

[6] F. Western and A. E. Ruark, J. Chem. Phys. **1**, 717 (1933); Phys. Rev. **45**, 69 (1934).

[7] A. V. Grosse, Phys. Rev. **42**, 565 (1932); J. Phys. Chem. **38**, 487 (1934).

[8] F. H. Bruner and H. Schlundt, J. Phys. Chem. **38**, 1183 (1934); M. Francis and Tcheng Da-Tchang, Comptes rendus **198**, 733 (1934), Phil. Mag. **20**, 623 (1935); E. Gleditsch and E. Foeyn, Comptes rendus **199**, 412 (1934).

[9] F. Western and A. E. Ruark, Phys. Rev. **44**, 675 (1933); ibid. **45**, 628 (1934).

[10] Lord Rutherford, Nature **123**, 313 (1929).

[11] F. W. Aston, Proc. Roy. Soc. **A140**, 535 (1933).

[12] J. L. Rose and L. P. Granath, Phys. Rev. **39**, 1017 (1932); ibid. **40**, 760 (1932).

[13] J. L. Rose and R. K. Stranathan, Phys. Rev. **49**, 916 (1936).

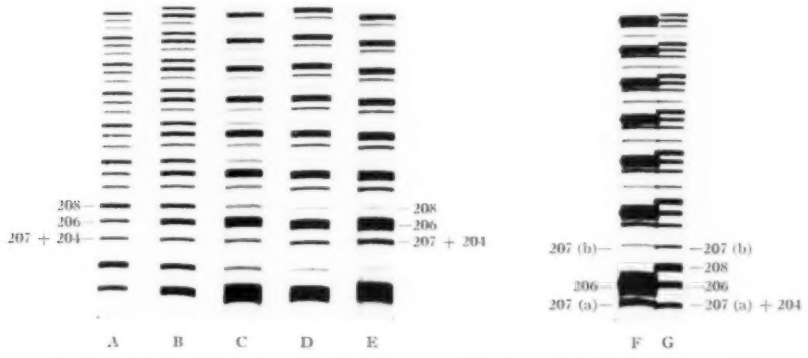

FIG. 1 (left). λ5372, etalon spacer 5.194 mm. A. Ordinary lead; B. Colorado carnotite; C. Wilberforce uraninite; D. Great Bear Lake pitchblende (Pb extracted by Riblett); E. Katanga pitchblende. (Right) λ5372 etalon spacer 3.561 mm. F. Katanga pitchblende; G. Ordinary lead.

intensities of the hyperfine structure components of the same line show that the proportions of isotopes are not the same. This can be seen from the photographs in Fig. 1 of the patterns of λ5372 with a 5.194 mm etalon spacer. All of the densitometer data were obtained from photographs with this spacer, for which the Pb^{204} component and both components of Pb^{207} appear as a single component. Due to the large proportions of Pb^{206} in these leads the wire screens with percentage transmissions from 14.8 to 67.3 which were previously used with ordinary lead could not be used singly in comparing the intensities of the Pb^{206} components with the components due to Pb^{207} and Pb^{208}. Although intensity marks can be made with some success with combinations of two or more screens it was thought better to use the above screens one at a time with a brown glass filter in front of the source. The transmission of the filter was found to be 16.5 percent for λ5372. The relative blackenings of the photographic plates from densitometer traces of the Pb^{208} and Pb^{207} components for an exposure of 100 percent transmission of light from the source were compared with an intensity-blackening curve for the Pb^{206} component in the same order of the interference pattern. The curve was obtained from photographs of equal exposure times with the wire screens and glass filter in front of the source. This method of estimating relative intensities is not so accurate as the method used for ordinary lead in which the intensity ratios of the components are not as large and where the average of several values can be found for the ratios from intensity-blackening curves for each of the components. The maximum error, however, in the results in Table I, row 4, should not be more than ±0.3 in the percentage abundance of any isotope.

All of the minerals from which the leads were extracted, with the exception of the Wilberforce uraninite, contain no more than a trace of thorium and therefore the Pb^{208} in these minerals must be due to contamination of ordinary lead. Chemical analyses of the thorium content and petrographic studies indicate that the Pb^{208} in the Wilberforce material is entirely the end product of thorium. With the previous results for the isotopic proportions or ordinary lead and the percentages in Table I it is possible to determine for the above leads the percentages of Pb^{207} and Pb^{206} (Ac D and Ra G), which are the end products of uranium. The ratio of these isotopes as shown in Table I, row 8, appears to vary with the age of the mineral. This is in accordance with the present theory concerning the origin of the actinium series.

ACTINIUM SERIES

It has been known for some time that Pb^{206} is the end product of U^{238} (U I) through the radium series and it was an early view that the actinium series was a branch of the uranium family. Piccard and others[3, 4] later suggested that the actinium series contains one or more

TABLE I.

		1	2	3	4	5	6
1. Mineral		Galena [a]	Carnotite [b]	Uraninite [c]	Pitchblende [d]	Pitchblende [e]	Pitchblende [f]
2. Geographic origin		Missouri, U. S. A.	Colorado, U. S. A.	Wilberforce, Canada	Great Bear Lake, Canada	Great Bear Lake, Canada	Katanga, Belgian Congo
3. Probable age from geologic evidences			Late Cretaceous to Early Tertiary [l]	Middle Pre-Cambrian [l]	(?) Pre-Cambrian [16]	(?) Pre-Cambrian [16]	Upper-Pre-Cambrian [l]
4. Isotopic constitution from hyperfine structure in percent	Pb^{208}	51.5 [12]	32.2 [h]	6.2 [i]	4.7 [h]	2.8 [h]	0.3 [h]
	Pb^{206}	26.3	52.2	86.6	86.2	88.8	93.4
	$Pb^{204}+Pb^{207}$	22.2 [g]	15.6	7.2	9.1	8.4	6.3
5. Mean mass number [j]		207.228	206.785	206.196	206.182	206.139	206.069
Changed to chemical scale [k]		207.20	206.75	206.17	206.15	206.11	206.04
6. Chemical atomic weight of Pb		207.22 [l]	206.59 [m]	206.195 [n]		206.054 [o]	206.027 [p]
			207.00			206.058	206.030
7. From hyperfine structure in percent RaG			35.75	86.6	83.8	87.4	93.2
Ac D			1.7	7.2	7.1	7.2	6.2
8. Ac D : Ra G ratio in percent			4.75	8.30	8.48	8.24	6.67
9. Age of mineral from Ac D : Ra G ratio in million years							
$\lambda(U\,I)=1.5\times10^{-10}yr^{-1}\left\{\frac{\lambda(Ac\,U)}{\lambda(U\,I)}\right.=10$			246	952	977	944	694
" $=11$			220	860	882	852	622
$\lambda(U\,I)=1.6\times10^{-10}yr^{-1}\{$ " $=10$			222	900	923	892	650
" $=11$			207	808	828	800	586
10. Pb : U ratio			0.0013–0.0053 [l]	0.162 [q]	0.114–0.273 [r]	0.201 [15]	0.07–0.084 [l]
11. Age of mineral from Pb : U ratio in million years			60	1050		1323	600
12. Isotopic constitution from mass spectrograph in percent	Pb^{208}	50.1 [s]		5.8 [11]		2.3 [11]	0.02 [11]
	Pb^{206}	28.3		85.9		89.8	93.3
	Pb^{207}	20.1		8.3		7.9	6.7
	Pb^{204}	1.5					
13. Mean mass number [j]		207.173		206.199		206.125	206.067
Changed to chemical scale [k]		207.14		206.17		206.09	206.04
14. Ac D : Ra G ratio in percent				9.67		7.72	7.18
15. Age of mineral from Ac D : Ra G ratio in million years:							
$\lambda(U\,I)=15.\times10^{-10}yr^{-1}\left\{\frac{\lambda(Ac\,U)}{\lambda(U\,I)}\right.=10$				1132		870	785
" $=11$				1016		784	705
$\lambda(U\,I)=1.6\times10^{-10}yr^{-1}\{$ " $=10$				1054		820	736
" $=11$				962		754	662

[a] Ordinary lead (test lead, Ag, Bi, etc. free) National Lead Co.
[b] Lead chloride residue from U. S. Radium Corp. Lead purified and reduced to a metal by Dr. E. W. Riblett (1932).
[c] Lead extracted from a single crystal of uraninite by Dr. C. M. Alter, Boston Univ. (1936).
[d] Lead extracted by Dr. Riblett from a portion of a large piece of pitchblende sent by Prof. Alfred C. Lane, Tufts College (1933).
[e] This lead obtained from Dr. J. P. Marble is from the same lot used by Marble, and Baxter and Alter for atomic weight determinations and by Aston for isotopic constitution analysis.
[f] Lead carbonate residue from Union Minière du Haut-Katanga. Purified and reduced to a metal by Dr. Riblett (1932).
[g] Pb^{207}, 21.4 percent; Pb^{204}, 0.8 percent.
[h] Pb^{208} and Pb^{204} from contamination of ordinary lead.
[i] Very little ordinary lead contamination; Pb^{208} probably all Th D.
[j] From above percentages assuming the masses of the isotopes to be integral.
[k] Mean mass number corrected for a packing factor of +1 and then converted to chemical scale; ratio of chemical (O = 16.0000) to the physical scale (O^{16} = 16.0000) is at least 1.00025.
[l] Present international atomic weight.
[m] 206.59, T. W. Richards and M. E. Lembert, J. Am. Chem. Soc. **36**, 1329 (1914); 207.00, T. W. Richards and C. Wadsworth, ibid. **38**, 2613 (1916).
[n] G. P. Baxter and A. D. Bliss, J. Am. Chem. Soc. **52**, 485 (1930).
[o] Atomic weights from same lot; 206.054, J. P. Marble, J. Am. Chem. Soc. **56**, 854 (1934); 206.058, G. P. Baxter and C. M. Alter, ibid. **57**, 467 (1935).
[p] These values from the same lot of curite; 206.027, G. P. Baxter and C. M. Alter, J. Am. Chem. Soc. **57**, 467 (1935); 206.030, O. Hönigschmid, reported in preceding reference. Other atomic weights from 205.97 to 206.048; G. P. Baxter and C. M. Alter, J. Am. Chem. Soc. **55**, 2785 (1933); O. Hönigschmid, R. Sachtleben, and H. Bandrexler, Zeits. anorg. allgem. Chemie **214**, 104 (1933); O. Hönigschmid and L. Birkenback, Ber. D. Chem. Ges. **56**, 1837 (1923).
[q] Above ratio by R. C. Wells reported in reference n. Other ratios range from 0.150 to 0.172; L. T. Walker, Univ. of Toronto Studies, Geol. Ser. No. 17, 42 (1924); H. V. Ellsworth, Am. Mineral. **15**, 455 (1930); Am. J. Sci. (5) **9**, 127 (1925); 0.1628 by F. Hecht and 0.1646 by E. Kroupa in Munich, reported by A. C. Lane at meeting of Committee on Measurement of Geologic Time, New York, Dec. (1935). For minerals containing thorium the ratio commonly used is Pb : U + 0.36 Th.
[r] This range for distinctly altered material to that which contains barite and silver; reference 2, page 3 (1932).
[s] F. W. Aston, Nature **137**, 613 (1936).

uranium isotopes genetically independent of U^{238} and U^{234} (U II). This hypothesis is substantiated by the mass spectrograph studies of Aston[11] and further by the results from hyperfine structure analysis in Table I for the relative abundance of Pb^{207} and Pb^{206} in uranium leads. The percentages of Pb^{207} by both methods are too large for Ac D to be the end product of a branching U I series. Since the end product of the actinium series, Pb^{207}, has an odd atomic weight, it can never arise by branching from an even atomic weight series, such as uranium, for all members of any series are either odd or even, and differ in mass by $4n$. Hahn[5] and Western and Ruark[6] have shown that there is probably only one actinouranium isotope and of the two probable masses, 235 and 239, it appears to have that of the former.

Also by separating protactinium from uranium minerals and comparing its activity with other radioactive constituents of the same minerals it has been shown[7, 8] that the actinium series is independent of the U I series and the Ac U : U I ratio is constant for all uranium minerals regard-

less of source, thorium content, and uranium concentration, and that the present activity ratio of the Ac U to the U I series is approximately 4 : 100. With the latter ratio, the relative abundance of Ra G and Ac D from mass spectra data,[11] and the Pb : U ratios for several minerals calculations have been made from which it appears that the ratio of the decay contants, $\lambda_{(Ac\ U)} : \lambda_{(U\ I)}$, is between ten and eleven.[7, 9, 10]

Probable Geologic Ages of the Minerals

From the above values and ratios of Ac D to Ra G it is possible to determine the probable geologic ages of the uranium minerals by use of the following relation:

$$\frac{\text{Ac D}}{\text{Ra G}} = \frac{\text{Activity Ac U}}{\text{Activity U I}} \cdot \frac{\lambda_{(U\ I)}}{\lambda_{(Ac\ U)}} \cdot \frac{(e^{\lambda_{(Ac\ U)}t}-1)}{(e^{\lambda_{(U\ I)}t}-1)}. \quad (1)$$

Geologic ages have been estimated from the proportions of lead and uranium in minerals but with this method care must be taken to be certain that the minerals have not been altered by leaching by surface waters, or by other external processes since they were originally formed. In many cases it has been extremely difficult to determine to what extent the minerals have been altered. The ranges of the Pb : U ratios in Table I show the varying effects of alterations in samples of mineral from the same source. The separation of lead isotopes by selective solution has never been observed and therefore it is difficult to see how alterations could have changed to any extent the Ac D : Ra G ratio of a mineral of a definite age.

Fig. 2 shows curves computed by Eq. (1) for variation of the Ac D : Ra G ratio in uranium lead with the age of the mineral. In plotting these curves two probable values, 10 and 11, for the ratio of the decay constants of Ac U and U I and also the limiting values of $\lambda_{(U\ I)}(1.5\times10^{-10}$ yr^{-1} and 1.6×10^{-10} yr$^{-1})$ in current use[9, 14] were substituted in the above equation. The ages of the minerals from the Ac D : Ra G ratios are shown in Table I, row 9. Which of the four values for each mineral is the most nearly

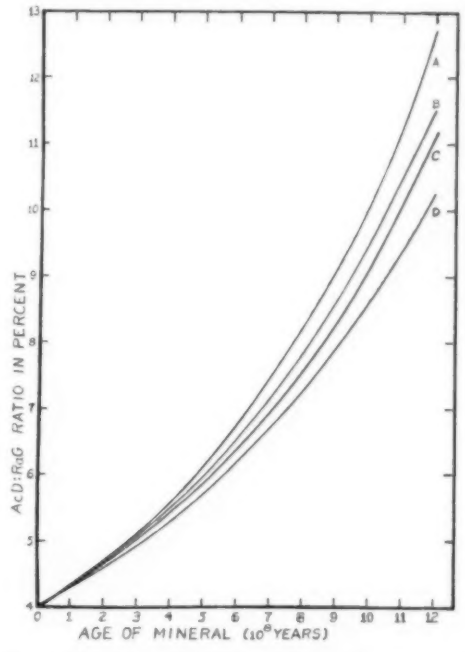

FIG. 2. Curves computed by Eq. (1); 4.0 percent present activity ratio of Ac U to U I. $\lambda_{(Ac\ U)}/\lambda_{(U\ I)} = 11$: *A*, $\lambda_{(U\ I)} = 1.6\times10^{-10}$ yr^{-1}; *B*, $\lambda_{(U\ I)} = 1.5\times10^{-10}$ yr^{-1}. $\lambda_{(Ac\ U)}/\lambda_{(U\ I)} = 10$: *C*, $\lambda_{(U\ I)} = 1.6\times10^{-10}$ yr^{-1}; *D*, $\lambda_{(U\ I)} = 1.5\times10^{-10}$ yr^{-1}.

correct cannot be determined until better experimental agreement is found for the decay constants of Ac U and U I. The ages, however, with the exception of the Great Bear Lake pitchblendes, are not far from age estimates by other methods.

The slightness of difference in the ages of the Great Bear Lake pitchblende from two samples with different proportions of ordinary lead contamination indicates that the age for this material from the Ac D : Ra G ratios is to be preferred to the much higher estimate by Marble[15] from the Pb : U ratio. He did not think the sample desirable for a highly accurate age determination but it was the best which had thus far come from the region. Also the large variation in the Pb : U ratio shows that many deposits of this mineral have been subject to alteration. Through incomplete geological studies there is a conflict of opinion of the age, ranging

[14] Radium-Standards Commission, Rev. Mod. Phys. **3**, 427 (1931); A. F. Kovarik and N. I. Adams, Phys. Rev. **40**, 718 (1932); R. D. Evans, Phys. Rev. **45**, 35 (1934); R. Schiedt, Akad. d. Wiss. Wien, Ber. **144**, 175, 191 (1935).

[15] J. P. Marble, J. Am. Chem. Soc. **58**, 434 (1936).

from Keweenawan to Kewatin.[16] From the above lead analyses it appears to have been formed at about the time of formation of the Wilberforce uraninite which is thought to be Middle Pre-Cambrian.

The method proved successful in showing that Colorado carnotite is a more recent formation. For very young minerals accurate ages cannot be expected since the Ac D : Ra G ratio is very sensitive to a small error in the content of Pb^{207}. If the percentage of Pb^{207} for the above lead were decreased 0.2 percent (within the limit of experimental error), the ratio of Ac D : Ra G would be changed from 0.0475 to 0.0420 and the ages from curves of Fig. 2, from approximately 200×10^6 yr to 60×10^6 yr.

Quantity of Lead Required

The Paschen-Schüler hollow cathode discharge tube[17] used in this work requires between two and four grams of pure metallic lead for a steady discharge. Only a small fraction of the lead is lost, however, after several days' operation. The major portion of the lead left in the stainless steel hollow cathode after an investigation can be removed with a steel blade and the remainder by placing the cathode in hot nitric acid for several minutes. After polishing the outside and inside with very fine emery cloth and washing, the cathode is ready to be used with another sample.

Some modification of this type tube will have to be made if leads are to be analyzed from rocks, meteorites, and other sources which contain very small quantities of lead. The more intense lines could just be detected with 15 mg of lead electrolytically deposited inside of a water-cooled cathode, which was tried some time ago by one of us (J. L .R.), of the type used by Kopfermann[18] with 100 mg of Th D. To operate this type of tube the surface of the deposited lead must be smooth, clean, and bright. The most satisfactory surfaces were obtained with a dilute lead perchlorate solution with a small amount of meat peptone added. The solution was put in the hollow cathode and a small lead wire electrode was placed in the center. To insure a firm coating the cathode should be rotated and only a few milliamperes of current used. Whether or not cathodes with very small amounts of deposited lead can be used for isotopic analyses with the success of the larger tube can be determined only by further investigations.

Acknowledgments

In conclusion the authors wish to express their indebtedness to Dr. R. L. Garman of the Department of Chemistry, Washington Square College, for the splendid microphotometer traces of the photographs, to those who have aided in providing and purifying samples of lead, and to the National Research Council for the grant-in-aid for hyperfine structure work in this laboratory.

[16] Bibliography, reference 15.
[17] J. L. Rose, Phys. Rev. **47**, 122 (1935).
[18] H. Kopfermann, Zeits. f. Physik **75**, 363 (1932).

The $2s\,^1\Sigma \rightarrow 2p\,^1\Sigma$ Bands of the Hydrogen Molecule

G. H. DIEKE, *Johns Hopkins University, Baltimore, Maryland*

(Received August 14, 1936)

The so-called $^1X \rightarrow 2p\,^1\Sigma$ bands of H_2 have been considerably extended and the analogous systems of HD and D_2 discovered. The discovery of the new bands shows that the properties of the upper level of these bands are considerably different from those assumed until now, and the new facts allow a quite unambiguous identification of this level as $2s\,^1\Sigma$. This state has an equilibrium distance of $1.0087 \cdot 10^{-8}$ cm slightly greater than the corresponding triplet level and is slightly less firmly bound. For the estimate of the significance and accuracy of the various constants the comparison of the three isotopic molecules is of great help. The $2s\,^1\Sigma$ state shows marked class B perturbations and the perturbing state is very probably $(2p\,\sigma)^2\,^1\Sigma$ which should lie roughly 3500 cm^{-1} above $2s\,^1\Sigma$. This would explain also the fact that the $2s\,^3\Sigma$ state does not show any perturbations.

§ 1. INTRODUCTION

THERE is a band system in the infrared part of the spectrum of the hydrogen molecule discovered by Richardson and Davidson[1] which is of especial interest from several points of view. The lower state of this system is the well-known level $2p\,^1\Sigma$ which is the initial state of one of the systems in the vacuum ultraviolet and the final state of the extensive and strong singlet systems found in the visible part of the spectrum. The initial state called ^1X by Richardson is much lower than any of the other initial levels of the visible bands. For this reason its interpretation should be comparatively simple. For there is only a small number of levels of such low energy possible and they should have rather simple properties. This is quite different from the situation for the higher states where many levels lying very closely together give rise to complicated interactions. Accordingly the interpretation of such highly excited levels must be expected to present great difficulties, and, as is well known, there are a great number of the levels found empirically by Richardson and his co-workers which have not yet been classified satisfactorily.

The surprising fact about the ^1X level is that it does not at all behave as one should expect at first hand for such a low lying level. If one restricts oneself to states for which only one of the two electrons is excited, the only possible theoretical level with which ^1X can be identified is $2s\,^1\Sigma$.[2] Weizel[3] emphasized the difficulties connected with this identification and proposed to identify the ^1X state with $(2p\sigma)^2\,^1\Sigma$, a state thus for which both electrons are excited. There were, however, also difficulties to this point of view, and Richardson[4] favored $2s\,^1\Sigma$ notwithstanding the objections which might be raised. The difficulties are of the following nature. The ^1X level shows strong irregularities which might be either due to uncoupling as in most of the other hydrogen levels or to some other kind of perturbation. Uncoupling for $2s\,^1\Sigma$ is out of the question, as that phenomenon is produced by the interaction with a level which differs only by the value of the quantum number Λ and such a level cannot exist for an s electron. Some other kind of perturbation would necessitate the presence of another level close to $2s\,^1\Sigma$ and, as Richardson points out, there does not seem to be any room for such a level in the energy level scheme of the hydrogen molecule. Another difficulty is that the moment of inertia calculated from Richardson and Davidson's bands is much larger than should be expected for the $2s\,^1\Sigma$ state. (This was one of Weizel's chief arguments in favor of his interpretation.) A further circumstance which made a definite decision difficult was the fact that the exact location of the electronic level was very uncertain. The reason for this was that there was no way of finding out whether Richardson's assignment of vibrational quantum numbers was correct or not,

[1] O. W. Richardson and P. M. Davidson, Proc. Roy. Soc. **A124**, 81 (1929). Some of the bands were also given simultaneously in a slightly different arrangement by Finkelnburg and Mecke (Zeits. f. Physik **54**, 597 (1929)). All the data are also found in Richardson, *Molecular Hydrogen and Its Spectrum* (Yale University Press, 1934).

[2] G. H. Dieke, Zeits. f. Physik **55**, 447 (1929).

[3] W. Weizel, Zeits. f. Physik **65**, 456 (1930).

[4] Richardson, *Molecular Hydrogen and Its Spectrum*, p. 308.

TABLE I. *The $2s\,{}^1\Sigma \rightarrow 2p\,{}^1\Sigma$ bands of H_2.*

J	ν	I		ν	I
	P branch			*R* branch	
	0→0				
0	—	—		9 024.68	5
1	8 922.38	3		112.16	4
2	908.51	5		223.06	7
3	919.82	3		356.57	3
4	956.37	5		511.82	6
5	9 017.90	5	blend	687.71	1
6	104.22	4			
7	214.74	1			
8	348.80	1			
9	505.49	90*d*			
	1→0				
0	—	—		11 350.51	9*b*
1	11 250.34	4		429.32	8
2	234.37	9		529.75	10*b*
3	236.99	7		646.32	6
4	263.11	10*b*		780.85	8
5	307.67	5		919.60	5
6	373.17	6			
7	447.78	1			
	2→0				
0	—	—		13 402.09	10*b*
1	13 317.22	10		447.76	10
2	285.91	10*b*		470.33	10
3	255.43	10			
4	203.59	10			
	2→1				
0	—	—		12 083.82	10*b*
1	12 000.89	9		131.44	7
2	11 973.41	10		157.81	9
3	948.54	8			
4	903.93	9			
	2→2				
0	—	—		10 802.36	1
1	10 721.05	0		851.72	0
2	696.83	4		881.21	0
3					
4	638.35	0*d*			
	3→0				
0	—	—		15 211.79	6
1	15 142.64	7			
2	095.67	8		237.22	?
3	039.34	5			
4	14 970.53	6			
	3→1				
0	—	—		13 893.44	10
1	13 826.20	10		915.23	9
2	783.00	10		924.66	10
3	732.32	10			
4	670.75	10			

J	ν	I		ν	I
	P branch			*R* branch	
	3→2				
0	—	—		12 611.92	1
1	12 546.36	0		635.39	1
2	506.50	4		646.03	2
3	460.55	2*c*			
4	405.23	2			
	3→3				
0	—	—		11 365.27	5
1	11 301.11	4		390.16	3
2	264.10	5		405.66	4
3	222.43	4			
4	172.64	4			
	4→1				
0	—	—		15 927.80	4
1	15 867.12	3		937.80	2
2	817.47	5		933.16	3
3	754.91	5		912.62	1
4	679.29	5			
5	590.02	1			
	4→2				
0	—	—		14 646.38	5
1	14 587.32	4		658.02	4
2	540.88	8*r*		656.59	6
3	483.16	5		640.91	4
4	413.75	9			
5	331.98	4			
	4→3				
0	—	—		13 399.61	4
1	13 342.00	1		412.70	2
2	298.34	7		414.14	9
3	244.94	3		402.76	0
4	181.28	10	blend		
	4→4				
0	—	—		12 186.60	4
1	12 130.38	1		201.03	1
2	089.44	4		205.08	3
3	039.86	1*c*		197.55	0
4	11 980.98	3			
5	912.22	0			
	4→5				
0	—	—		11 006.61	00
1	10 951.68	1			
2	913.07	5		028.78	00
3	867.07	3			
4	813.00	3			
5	749.89	2			

in other words, whether what according to Richardson's numbering should be the vibrationless electronic state had not perhaps several quanta of vibrational energy. In that case there should be additional bands in the hitherto photographically inaccessible infrared, and the position of the ^1X level would have to be lowered by several thousand wave numbers.

With this state of affairs it seemed desirable to see whether an investigation of the HD and D_2

TABLE II. *The $2s\,{}^1\Sigma \rightarrow 2p\,{}^1\Sigma$ bands of HD.*

J	P branch ν	I		R branch ν	I
		0→0			
0	—	—		8 949.49	0
1	8 872.37	0		9 015.49	2
2	861.73	0		099.24	3
3	869.86	1		200.34	3
4	896.80	3	$+D_2$	318.29	0
5	942.59	1		452.55	0
6	9 006.99	1			
7	089.80	1			
8	190.64	0	?		
		1→0			
0	—	—		10 988.26	3
1	10 913.66	3		11 049.10	5
2	900.44	4		125.10	6
3	903.43	5		216.06	6
4	922.67	5		321.18	6
5	958.29	4	$+H_2$	439.87	5c
6	11 009.87	4		571.67	5
7	077.15	4			
8	159.77	3			
9	257.11	00			

J	P branch ν	I		R branch ν	I	
		2→0				
0	—	—		12 862.28	6	
1	12 791.84	7		913.96	7	
2	774.47	9		971.14	2	
3	768.10	10	$+D_2$			
4	768.80	4				
		2→1				
0	—	—		11 714.25	5	$+H_2$
1	11 645.87	5		767.96	7	
2	631.03	7		827.76	3	
3	628.65	7				
4	634.01	4				
		2→2				
0	—	—				
1	10 527.87	0		10 595.93	0	
2	515.27	1		649.95	0	
3	516.09	2				

spectra would not overcome the difficulties mentioned above. Since the early studies on the spectra of isotopic molecules, it has been known that any ambiguity in the assignment of vibrational quantum numbers can be removed if two or more isotopic forms of the same molecule are available. The results obtained with other band systems of H_2, HD, and D_2 seemed to make it rather probable that a study of the $^1X \rightarrow 2p\,{}^1\Sigma$ bands of HD and D_2 would also lead to a solution of the other difficulties. It was fortunate that in the meantime the new plates had become available which allowed the photography of the spectrum beyond 10,000A. This allowed a direct check of some of the results obtained. It will be seen that all the results support the identification of the initial state of the bands with $2s\,{}^1\Sigma$.

§ 2. EXPERIMENTAL PROCEDURE

The procedure for obtaining and measuring the plates was essentially the same as described previously.[5] In collaboration with Drs. C. R. Jeppesen and D. H. Rank the spectrum was extended to about 11,700A. Details of these measurements will be published shortly. A part of the wave numbers given in the subsequent tables is subject to small systematic corrections of a few hundredths of a cm^{-1}. The writer is at present engaged in a complete revision of the entire wave-length material, and different parts of the spectrum are at present at different stages of completion. The corrections are of such a nature that they will affect only inappreciably or not at all the values of the constants given in this paper.

Tables I–III give the wave numbers and intensities of the bands in question for H_2, HD and D_2. It will be seen that the data are most complete for D_2. That is partly due to the fact that because of the larger moment of inertia of D_2, the bands will be better developed so that the lines go to higher values of J. Also, in general, it can be expected that there will be more bands in a given system. In our particular case more care has been taken to obtain plates of great intensity for D_2 than for H_2. For HD it is in general more difficult to obtain as complete data, as the HD spectrum cannot be obtained without the lines of H_2 and D_2 being present at the same time and confusing the HD spectrum.

For H_2 the 2→0, 2→1, 3→0, 3→1, and 3→2 bands agree with Richardson's analysis except that Richardson's values of OV' are raised by one. Richardson gives some lines with higher J values than those included in the table, but their reality seems doubtful, and therefore they have been omitted. I have some alternative lines to

[5] G. H. Dieke and R. W. Blue, Phys. Rev. **47**, 261 (1935).

TABLE III. *The $2s\,{}^1\Sigma \rightarrow 2p\,{}^1\Sigma$ bands of D_2.*

J	ν	I		ν	I	
	P branch			*R* branch		
	0→0					
0	—	—		8 859.83	00*d*	
1	8 808.23	00		904.24	1	
2	800.96	0		960.53	1	
3	806.16	1		9 028.67	3	
4	823.91	0*d*		108.44	2	+HD
5	854.06	1		199.45	2	
6	896.78	2	+HD	301.61	0	
7	951.73	1		414.60	1	
8	9 018.92	0		414.60		
9	098.19	0*d*				
	1→0					
0	—	—		10 546.91	5	
1	10 496.50	5		588.40	7	
2	487.85	5		640.59	5	
3	490.30	7		703.23	7*b*	
4	503.90	6	blend	776.02	4*b*	
5	528.65	7		859.03	6	
6	564.33	4		951.70	4	
7	611.34	7		11 053.82	5	
8	669.05	4		164.96	3	
9	737.48	5		284.		
10	816.28	6				
11	905.38	3				
	1→1					
0	—	—				
1	9 554.83	1		9 646.75	00	
2	547.64	0				*c*
3	552.24	2		765.23	2	
4	568.65	1		841.11	0	
5	596.86	2		927.35	1	
6	636.67	00*d*		023.92	0	
7	688.15	2		130.56	1	
8	750.95	0				
	2→0					
0	—	—		12 137.31	4	
1	12 088.46	6		175.71	6	
2	078.25	6		223.21	6	
3	077.59	7		279.44	7	
4	086.51	6		340.76	3	
5	104.88	7		418.44	5	
6	129.13	3				
7	170.73	5				
	2→1					
0	—	—		11 195.02	2	
1	11 146.89	3		234.15	3	
2	138.10	3		283.06	2	
3	139.45	5*b*		341.47	4	
4	151.33	3		405.61	3	
5	173.12	4		486.72	4	
6	201.43	2				
7	247.57	2				
	2→2					
0	—	—		10 272.12	3	
1	10 224.61	5		311.86	5	
2	217.10	4		362.05	4	
3	220.46	6		422.32	4	
4	234.62	4		488.94	1	
5	259.44	5		573.03	4	
6	291.25	1				
7	341.47	4				

J	ν	I		ν	I	
	P branch			*R* branch		
	2→3					
0	—	—				
1	9 320.54	00		9 407.63	00	
2				458.99	0	
3	319.34	2	blend?	521.05	0	
4	335.49	00*d*		589.81	0	
5	363.07	0		676.89	0	
6	398.12	1				
7	451.90	0				
	3→0					
0	—	—		13 589.02	2	
1	13 543.44	4		620.60	4	
2	529.95	3		656.66	3	
3	522.53	10		693.71	4	
4	520.06	9*c*				
5	519.17	9*c*				
	3→1					
0	—	—		12 646.71	3	
1	12 601.83	8		679.01	7	
2	589.82	6		716.52	5	
3	584.47	7		755.73	5	
4	584.78	6				
5	587.37	7				
	3→2					
0	—	—				
1	11 679.83	0		756.69	(3*d*)	+HD
2				11 795.55	1	
3	665.10	4*c*	blend			
4						
5	673.76	1*d*				
	3→3					
0	—	—		10 819.21	2	
1	10 775.54	2		852.71	3	
2	765.99	5		892.61	1	
3	764.12	4		935.36	2	
4	769.08	2				
5	777.40	2				
	3→4					
0	—	—		9 932.11	00	
1	9 889.12	0		966.21	2	
2	880.24	1*v*		10 007.05	0	
3	880.24	1*v*		051.35	1	
4	887.12	0				
5	897.96	00				
	3→5					
0	—	—				
1	9 019.67	00*d*		9 096.64	00	
2						
3	012.95	00*d*		084.19	00	
	4→0					
0	—	—		14 950.72	1*b*	
1	14 878.80	0		929.27	1	
2	856.31	0		939.54	00	
3	831.14	1		944.72	1*c*	
4	802.80	0				
5	770.07	0*c*				

TABLE III.—*Continued.*

J	ν	I	ν	I	
	P branch		R branch		
	4→1				
0	—	—	13 973.04	2	
1	13 937.13	4	987.65	5	
2	916.10	2	999.36	3	
3	893.11	5	006.64	5	
4	867.60	3			
5	838.28	4			
	4→2				
0	—	—	13 050.10	2*d*	
1	13 014.90	1	065.41	3*c*	
2	12 995.16	1	078.40	1	
3	974.02	3	087.53	2	
4	950.96	2			
5	924.68	3			
	4→3				
0	—	—	12 145.51	1	
1	12 110.82	2	161.32	2	
2	092.22	2	175.45	0	
3	072.73	3	186.28	1	
4	051.94	2			
5	028.31	2			
	4→4				
0	—	—	11 254.12	0*d*	
1	11 224.31	1	274.81	2	
2	206.74	0			confused
3	188.79	3	302.31	3	
4	169.97	2			
	4→5				
0	—	—	10 384.50	1	
1	10 354.75	3	405.32	3	
2	338.13	2	421.39	1	
3	321.61	2	435.18	2	
4	304.70	4			
5	285.95	3			

substitute for them, but they are not very satisfactory either and therefore are not included in the table. The bands with the initial vibrational quantum number 4 have been greatly extended. Of the 1→0 band Richardson gives only the pair $R0$ and $P2$. The 0→0 band lies in a region for which hitherto no measurements existed.[6] Naturally all the HD and D_2 bands are new.

§ 3. THE FINAL STATE $2p\ ^1\Sigma$

We shall not discuss in this paper the properties of the final state of the bands. This state is also the final state of a number of other bands in the visible and it will be discussed together with those bands in another paper. When it was necessary to use the constants of that state as, e.g., for the calculation of the zero lines of the bands, use has been made of the results of the analysis of the $3d\rightarrow 2p\ ^1\Sigma$ systems of HD and D_2 by M. Lewis and the author which will be published soon.

§ 4. THE VIBRATIONAL QUANTUM NUMBERS

If there are two isotopic molecules the correctness of the assignment of vibrational quantum numbers can be ascertained in a very simple way. If the electronic frequency of the band system is calculated it should have approximately the same value for the two molecules. If that is not the case the vibrational quantum numbers have to be adjusted in such a way that the changed new electronic frequencies satisfy the condition. If we use just the quadratic approximation $\omega(V+\frac{1}{2})-x(V+\frac{1}{2})^2$ for the vibrational energies of H_2 and D_2 we obtain the values 8368.6 and 8426.5 for the values of the electronic frequencies, which can be regarded as agreement in a case like ours. For the comparatively large discrepancy of about 58 cm^{-1} there are two reasons. In the first place in a molecule like the hydrogen molecule relatively large electronic shifts must be expected. The largest shift so far observed is 25.5 cm^{-1},[7] and it is likely that it is larger for our system. In the second place it is certain that the simple quadratic formula used to extrapolate to the electronic frequency is inadequate, but it is useless to try a more elaborate formula because of the irregularities in the initial state. Nevertheless the agreement can be regarded as conclusive proof for the correctness of the vibrational quantum numbers, as increasing the vibrational quantum numbers of the upper state by one[8] would produce a discrepancy of more than 900 cm^{-1}, in the electronic frequencies. Instead of comparing H_2 with D_2 we could just as well have compared HD with H_2 or D_2 with the same result.

[6] Richardson (Nature **135**, 99 (1935)) announces the discovery of bands which have the $V=0$ level of ^1X as final state. Whether this level is identical with our $V=0$ or $V=1$ level cannot be ascertained from his description.

[7] G. H. Dieke, Phys. Rev. **47**, 661 (1935).

[8] Decreasing the vibrational quantum numbers is not possible because otherwise there would be no place for the bands around 8900 (0→0 bands with the correct numbering).

TABLE IV. *Rotational differences of the 2s $^1\Sigma$ level.*
$R(J)-P(J)$

J \ V	0	1	2	3	4
			H_2		
1	189.76	178.98	130.54	89.04	70.68
2	314.55	295.38	184.41	141.54	115.70
3	436.47	409.33			157.72
4	555.45	517.74			
5	669.81	611.93			
			HD		
1	143.12	135.44	122.11		
2	237.51	224.66	196.70		
3	330.48	312.63			
4	421.49	398.51			
5	509.96	481.58			
6		561.80			
			D_2		
1	96.01	91.91	87.25	77.17	50.50
2	159.57	152.73	144.96	126.70	83.24
3	222.52	212.93	201.85	171.22	113.54
4	284.59*	272.31	254.30		
5	345.13	330.41	313.58		
6	404.86	387.37			
7	462.90	442.44			
8		495.91			

§ 5. ROTATIONAL STRUCTURE OF $2s\ ^1\Sigma$

Table IV gives the rotational differences $R(J)-P(J)=F(J+1)-F(J-1)$ of the upper level. These values can be used to represent the rotational levels by the usual formula

$$F_V(J)=B_VJ(J+1)-D_VJ(J+1). \qquad (1)$$

It is found that this formula is quite adequate for the lowest values of the vibrational quantum number V, but that for the higher values of V there are marked deviations from the regular formula. The rotational constants are collected in Table V. Those values for which the formula is inadequate are marked by an asterisk. They were calculated from the first *two* differences of Table IV only and cannot be regarded as having much significance. The others were calculated by a least-square formula from the first *three* differences.

The most striking feature about the constants in Table V is the rapid decrease of the value of B_V with the vibrational quantum number. The decrease is too irregular to be represented by the usual formula

$$B_V=B_e-\alpha(V+\tfrac{1}{2})+\beta(V+\tfrac{1}{2})^2. \qquad (2)$$

As the rapid decrease of B_V and its irregularity are obviously connected with the perturbations, and the $V=0$ and $V=1$ level are practically free of them, we can apply the above formula, with neglect of β to B_0 and B_1 and calculate an approximate value of B_e. The values so obtained and the moments of inertia I calculated from them are

	H_2	HD	D_2
B_e	32.679	24.568	16.373
$I\cdot10^{40}$	0.8464	1.1258	1.6892

The values for D_2 are probably most reliable, as it is less affected by the perturbations than the two other molecules and also the formulas used are a better approximation. The value of the equilibrium distance is found to be $r_e=1.0087\cdot10^{-8}$ cm. That this value and the values of B_e from which it is derived are not far from the correct ones can be ascertained by a comparison of the three isotopic molecules. The ratios of the B_e values are

	HD : H_2	D_2 : H_2	D_2 : HD
empirical	0.7517	0.5010	0.6664
theoretical	0.7502	0.5005	0.6671

The discrepancies between the empirical and the theoretical ratios are small and of the same order of magnitude as for other states of the hydrogen molecule.[5]

The values of D_0 are of the right order of magnitude which can be seen again by observing that the isotopic ratios have about the correct values. The empirical ratios 0.556, 0.233, 0.419 are all slightly smaller than the theoretical values 0.563, 0.250, 0.445. This means that the values for the lighter molecules are too big in proportion and is an indication that the per-

TABLE V. *2s $^1\Sigma$. Rotational constants.*

V=	0	1	2	3	4
H_2 B_V	31.770	29.952*	24.23*	15.35*	11.930
D_V	0.0228	0.0277*	0.414*	0.086*	0.0256
HD B_V	23.924	22.636	20.863*		
D_V	0.0123	0.0118	0.085*		
D_2 B_V	16.032	15.350	14.583	13.01*	8.49*
D_V	0.0053	0.0054	0.0063	0.0240*	0.0116*

turbations which affect so strongly the higher vibrational levels have also a very slight influence on the $V=0$ level. The D_V values for the higher V are abnormally large, and, as mentioned before, this must not be taken that the actual D_V have these values but rather as an indication that the simple formula for the rotational energy breaks down. The value of D_V can be taken as a direct indication for the degree to which the level is perturbed.

§ 6. The Vibrational Constants

Table VI gives the origins of all the bands found so far calculated in the usual way. The values marked by an * again refer to the perturbed bands. These latter values have been calculated from the $P(1)$ line only by adding to it the rotational energy $F(1)$ of the final state. Table VII gives the vibrational differences of the $2s\,{}^1\Sigma$ state. The vibrational differences of the $2s\,{}^3\Sigma$ state as a representative of a normal state are included in small print for comparison.

The table shows immediately the difference between the $2s\,{}^3\Sigma$ and the $2s\,{}^1\Sigma$ states. For the former the second differences are approximately constant and the small variations which do occur are very regular. For $2s\,{}^1\Sigma$, however, the second differences are very irregular, so that the formula

$$F_V=\omega(V+\tfrac{1}{2})-x(V+\tfrac{1}{2})^2+\cdots \qquad (3)$$

for the vibrational energy is no more a good approximation. Nevertheless, for lack of anything better, we can use the formula to calculate from the first two differences the constants ω and x. The values for ω are 2588.9, 2204.4, and 1784.5, respectively, and the values for x are 130.5, 81.6 and 48.1. As could be expected the isotopic ratios show that the values of x must be considerably wrong and that the values of ω are less though quite appreciably affected.

		$HD:H_2$	$D_2:H_2$	$D_2:HD$
ω	empirical	0.8514	0.6893	0.8095
	theoretical	0.8662	0.7074	0.8168
x	empirical	0.625	0.369	0.590
	theoretical	0.750	0.501	0.667

The values of all these constants are too low, but the values for D_2 must be more nearly correct than those for the two other molecules.[9]

The electronic frequencies of the bands systems have been discussed in § 4.

Table VI. *Origins of the $2s\,{}^1\Sigma \rightarrow 2p\,{}^1\Sigma$ bands.*

V'/V''	0	1	2	3	4	5
			H_2			
0	8 961.23					
1	11 289.19*					
2	13 356.07*	12 037.81*	10 736.33*			
3	15 181.49*	13 863.12*	12 581.64*	11 334.93*		
4		15 904.02	14 622.58	13 375.79	12 162.85	10 982.86
			HD			
0	8 901.72					
1	10 943.02					
2	12 821.18*	11 673.91*	10 554.86*			
3						
			D_2			
0	8 827.98					
1	10 516.22	9 573.86				
2	12 108.17	11 165.88	10 242.34	9 338.28		
3	13 563.16*	12 620.82*	(11 698.18*)	10 793.21*	9 906.22*	9 036.18*
4	14 898.52*	13 956.12*	13 033.25*	12 128.59*	11 241.60*	10 371.56*

Table VII. *First and second vibrational differences of $2s\,{}^1\Sigma$ and $2s\,{}^3\Sigma$.*

	V	H_2 Δ_1	H_2 Δ_2	HD Δ_1	HD Δ_2	D_2 Δ_1	D_2 Δ_2
$2s\,{}^1\Sigma$	1	2 327.96		2 041.30		1 688.24	
			260.98		163.14		96.26
	2	2 066.98		1 878.16		1 591.98	
			241.64				137.01
	3	1 825.34				1 454.97	
			−215.56				119.64
	4	2 040.90				1 325.33	
$2s\,{}^3\Sigma$	1	2 524.35		2 202.75		1 814.97	
			136.03		102.72		69.15
	2	2 388.32		2 100.03		1 745.82	
			132.10		100.08		67.56
	3	2 256.12		1 999.95		1 678.26	
			129.22		97.92		66.18
	4	2 126.90		1 902.03		1 612.08	

§ 7. The Perturbations

It was mentioned in the introduction that there was considerable doubt whether the irregularities observed in many of the bands were due to decoupling or ordinary perturbations. This question can be answered now satisfactorily. If the irregularities were due to decoupling they should be the same or even larger for the $V=0$ level,

[9] For this reason, if the exact value of, e.g., ω for H_2 is desired, it would be more nearly correct to take the D_2 value and multiply it with the correct isotopic factor than to use the value derived from the H_2 bands. This is true for most of the constants of the hydrogen molecule, and the cause is that all interactions which are usually difficult to express in a satisfactory formula are much less for D_2 than for the other two molecules.

TABLE VIII. *Differences between observed and calculated rotational $2s\ ^1\Sigma$ levels of D_2.*

	$J=0$	1	2	3	4	5	6	7
$V=0$	−0.04	0.01	−0.01	0.02	0.00	0.04	0.00	−0.04
1	0	.01	.00	.01	.04	−.05	.16	.39
2	0	−.01	−.02	.00	.01	−2.41	1.41	
3	0	−.19	−.28	.11	−.32			
4	0	−.11	−.12	.02	−.18			

whereas it was seen in § 5 that that level is perfectly normal. This shows that they must be produced by the accidental presence of another level in the vicinity of $2s\ ^1\Sigma$. Much can be learned of the nature of this level by a careful scrutiny of the perturbations. However, it is likely that bands coming from this perturbing level can be found empirically which will allow a much more thorough discussion of the perturbations and therefore only the most outstanding features of the perturbations will be mentioned now and the rest reserved for a future paper.

In order to give an idea of the kind and magnitude of the perturbations the differences between the observed rotational levels and those calculated by formula (1) are given for D_2 in Table VIII. The level $J=0$ is taken to be zero except for $V=0$ where it comes from an obviously poor line. The table shows that the agreement for $V=0$ is as good as can be expected. The discrepancy for $V=1$, $J=6$ and 7 may be the beginning of a weak perturbation or it may be due to the fact that the constants B and D do not have quite the correct values, as they were calculated from the first few rotational levels only. The first view is more likely correct as there is definitely a weak perturbation in the $V=1$ level of H_2. $V=2$ is quite regular up to $J=4$. $J=5$ and 6 however show marked perturbations. $V=3$ and 4 behave both very similarly. They show marked irregularities but the actual value of the perturbations must be larger than the values in the table as the constants were calculated so as to give as good an average fit of the rotational differences as possible and probably are very different from the unperturbed constants. The values for $J=5$ and 6 must be expected to be much more strongly perturbed, but unfortunately they have so far escaped discovery.

The $V=0$ level of H_2 is regular. The $V=1$ level seems to have a definite perturbation for small J. $V=2$ is very strongly irregular as indicated by the abnormally large value of D in Table V, the $V=3$ level less so, and the $V=4$ level seems again to be quite regular.

There are two types of perturbations which have widely different characteristics and causes.[10] Class A perturbations arise from the interaction between rotation and electronic motion, and therefore the nonrotating molecule cannot be perturbed. The two levels influencing each other have values of the quantum number Λ different by one.

On the other hand class B perturbations arise from the interaction of vibration and electronic motion, and the two levels perturbing each other must have the same value of Λ. In both cases the perturbations appear primarily as irregularities in the rotational structure, as the relative distance of the perturbing levels which enters quite prominently into the magnitude of the perturbations is dependent on the rotational quantum number.

We see immediately that the perturbations in our case must belong to class B. For the irregularities in the vibrational differences of Table VII shows that we have here vibrational perturbations, i.e., that even the rotationless molecule is affected, and this can happen only for class B. This is the first case of this type of perturbation in the hydrogen molecule. We know now that the level causing the perturbations must also be a $^1\Sigma$ level which must besides have the same symmetry properties as the $2s\ ^1\Sigma$ level.

All the perturbed vibrational levels are lower than their expected position except the $V=4$ level of H_2 which is higher. This means that the perturbing level must now lie below it. The perturbing level has probably a much larger moment of inertia than $2s\ ^1\Sigma$ and therefore no typical rotational perturbations can arise, which is just what is observed. However, the possibility that the $V=4$ vibrational level belongs perhaps to a different electronic state cannot be entirely disregarded. Further experimental evidence will clear up this point.

[10] G. H. Dieke, Phys. Rev. **47**, 870 (1935); J. H. Van Vleck, J. Chem. Phys. **4**, 327 (1936).

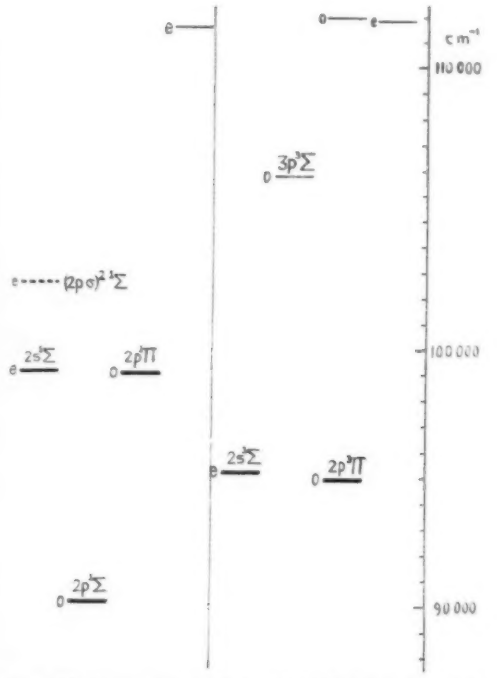

FIG. 1. The two quantum states of the hydrogen molecule. A few of the next higher levels are also given.

§ 8. THE NATURE OF THE UPPER STATE

If we review the facts presented in the preceding paragraphs we see that all the evidence against identifying the upper level of our bands with $2s\,{}^1\Sigma$ has disappeared. The internuclear distance $1.0087 \cdot 10^{-8}$ is only slightly larger than $0.9868 \cdot 10^{-8}$, that of $2s\,{}^3\Sigma$. The relative magnitudes of the vibrational constants of these two states shows that the binding of the singlet level is less strong than that of the triplet level which is undoubtedly due to the fact that the former is influenced by the perturbing level and takes some of its characteristics. Fig. 1 shows that the position of all the known two quantum levels. It is seen that the position of the $2s\,{}^1\Sigma$ level is just where it would be expected from analogy with the triplet system.

Finally there remains the identification of the perturbing level. From the facts of the preceding paragraph it follows that it must be a ${}^1\Sigma_g$ state, and there is no possibility for such a state with only one electron excited. We must therefore look for a state with two excited electrons and among these $(2p\sigma)^2\,{}^1\Sigma$ is the most probable one. All the arguments which Weizel[3] brought forward to show that this state can be expected to lie in the right region and to be a discrete state notwithstanding the fact that the $2p\sigma$ state of the H_2^+ ion is continuous still hold. The $2p\sigma$ state of the H_2^+ ion is for not too small internuclear distances a very low state. It is not discrete, however, but a continuous, repulsive state. This is not necessarily a difficulty, as the interaction energy of two such electrons might produce a minimum in the potential energy curve and give thus a discrete state. It must be assumed, that the equilibrium distance for such a state is quite large. Of course, none of these arguments are conclusive, and they make only plausible the existence of this state with the required properties. A more direct calculation would be highly desirable, but, unfortunately, is far from simple.

There is an additional argument in favor of $(2p\sigma)^2\,{}^1\Sigma$ as the perturbing state. All the electronic states of the hydrogen molecule occur in pairs, one each for the triplet and one for the singlet system, except when the two electrons have identical quantum numbers. In that case the triplet level is missing. The $2s\,{}^3\Sigma$ state which is the lower level of the Fulcher bands shows no trace of any perturbation whereas we have seen that the $2s\,{}^1\Sigma$ state is strongly perturbed. This difference in the behavior of the two analogous states is perfectly explained by the assumption that $(2p\sigma)^2\,{}^1\Sigma$ is the perturbing level. For there is no analogous level in the triplet system and therefore no possibility for any perturbations of $2s\,{}^3\Sigma$.

The position of the perturbing level can be roughly estimated from the character of the perturbations. It should be about 3 500 cm^{-1} above the $2s\,{}^1\Sigma$ level although this figure is not very trustworthy as it involves several assumptions. In any case the $(2p\sigma)^2\,{}^1\Sigma$ state should lie in this general neighborhood.

The Scattering of Protons by Protons*

M. A. Tuve, N. P. Heydenburg and L. R. Hafstad, *Department of Terrestrial Magnetism, Carnegie Institution of Washington, Washington, D. C.*

(Received August 11, 1936)

By counting several thousand scattered protons at each angle and voltage with a linear amplifier, the numbers of protons scattered or projected by recoil through angles from 15° to 45° from a carefully defined mono-energetic proton beam in passing through 2 mm path length of pure hydrogen gas at a pressure of 12 mm have been measured for proton beam energies of 600, 700, 800, and 900 kv. The angular resolution for the slit systems was about 2°. The high voltage was constant to within one percent and was measured directly to about two percent with a specially calibrated 10,000-megohm corona free voltmeter resistor. The spread in energy of the primary protons did not exceed one percent. At 600 kv the observed numbers at all angles are roughly two-thirds of the values predicted by Mott's formula. The curves for this observed "Mott ratio" *versus* angle change progressively as the voltage is increased and at 900 kv the observations show two-thirds of the Mott value at 15°, 1.4 times Mott at 30°, and 4.0 times Mott at 45°. Measurements of the scattering of protons by deuterium, helium, and air, together with "vacuum-scattering" tests which eliminate slit scattering and unknown vapors, have led to the conclusion that the observed anomaly is not due to a contamination and must be ascribed to a proton-proton interaction at close distances (less than 5×10^{-13} cm) which involves a marked departure from the ordinary Coulomb forces. The observed curves lead quantitatively to a simple theoretical interpretation on the basis of wave mechanics, as shown in the accompanying paper by Breit, Condon and Present. A new scattering apparatus is under construction to eliminate possible small errors in the angular measurements and to permit observations (with Geiger point-counters) at lower voltages.

(A) Introduction

THE statistical study of collision processes, by observations on the number, energy, and angular distribution of the scattered particles after collision, has been recognized for many years as a basic method for obtaining intimate knowledge of the nature and magnitude of the interaction forces between particles when they are brought into close proximity with each other. The application of this method by Rutherford and his colleagues using alpha-particles for the quantitative demonstration that atoms have a nuclear structure was followed by their similar studies demonstrating the failure of the Coulomb law of repulsion when alpha-particles and other atomic nuclei approach within distances of the order of 10^{-12} cm between centers. The study of the scattering of protons by protons in order to acquire basic information regarding the interaction forces between these primary constituents of nuclear structure (then thought to be protons and electrons) was one of the stated objectives of the program of high voltage research begun here in 1926 with the general aim of investigating the simplest and most basic manifestations of magnetic and electric forces which can be conceived or enunciated. At about the same time Gerthsen[1] initiated a series of researches on the properties of high speed protons in the region below 100 kv, culminating (1931) in his verification (for this range of energy) of Mott's theoretical formula for the scattering of protons by protons which is based on the wave mechanics and on the Coulomb law of repulsion.[2] Since the classical "closest distance of approach" at these voltages is of the order of 10^{-11} cm it was not surprising to find agreement with predictions based on the Coulomb law. However, if the proton energy is raised to 400 kv all large angle collisions involve protons which have approached (classically) to a distance between centers which is smaller than the distance 4×10^{-13} cm for which Chadwick and Bieler demonstrated (1921) the breakdown of the Coulomb law between protons and helium nuclei (for head-on collisions of fast alpha-particles in hydrogen; 8×10^{-13} cm for oblique collisions). Anomalous deviations from Mott's formula might accordingly be expected at large

* A brief account of this paper was delivered at the Tercentenary Conference of Arts and Sciences at Harvard University, September, 1936.

[1] Gerthsen, Ann. d. Physik **86**, 1025–1036 (1928); **3**, 373–408 (1929); **9**, 769–786 (1931).

[2] N. F. Mott, Proc. Roy. Soc. **A126**, 259–267 (1930); also Mott and Massey, *Theory of Atomic Collisions* (Oxford, 1933).

angles (limiting angle 45°) for proton-proton collisions at voltages of this order or higher, since it has long seemed probable that the proton must have a "size" (region of dimensions in which the Coulomb repulsion fails to hold) much in excess of its "classical diameter" (10^{-16} cm) and roughly of the dimensions of the other nuclei of which it is a demonstrated constituent.

The first attack on the experimental problem of proton-proton scattering at high voltages was made by Wells[3] in this laboratory in 1933–34. He photographed in a hydrogen filled cloud chamber the tracks of the recoil protons of various velocities produced by polonium alpha-particles bombarding thin Cellophane or paraffin sheets. Stereoscopic pictures of 200,000 tracks (15,000 expansions) resulted in a total of only 33 collisions which were finally accepted as valid; of this number 11 collisions were in the range 450 to 900 kv, only three of these lying in the interesting range 25°–45°. Collisions observed along tracks in a cloud chamber are twice distributed—with respect to voltage (distance from end of track) and with respect to angle—and consequently large numbers of collisions must be observed before statistical validity is achieved. The problem of establishing suitable criteria for accepting or rejecting collision forks is another difficulty inherent in this method. No theoretical conclusions were drawn from Wells' experiments and this method was abandoned by us since the possibility existed of carrying out the experiment of directly counting the protons scattered in hydrogen gas with our high voltage technique, then in process of perfection for quantitative work.

Similar cloud chamber experiments were carried out by White[4] at Berkeley in 1934–35 who used protons from a small cyclotron. The spread in energy among and along White's proton tracks (roughly 1000 kv to zero for most tracks) was somewhat smaller than for Wells' (maximum 1500 kv to zero; half of tracks 750 kv to zero) tending to a slightly increased emphasis in White's data on the collisions above 500 kv. In a total of 300,000 tracks White observed a total of 95 collisions occuring at energies between 450 and 900 kv. White concluded that Mott's formula was valid below 600 kv, and concluded further that a large anomaly became evident for large angle collisions occurring in the region of 600–750 kv (scattering too infrequent in the range 25° to 30° and too frequent by a factor of about 10 at 40° to 45°). This conclusion was based on the observation of "13.5 collisions" in the range 35° to 45°, where two collisions were expected, and on the observation of "1.5 collisions" in the range 25° to 30° where three collisions were expected on the basis of Mott's formula. A total of five collisions observed by White between 25° and 45° in the range 750 to 900 kv gave a crude check on this anomaly. A comparison of White's results with the data we have obtained by electrical counting methods is shown in Fig. 10. Although we find a considerable anomaly at 900 kv our results differ from those of White in the region 600 to 750 kv covered by his data. Within the statistical accuracy of his experiments the anomaly we find would not be detectable.

The fact that Bethe's correction (unpublished) of the usual range energy curve for protons raises the center of gravity of White's group for 600 to 750 kv to an actual voltage of about 720 kv, with corresponding changes in the other cloud chamber numbers, gives rise to no important alterations in the above discussion. White's conclusions as to the existence of an anomaly was based on a total of 18 observed particles at high angles with energies over 600 kv. In our final experiments a total of 21,540 particles in the same region were observed.

Profiting by our experience with Wells' work here, we chose to defer work on the proton-scattering problem until it became feasible to make a direct measurement by electrical methods of the scattering of large numbers of protons in gaseous hydrogen from the proton beam produced by our 1200-kv electrostatic generator and accelerating tube. For such a quantitative problem, however, it was clearly essential to have sufficient steadiness of experimental conditions as well as accurate knowledge and control of the voltage and composition of the ion beam. The discovery during 1934–35 of sharp nuclear resonance phenomena under bombardment by protons gave us a suitable test object for our technique. It also showed the primary need for

[3] W. H. Wells, Phys. Rev. **47**, 591–596 (1935).
[4] White, Phys. Rev. **49**, 309–316 (1936).

an accurate and reliable voltmeter, and for a tube having properly aligned electrodes before repeatable results could be obtained.

The need for a suitable voltmeter was met by the development of a 10,000-megohm corona-free voltmeter resistor which was constructed and tested during the summer of 1935 with the help of Dr. R. G. Herb. This voltmeter, together with a new tube with accurately aligned electrodes, was used for a study of the proton resonances with lithium and fluorine targets until a reference voltage scale was established by sharp resonances at 320, 440, 890, and 940 kv.[5] As already reported, the limit of fluctuation of the voltage was measured and found to be less than ± 0.5 percent R.M.S. The quantitative "repeatability" of observations with this equipment and technique was carefully tested and adequately demonstrated during these studies of nuclear effects varying extremely rapidly with voltage.

Having thus finally satisfied ourselves that quantitatively reliable results could be obtained, we returned to the proton-scattering problem. In this paper we will describe our experiments as thoroughly as possible in order to give an adequate critical basis for their evaluation. The theoretical aspects of the results are being very completely treated in the accompanying paper by Breit, Condon, and Present.

(B) Numerical Values for Coulomb Scattering

The classical formulas for nuclear scattering* based on the perfectly elastic collisions of massive charged particles obeying the inverse square law of Coulomb repulsion were given by Rutherford[6] and Darwin.[7] For convenient reference the formulas are again recorded here, with slight changes in notation which make them more immediately applicable to collisions of unlike particles. For incident particles of mass M impinging on "target" nuclei of mass m, the general formula can be resolved into special formulas for the three cases $M<m$, $M=m$, and $M>m$. If N_0 is the number of particles per second in the incident beam, having mass M, charge Ze, and kinetic energy T, then the numbers of primary particles N_s scattered per second into a solid angle ω at an angle θ with respect to the initial beam by a "target" having N_t nuclei per unit area of mass m and charge $Z'e$ are as follows: For $M<m$,

$$N_s=(1/4)K(ZZ')^2\{\csc^4(\theta/2)-2(M/m)^2+[1-(3/2)\sin^2\theta](M/m)^4+\cdots\},$$

where $K=N_0N_t\omega e^4/4T^2=0.512$ for $T=1000$ ekv and $(N_0N_t\omega)=10^{26}$. For $M=m$, the recoil nuclei (N_R) are indistinguishable from the scattered particles (N_S), and for the sum of the two the formula is

$$N_S+N_R=4K(ZZ')^2\cos\theta\csc^4\theta(1+\tan^4\theta).$$

For $M>m$, the recoil particles alone will in general be observed and for these the formula is

$$N_R=K(ZZ')^2(M/m)^2\sec^3\theta.$$

With an initial beam intensity of 10^{10} particles per second, and a target density $N_t=10^{18}$ nuclei per square centimeter (about 0.5-mm equivalent stopping power of air) the calculated number of scattered particles per second N_s to be expected in a solid angle $\omega=0.01$ steradian at a primary beam velocity corresponding to 1000 ekv (1.39×10^9 cm/sec. for protons; 0.98×10^9 cm/sec. for deuterons; 0.70×10^9 cm/sec. for alpha-particles) as calculated from the above formulas for a series of typical elements and angles are listed in Table I. The orders of magnitude of the expected scattering for various elements, voltages, and angles are important considerations in connection with the effects of possible contaminations. To convert to a primary beam energy of V kv multiply the tabulated values by $(1000/V)^2$. The use of 4.80×10^{-10} instead of 4.77×10^{-10} for the value of e would raise the values given in this table by nearly three percent.

For the collisions of like particles, that is, protons in hydrogen or alpha-particles in helium, Mott[2] worked out the corrections to be applied on account of the quantum-mechanical identity of the two particles. For angles near zero the Mott formula predicts the same scattering as the Rutherford-Darwin values for all velocities and at 45° the Mott value is always half that of

[5] Hafstad, Heydenburg and Tuve, Phys. Rev. **50**, 504 (1936).

* A misprint occurs in the formula given in Rutherford, Chadwick, and Ellis, *Radiations from Radioactive Substances* (Cambridge, 1930), p. 243, Eq. (8).

[6] Rutherford, Phil. Mag. **21**, 669–688 (1911).

[7] Darwin, Phil. Mag. **27**, 499–506 (1914).

TABLE I. *Numbers of scattered particles predicted by the Rutherford-Darwin formulas.* Initial energy, 1000 kv (500 kv accelerating potential for alpha-particles); initial beam $N_0 = 10^{10}$ primary particles; target-density $N_t = 10^{18}$ nuclei per cm^2; solid angle of detection $\omega = 10^{-2}$ steradian.

	Proton scattering						
	Scattered and recoil protons		Scattered protons				
Angle	H^1	(H^1 Mott)*	D^2	He^4	Li^7	C^{12}	Al^{27}
°							
10	2213	2150	2218	8875	19940	79900	375000
15	443	416	439	1757	3954	15840	74300
20	142	124	140	562	1264	5015	23720
25	60.7	45.2	58.0	232	525	2092	9820
27.5	42.9	32.0	....	....	....	....	....
30	31.5	22.0	28.4	114	256	1026	4823
32.5	23.5	15.7	....	....	....	....	....
35	19.1	11.6	15.6	62.5	141	563	2644
37.5	14.9	8.94	....	....	....	....	....
40	13.7	7.25	9.26	37.3	83.8	335	1578
42.5	12.2	6.26	....	....	....	....	....
45	11.6	5.78	5.89	23.8	53.7	214	1006
50	11.5	6.06	....	....	....	....	....
60	16.9	11.9	1.98	8.18	18.4	73.7	346
90	....	....	0.443	1.98	4.56	18.4	86.3
135	....	....	0.102	0.637	1.53	6.28	29.6
150	....	....	0.0877	0.522	1.27	5.24	24.7

	Deuteron scattering				Alpha-particle scattering				
			Scattered deuterons		Recoils only			Scattered alpha-particles	
Angle	Recoil protons H^1	Scattered and recoil D^2	He^4	Be^9	H^1	H^2	Scattered and recoil He^4	C^{12}	Al^{27}
°									
10	4.83	2213	8870	35460	53.6	19.3	35420	319200	1500000
20	5.55	142	560	2243	61.7	22.2	2280	20200	94900
30	7.08	31.5	114	456	78.6	28.3	504	4100	19200
40	10.2	13.7	37.0	149	114	40.8	220	1338	6300
45	13.0	11.6	23.6	95.3	145	52.2	185	855	4028
60	36.8	16.9	7.92	32.5	408	147	270	290	1380
90	∞	....	1.77	7.98	∞	∞	....	69.5	342
135	....	....	0.450	2.60	....	....	....	21.2	115
150	....	....	0.348	2.14	....	....	....	17.2	95.3

* Values predicted by Mott's formula.

Rutherford and Darwin, while the corrections for other angles depend on the velocity as indicated in Fig. 1 taken from Mott's paper. For the values of primary proton energy we have examined experimentally, the dependence on velocity is about one percent and we have used the Mott correction for $v = \infty$ (curve *I* in Fig. 1) in computing our predicted Mott values. A tabulation of these calculated values, for the actual thickness of target, solid angle, and other constants of our apparatus, together with the ratios of our observed values to the Mott values, is given in Table II (see Section *F*).

(C) Design and Constants of the Scattering Apparatus

The construction of the scattering chamber is indicated in Figs. 2 and 3. The primary proton beam, freed from other ions to a high degree of purity by magnetic analysis, was intentionally spread into a diffuse target spot 1.5 to 3 cm in diameter by a slight defocusing of the tube (slight change of voltage across the first tube section, next to the ion source). This insured a nearly constant proton current entering the 2.0-mm hole of the diaphragm system which

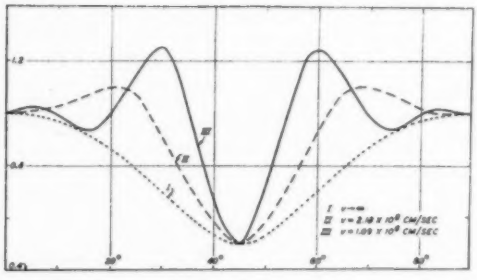

FIG. 1. Ratio of quantum theory scattering to classical scattering for protons, according to Mott.

defines the proton beam in the scattering chamber, regardless of slight motions of the (magnetically deflected) proton spot due to residual voltage fluctuations. The total proton current was of the order of several microamperes, whereas the proton beam passing through the scattering chamber was between 0.005 and 0.03 microampere in the different runs. The apertures of these diaphragms and of the detector slit system were selected to give a reasonable number of scattered protons (at least 50 per minute) into the ionization chamber at the highest voltages and angles, without giving rise to overwhelming numbers of counts at the lower angles and voltages, the hydrogen pressure and proton current necessarily being held constant during each run.

The slit systems

In experiments on alpha-particle scattering it has been customary to use very crude angular resolution, the observations frequently covering a zone of 20° or more. In the present experiment ample primary intensity was available and corresponding resolution could be obtained. The angular resolution of our slit systems was approximately 2°. The details of the diaphragms and slits are shown in Fig. 4. The terms "central zone" and "extreme limits" used in Fig. 4 to describe the angular definition may be understood by reference to Fig. 5. To make clear the fact that scattering from the whole diameter of the primary beam is observable in the ionization chamber the "plan" of the detector slit system, viewed from the direction of the primary beam when set for a scattering angle of 90°, is shown in Fig. 6.

The mounting of the slit systems to insure that the axis of rotation of the ground joint is perpendicular to the beam and to the detector slits, and furthermore intersected by the axis of the detector slit system, is a matter of importance when angular measurements with an accuracy of one-fifth degree become necessary or desirable, as is the case for proton scattering at 15° or less. A new scattering chamber designed for greater angular accuracy is now under construction, but it seems likely that in this original apparatus the requirements of perpendicularity must have been met within at least 1° or 2°. The intersection of the axes of the ground joint, primary beam diaphragms and detector slits was examined by the insertion of rods in the diaphragm and slit systems and the junction of the rods at the axis of rotation was watched while changing the "angle of scattering" through 90°. No appreciable error was visible, indicating that the axes intersected within perhaps ½ mm or better. The zero position of the angular scale was similarly checked by inspection. After considering second-order angular corrections of various kinds, we have concluded that except for possible errors contributing effectively to the zero error in the angular scale, this apparatus seems to have been essentially satisfactory in respect to angular measurements.

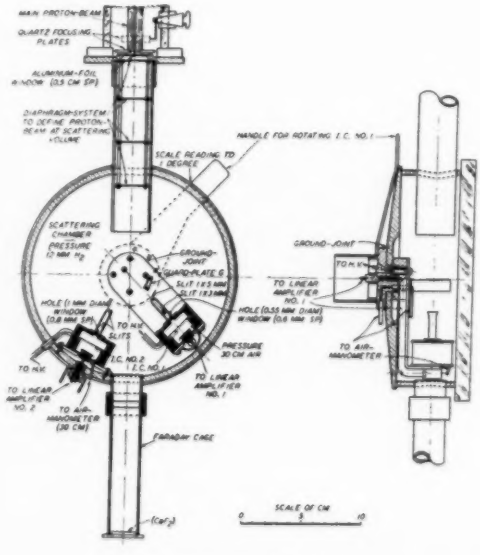

FIG. 2. Proton-scattering apparatus.

No special effort was made in the design to insure the accuracy of the "zero" of the scale for it appeared advisable in any case to eliminate the error from this cause by taking observations at both sides of the beam. However, in practice, early tests for protons scattered in the detecting chamber with a vacuum in the scattering chamber showed the presence of some multiply-scattered protons from slit edges of the diaphragm system at angles of 20° and less and caused us to insert the guard plate *G* shown in Fig. 4 (in the right-hand diagram the guard *G* appears as an unlabeled rectangle projecting into the scattering chamber). Since the presence of this plate precluded the possibility of observations on both sides of the beam, the second ionization chamber was also installed for use as a "current monitor" as will be discussed below.

A special series of observations to determine the zero might well have been taken after the measurements reported in this paper were completed, but by an oversight the assembly screws holding the ionization chamber and arm were removed and replaced before such observations were made, and careful examination showed that we could not be certain that the original setting for zero angle could be reproduced by such replacement with sufficient accuracy.

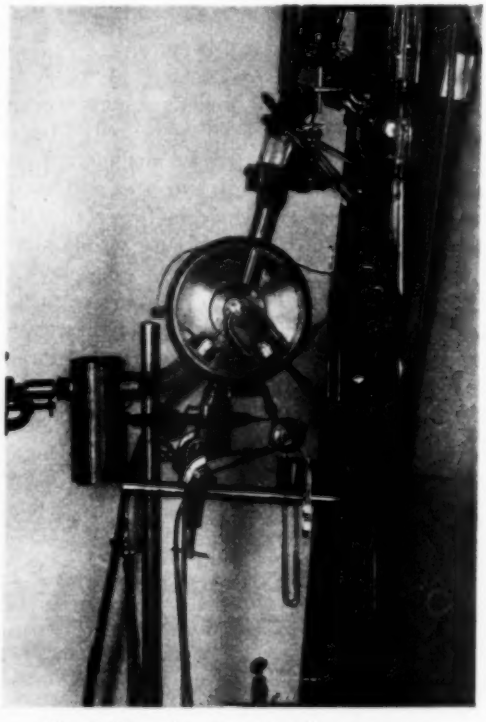

FIG. 3. View of proton-scattering apparatus.

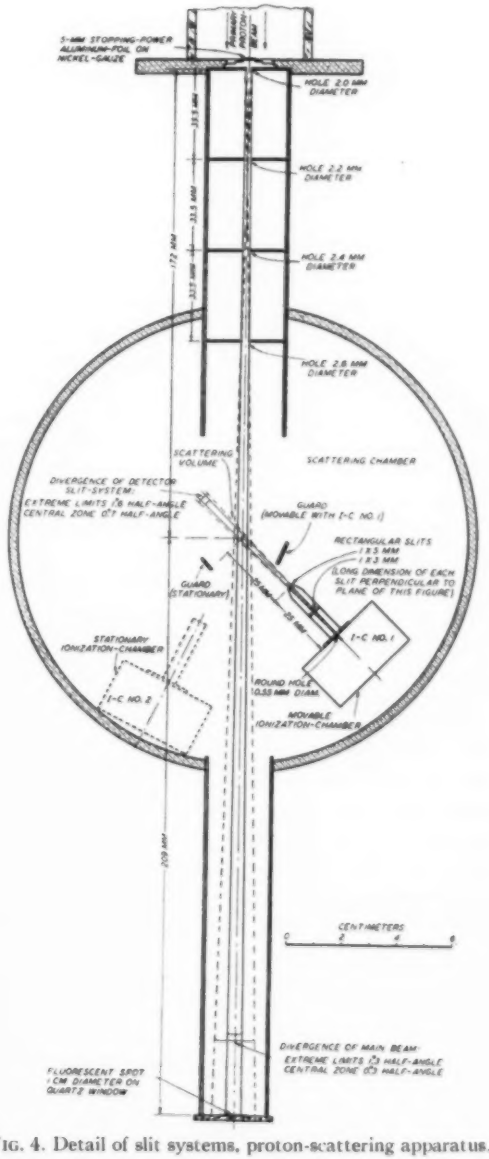
5-MM STOPPING-POWER ALUMINUM-FOIL ON NICKEL-GAUZE
HOLE 2.0 MM DIAMETER
HOLE 2.2 MM DIAMETER
HOLE 2.4 MM DIAMETER
HOLE 2.8 MM DIAMETER
SCATTERING VOLUME
SCATTERING CHAMBER
DIVERGENCE OF DETECTOR SLIT-SYSTEM: EXTREME LIMITS ½° HALF-ANGLE CENTRAL ZONE ¼° HALF-ANGLE
GUARD (MOVABLE WITH I-C NO. 1)
RECTANGULAR SLITS 1.5 MM 1.3 MM (LONG DIMENSION OF EACH SLIT PERPENDICULAR TO PLANE OF THIS FIGURE)
GUARD (STATIONARY)
I-C NO. 1
STATIONARY IONIZATION-CHAMBER
I-C NO. 2
ROUND HOLE 0.55 MM DIAM.
MOVABLE IONIZATION-CHAMBER
CENTIMETERS
DIVERGENCE OF MAIN BEAM: EXTREME LIMITS ½° HALF-ANGLE CENTRAL ZONE ¼° HALF-ANGLE
FLUORESCENT SPOT 1 CM DIAMETER ON QUARTZ WINDOW

FIG. 4. Detail of slit systems, proton-scattering apparatus.

The scattering gas

As may be seen from a consideration of the diagrams in Figs. 4 and 5, the actual gas target

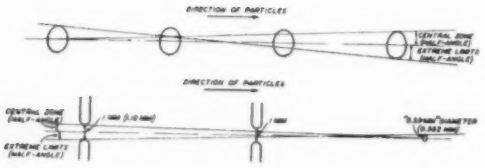

FIG. 5 (above). Diaphragm system—primary beam and (below) slits and diaphragm detecting chamber. These sketches are not drawn to scale.

which scatters protons into the detecting chamber is an odd shaped section of the path of the primary beam and its volume, as well as shape, depends on the angular setting of the detecting chamber. When the latter is at 90°, the scattering volume is a drum shaped section of the primary beam with its flat faces (not quite parallel) separated by about 2 mm. As the angle of observation is decreased toward 0° it is obvious that the principal effect is an increase in the thickness of the scattering volume (measured along the primary beam), which varies inversely with the sine of the angle of observation. As stated previously, the whole cross-sectional area of the primary beam is included in the solid angle subtended by the detector slit system, and the dimensions of the latter along the beam, by determining the thickness of the target volume, determines the number of target atoms which scatter toward the small hole in the detecting chamber. Hence to obtain the number of scattered protons to be expected at any angle on the basis of Mott's formula we have taken for the target volume at the angle θ the target volume at 90° divided by $\sin\theta$, neglecting all other corrections as of the second order and unimportant. The solid angle subtended by the detector is obviously independent of the rectangular slits and depends on the round hole in the detecting chamber only, but the size of this hole and the short dimension of the 1 mm by 5 mm detector slit together determine the scattering volume.

The actual pressure of hydrogen gas used in all of our experiments to date has been 12.0 mm, measured by a small mercury manometer with an accuracy probably not much better than five percent. The manometer was connected to the scattering chamber through a U-tube immersed in a slush of solid CO_2 and alcohol. As each series of observations is made on a separate filling of hydrogen the error in the pressure measurement should average out to within several percent over a number of runs at one voltage. The number of target nuclei was computed for a temperature of 20°C and no temperature corrections were made, the temperature of our basement observing laboratory being within about 3°C of this value at all times during the observations.

That multiple scattering in the gas may be neglected is apparent from the fact that taking account of all of the small angle deflections at this pressure in a path length of 10 cm above the scattering volume, by calculation a scattering through 2.5° followed by a second deflection of 17.5° would account for only one in 2000 of the protons observed at 20°. For higher values of these angles the multiple scattering correction becomes rapidly even less. Upper limits for the values of these corrections have been estimated from the Rutherford-Darwin scattering values for an energy of 500 kv. The total number of protons scattered or recoiling from the scattering volume under observation through all angles above 15° (to 75°) is approximately one in 10^6 at 800 kv, the actual number observed at 45° being about 10^{-11} of the original beam.

The purity of the hydrogen used to fill the scattering chamber is of obvious importance, and tests for contaminations will be described below. For filling the chamber we used a palladium tube immersed in a bulb of tank hydrogen and heated by radiation from a nearby coil of resistance wire to perhaps 300°C (far below any visible glow). The U-tube of the manometer, cooled to CO_2 temperature for at least an hour in advance of any measurements, insured against mercury or other local vapors, and a "thermocouple Pirani-gauge," connected to the scattering volume and capable of detecting a few thousandths of a

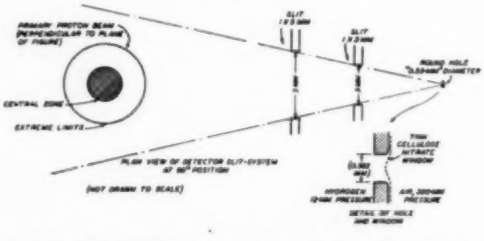

FIG. 6. Detector slit system as viewed along primary beam when set for scattering angle of 90°.

millimeter pressure, showed no appreciable development of pressure in the scattering chamber when pumped out to a high vacuum and left disconnected from the pumps for some hours. A manometer indicating the pressure of air in the ionization chambers showed no appreciable change over a period of several weeks, indicating that the thin windows did not leak.

Since the final result of our experiments is a series of ratios of absolute values, for different voltages and angles, the observed numbers of scattered particles divided by expected numbers predicted by Mott's formula, without any reference value to which the results may be "normalized" or by which these ratios may be checked, it is highly important at every point to guard against slips or omissions which will affect the absolute values of either the expected Mott numbers or the observed numbers of scattered particles. Consequently separate and independent calculations were made by four individuals for the number of scattered protons to be expected on the basis of Mott's formula for the dimensions of apparatus given in Fig. 4, each making a separate estimate of the corrections to be applied for the peculiar solid angle situation arising from the round-and-square combination of the detector slit system. These calculations agreed within one-half percent in giving a value of 464 scattered and recoil protons (indistinguishable) per minute per microampere into the detecting chamber, for a primary proton beam energy of 1000 kv and an angle of 45°, including the correction $1/\sin\theta$ for variation of target volume with angle. This number is for a hydrogen pressure of 12 mm at 20°C. Accurate measurements of the exact dimensions of the detector slit system were intentionally postponed until all other observations were completed. Hence throughout our work, and in all of the curves and comparisons in this paper except Table II and the final curves (see Fig. 15), the value 464 given above was taken as the "Mott standard."

The number of protons in the primary beam

One of the major problems of the experiment was that of obtaining a sufficiently accurate measurement at all times of the number of protons per second which pass through the scattering volume as the primary beam, a quantity which obviously affects in direct ratio the absolute value which is arrived at as the "observed scattering" and which must be compared finally to another absolute value calculated from Mott's formula. To eliminate a suspected source of error the Faraday cage at the bottom of Fig. 2 was increased to 60 cm length. However, this deep Faraday cage beyond the scattering volume is obviously useless when the apparatus is filled with hydrogen for scattering observations, since each proton in the main beam produces about 20 ion pairs per mm path in the gas, and the collection of a small percentage of these ions, due to contact potentials or other stray effect, gives rise to enormous errors in the current measurement (observed currents under these conditions were actually -10 to $+20$ times the known current in the beam).

Although a better method undoubtedly can be achieved later for measuring the proton current continuously in these experiments, we have made use of the known constancy of our experimental conditions and obtained our proton beam current values as follows: The equipment was first operated at the desired voltage and current for half an hour to attain maximum steadiness, then a current measurement was made by means of the Faraday cage with a high vacuum in the scattering chamber, then the chamber was filled with hydrogen and scattering observations were made at the various angles; finally the scattering chamber was pumped out again to a high vacuum and the measurement of "vacuum current" was repeated. If the latter failed to agree with the current measured at the start within the necessary limits the whole "run" was discarded. Each "run" required from 50 to 80 minutes, usually not over 60 minutes. During all of our final "runs" only one or two were discarded from this cause, however, as more or less continuous check on the current was obtained by using the 20° scattering as a "monitor" position, repeated after every one or two observations at any other angle. Any abrupt change in the 20°-value called our attention to trouble, and stopped the run. This happened once or twice by reason of trouble in the amplifier or ion source circuits. A progressive change up to say 15 percent between initial and final "vacuum currents" was permissible because the monitor readings (at 20°)

made the necessary correction possible to within the desired accuracy of say three percent for single observations. A further check on the constancy of the current was obtained by measuring the total proton current striking the aluminum foil window above the 2-mm beam diaphragm. This current was very steady but of course took no account of the lack of perfectly uniform current density in the diffused spot, which moved slightly on account of various causes, including changes in temperature of the deflecting magnet. The whole apparatus shown in Fig. 2 was insulated from ground and at the bottom of a deep Faraday cage to permit this measurement. A much better arrangement would have been to have selected by a preceding diaphragm system a portion, roughly 3 mm in diameter, of the diffuse spot above the aluminum foil window centered on the 2-mm diaphragm beneath, for this "total current monitor." The beam currents in various runs were set as desired for suitable numbers of counts (depending on voltage and on the range of angle in which greatest accuracy was desired in a particular run), and ranged from 0.005 to 0.03 microampere. These Faraday cage currents were measured on a sensitive galvanometer permanently mounted and calibrated at various scale values at frequent intervals during the weeks of observation. The calibrations of the galvanometer were made with two completely different sets of resistances and Weston voltmeters which agreed within one percent.

The chief objection to our current measurements arises from the presence during some of the days of an erratic changing of the current through a range as large as 10 or even 15 percent with steady periods of one-half to two minutes between shifts. With this happening we endeavored to obtain average values by observing counts and currents during periods of many minutes. Another circumstance required the discarding of a few of our values for the "final vacuum current." This was the fact that the scattering chamber was evacuated at the end of a "run" by means of a Hyvac pump, the final pumping to a high vacuum being done by opening a cock to the main tube (above the aluminum foil window). If this cock was opened too hurriedly a burst of hydrogen would be let into the high voltage tube while operating, with a resultant disturbance of the steady conditions which sometimes altered the current into the scattering apparatus by 50 percent, an actual shift or other effect on the focal spot being visible. The readings of the monitor at 20° allowed the "initial vacuum current" to be used for computing these runs.

As described below, we finally chose to reduce the effect of the uncertainty of our current values by making a considerable number of independent runs at such voltages taking the averages of scattering values (Mott ratios) obtained as the true value, with the fluctuations among all observations giving some criterion of the errors arising from all nonsystematic causes.

Velocity of the protons at the scattering volume

Since the theoretical scattering varies inversely as the square of the energy a small systematic error in the voltage measurements might easily give rise to a small apparent but false anomaly or, given a true anomaly of considerable magnitude such as we have found, might cause a specious variation of the observed anomaly with voltage in a way which might be very confusing in any theoretical analysis of the results. This was one of the reasons for the development of the 10,000-megohm voltmeter resistor, use of which gave a direct measurement (to two percent, differences to one percent) of the energy of the primary protons striking the aluminum foil window of the scattering chamber. This foil was estimated by weight to have a stopping power of 5-mm air equivalent. As a check on this thickness a calcium fluoride crystal was placed at the bottom of the Faraday cage (see Fig. 4) and with a vacuum in the scattering chamber the tube voltage was measured which gave the protons sufficient energy to excite the known fluorine gamma-ray resonances (890 and 940 kv) after passing through the aluminum window. At the voltages of these resonances the stopping power of the window was found to correspond to 5-mm air equivalent. At the usual pressure of 12.0 mm, the loss in range (energy) of the primary beam in passing through the hydrogen between the window and the scattering volume under observation was 0.5-mm air equivalent by calculation from ordinary stopping power values. To obtain

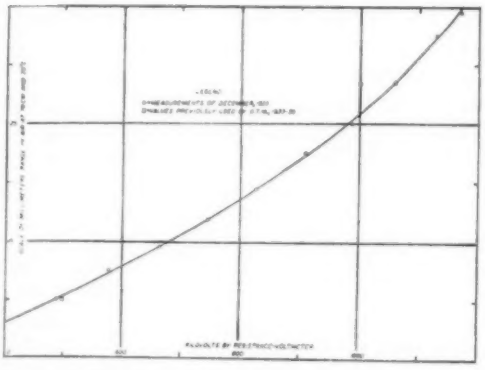

FIG. 7. Visual range curve for proton beam in air.

the actual energy of the protons at the scattering volume the slight differences between aluminum, hydrogen, and air in the rate of variation of proton range with voltage were neglected (obviously trivial) and the constant value of 5.5 mm was subtracted from the range of protons at the actual measured voltage to give the range, and hence the voltage, of the protons at the scattering volume. For making this correction it was sufficiently accurate to use our own curve for the "visual range" of protons as a function of voltage, shown in Fig. 7. This curve was obtained with the 10,000-megohm voltmeter resistor, and is based on the visually estimated range in air of the direct proton beam passing out from the tube through a copper-foil window, correction for which was made by inserting duplicate copper foils and noting the decreased visual range. It is possible that the proton range measured in this way exceeds by one or two mm the "extrapolated range" customarily meant in range measurements, but this should not give rise to any serious error in our estimates of the proton energy at the scattering volume.

Counting the scattered particles

To avoid ambiguity or misidentification of the particles entering the observing chamber, a linear amplifier was used for detection, with continuous monitoring of the counted particles by means of a cathode-ray oscillograph. A considerable restriction of the range of voltage and of higher angles over which scattering observations could be made arose from the use of this detector, since the scattered protons were required to have a definite and rather large residual range after collision or they would not be counted. The linear amplifier operates under a serious handicap with this apparatus because of the large electrical capacity of the connection from the ionization chamber through the rotating ground joint to the input grid. This wire gave trouble at first from mechanical vibration (which was electrically reproduced by the amplifier) and had to be surrounded by ceresin throughout its long shielding tube down the rotating arm and out through the ground joint. The high voltage lead to the chamber had to be similarly shielded by a grounded metal tube to prevent a glow discharge in the low pressure gas in the scattering chamber. Similarly the high voltage electrode of the chamber had to be entirely enclosed inside the grounded sheath containing the window (see Fig. 2). With its usual ionization chamber this linear amplifier will record moderately fast protons with a chamber depth of only two mm, whereas the lower limit for satisfactory recording with this scattering chamber has been found both by variation of angle and of voltage to be 7.4 mm (normal air) residual range for slow protons. The ionization chamber, 15 mm deep, was filled with air to a pressure of about 30 cm. The window covering the hole in the ionization chamber, to keep this air from the scattering chamber, was made by dropping collodion on a water surface. These films were found by a rough interferometer measurement to have a stopping power of 0.6 to 1.0 mm, and accordingly the slight bulge of the window into the hole due to the air pressure (see Fig. 6) made no appreciable difference in the counting as might be feared by reason of the particles traveling through the window thickness at an angle less than 90° near the edges of the hole. The lower limit of proton range to which the amplifier will respond reliably is of particular importance in connection with the expected symmetry of proton-proton scattering about 45° and will be discussed below.

The actual counting of the particles was carried out by a scale-of-eight thyratron circuit (Wynn-Williams) which had previously been used with the same linear amplifier and had been tested for missing at high speeds and other features during extended quantitative observations on the alpha-

particle excitation function of lithium, and numerous other less exact investigations.

It would have been a great relief to have had a check on the absolute value features of our results by making observations on the scattering of protons by some gas which could be relied on to show no anomaly at these voltages, just as the gold foils were used in the classical alpha-particle experiments. Bromine or iodine might serve if the chamber were properly designed, but problems of purification and the necessity for an atomic number of uncertain but considerable magnitude to avoid a possible anomaly seem to eliminate nearly all other gases except possibly argon. Due to difficulties in accurately measuring the small number of scattering atoms of high atomic number which would be required, no metal foil substitute for a gas target seems feasible. In the face of the difficulties which arise when such an absolute value calibration by a heavy atom target is attempted we decided that our results would be more reliable if we made in the first experiments a straightforward absolute comparison with Mott's formula which depended on slit dimensions, gas pressure, and proton current measurements.

(D) Preliminary Survey Observations

As usual, the first month of observations was spent in eliminating troubles and reducing the errors from various causes which were found to be important. By the beginning of February, 1936, it seemed definitely necessary to conclude that the counts differed from our expectations on Mott's formula in their variation with angle and with voltage as well as in absolute magnitude. Accordingly we undertook to make a preliminary survey over the range of voltage available, to indicate the magnitude of the deviations found within an error of perhaps 20 percent.

Two sets of curves were obtained, one involving observations at arbitrary fixed voltages varying from 625 to 981 kv (at the scattering volume) and a second set attempting to obtain the variation in counts at fixed angles as the voltage was changed. The latter was very difficult, or rather unreliable, due to the small but important changes in the target current and target spot area with voltage (the deflecting magnet naturally requires a different setting for each voltage) even though the focus controls were left unaltered or so changed as to duplicate the same appearance of spot at each voltage. These curves were taken during a period of about two weeks and are shown in Figs. 8 and 9. Fresh hydrogen was used for each curve, sometimes several different fillings being used for different points or portions of a curve. Some of the measurements made were discarded because of current measurement troubles. Among the fixed voltage curves of Fig. 8, the curve for 696 kv was considered as definitely too low, other separate observations so indicating as well as the variable voltage data of Fig. 9. The curve for 981 kv was based on only the four observations shown and was included primarily for "inspection purposes" as the voltage could be held steadily at this value (actual tube voltage about 1100 kv) during only 15 minutes on a single day. However, the data of Fig. 9 for fixed angles, taken independently from the data on Fig. 8 and much of it only one or two points per filling of hydrogen (several points per day), seemed to check reasonably enough for the purposes of a survey demonstrating the existence of an anomaly. The dotted portions of the curves of Fig. 9 are filled in from the data of Fig. 8, indicating this agreement. A comparison of these data also was made with the results of White as shown in Fig. 10.

These survey data, in the form of Figs. 8 and 9, were sent to Professor Breit, then at the Institute for Advanced Study at Princeton, February 15, 1936. Professor Breit and Professor Condon had already calculated the various numerical tables for the computation of the phase shifts and the expected deviations from Mott's formulas using different assumed potential distributions to represent a proton-proton interaction, and they promptly informed us of the theoretical possibilities by which our observed results might be accounted for at different voltages. Their theoretical analysis showed that a potential smaller than the "^1S neutron-proton potential" did not account for the observed anomaly unless the magnitude of the potential was varied with the incident proton energy. In view of the possible importance of such a conclusion, as well as the desirability of not causing unnecessary confusion, it was decided to postpone detailed publication

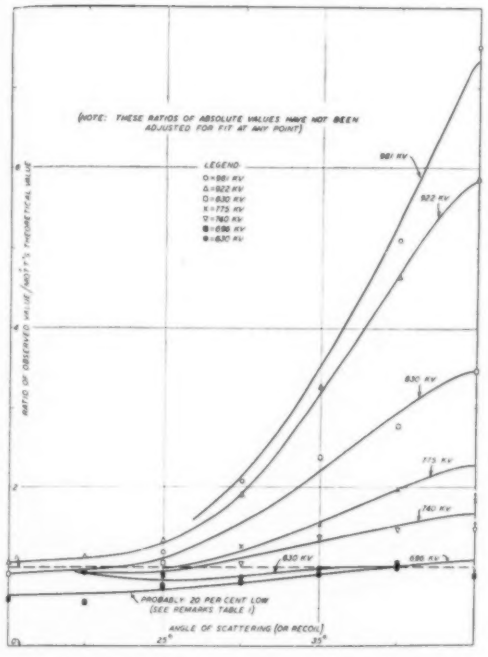
(NOTE: THESE RATIOS OF ABSOLUTE VALUES HAVE NOT BEEN ADJUSTED FOR FIT AT ANY POINT)
LEGEND:
981 KV
922 KV
830 KV
775 KV
740 KV
630 KV
PROBABLY 20 PER CENT LOW (SEE REMARKS TABLE I)
ANGLE OF SCATTERING (OR RECOIL)

FIG. 8. Scattering of protons by protons for constant voltages at different angles [preliminary survey].

until possible errors could be ascertained by an extensive repetition of the experiments. These survey observations essentially comprised only a single curve for each voltage, and weighty conclusions regarding the success or failure of representing the proton-proton interaction by a potential function seemed premature. Our observations taken since and reported at the April meeting of the Physical Society have confirmed the magnitude of the interaction potential obtained in the above preliminary survey almost exactly for 800 kv. The unaccountable variation with the voltage of the incident protons disappeared when the data from numerous runs at each voltage were averaged, as reported below.

In response to several requests for these preliminary data on the part of other theoretical physicists working on mass defects and other problems involving an assumed proton-proton interaction, however, we sent copies of these two sets of survey curves March 18, 1936, to those interested, accompanied by a memorandum written by Professors Breit and Condon giving the results of their calculations using exact theoretical equations and the conclusions to be drawn from these data as to the magnitude of the interaction potential indicated if later experimental results removed the disturbing variation of the interaction potential with voltage. This material reached Professor Bethe just in time to be discussed by him in his excellent paper in the April issue of the *Reviews of Modern Physics*, where he presents an essentially similar, although approximate, theoretical treatment.

(E) Search for Errors Arising from Contaminations or Other Causes

It is to a considerable extent a dangerous procedure to ascribe an apparent anomaly, that is, an observation of excess scattering at high angles, to an actual deviation of the proton-proton forces from the Coulomb law, since nearly every conceivable error in any scattering experiment leads to the expectation of an excess of counts at high angles, where the scattered particles should be relatively few. Furthermore, as mentioned above, it has been known for many years that protons of 400-kv energy colliding with other protons at rest must approach, on a Coulomb calculation, within a distance which is smaller than the distance for which the collisions of alpha-particles with protons already show an anomaly. This same approximate distance for the radius of action of non-Coulombian forces has been assumed from the first in all calculations of nuclear mass defects, so that the appearance of

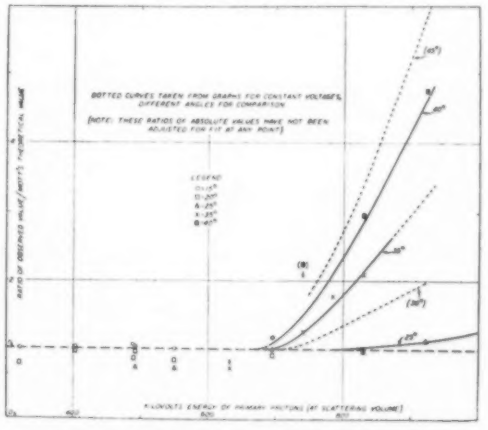
DOTTED CURVES TAKEN FROM GRAPHS FOR CONSTANT VOLTAGES, DIFFERENT ANGLES FOR COMPARISON
(NOTE: THESE RATIOS OF ABSOLUTE VALUES HAVE NOT BEEN ADJUSTED FOR FIT AT ANY POINT)
LEGEND

FIG. 9. Scattering of protons by protons for constant angles and different voltages [preliminary survey].

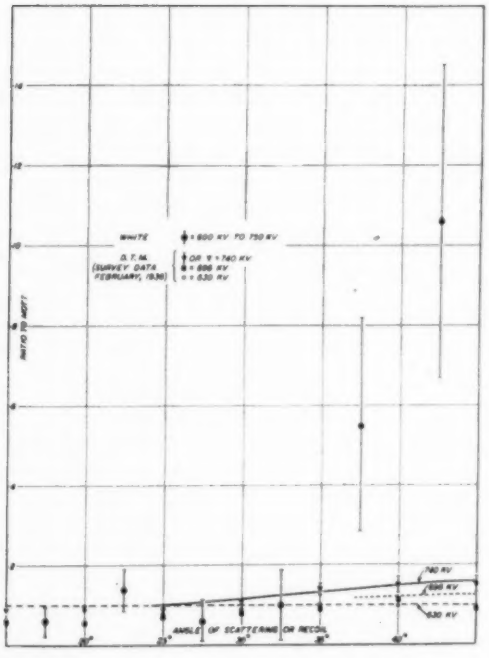

FIG. 10. Proton-proton scattering, comparison with White.

excess scattering at large angles, above 400 kv, simply indicating the existence of nuclear forces within this distance of approach which are considerably larger than the Coulomb repulsion, may make the observer unduly prone to accept such a result at face value. In view of this situation we spent the period from early February until the middle of April endeavoring to "break down" the results of our survey, to see whether the apparent anomaly might be explained in terms of an unsuspected contamination, multiple scattering, or other spurious cause.

The use of the linear amplifier as the detecting device removes at once a number of possible suspicions regarding our results, since the verification of the identity of the counted particles as protons, and also the measurement of their energy as the correct energy for primary protons which have lost approximately half of their initial energy in being scattered to about 45° by another proton, insures against counting, for example, any large number of protons which have been scattered by some heavier contamination. Such protons would retain nearly their entire primary energy and accordingly could be counted out to very high angles. Actually, for the highest voltage with which we have worked (900 kv) the amplifier is missing some of the counts at 50°, and counts no particles at all above 60° (fewer than five percent of 45° count). This observation alone puts certain limits on the number of scattered protons which might be due to the presence of a gas contamination of high atomic number, even though counts from such a cause do change rapidly with angle [varying as $Z^2 \operatorname{cosec}^4 (\theta/2)$].

To check on the possibility that an unknown vapor of condensible gas, such as an organic vapor, CO_2, or a trace of H_2O, might be present in the scattering chamber, several runs were made both with hydrogen and with a vacuum in the chamber during which the usual CO_2 slush on the mercury trap was replaced by liquid air. No differences from our usual results with CO_2 cooling were observed.

The possibility of multiple scattering in the hydrogen itself being responsible for the increased high angle counts was discussed and dismissed in an earlier section.

That the agent responsible for the observed anomaly could hardly be a frequent but "accidental" contamination of any kind, which should fluctuate in percentage in different runs or with length of time the scattering chamber had been filled before the observations were taken or otherwise show itself in the form of large fluctuations in the observed Mott ratios, seemed eliminated by the general consistency of our observations. The nonsystematic contamination of this kind which seemed reasonably possible was air, and accordingly observations with the same apparatus were made on the scattering of protons by air. Similarly, the only systematic contaminations which might be introduced while the scattering chamber was being filled through the palladium tube (other than vapors eliminated as above) seemed to be deuterium (a known contamination to something under one part in 1000) and possibly helium. Accordingly these gases were also investigated with the same apparatus.

For convenience in understanding the interpretation of the measurements on deuterium, helium, and air let us refer briefly to the hydrogen

anomaly itself. Fig. 11 shows on a direct scale of counts *versus* angle (not Mott ratios as in Figs. 8 and 9) the magnitude of the anomaly to be explained. It is to be noted that at 15° the predicted Mott value (these counts all involve the $(1/\sin\theta)$-correction for change of scattering volume with angle) is only slightly below the Rutherford-Darwin ("classical") value, while the observed counts are lowest of all three. At 30° the observed counts lie between the Mott and the Rutherford-Darwin predictions, while at 45° the Mott, Rutherford-Darwin, and observed values are in the ratio 1 to 2 to 3. (These observed values are our averaged values for 800 kv.) Referring to Fig. 12, it is now seen that such an anomaly could not be produced by a contamination of the hydrogen by any one of the three suspected gases. If either helium or air gave rise to the anomaly at 45° they would correspondingly give such an anomaly at all lower angles since their observed variation with angle so nearly corresponds to the variation predicted for hydrogen by the Mott formula and indeed at 15° the observed counts should be higher than the Mott value by a factor of 3, instead of the observed counts of only 80 percent of the Mott values. It may be pointed out that the possibility that the observed anomaly might be ascribed to an error in the absolute value calibrations can be eliminated by a similar argument. The actual scattering observations with helium and air were made at arbitrarily higher pressures (just sufficient to be read feasibly on the manometer) and the number of counts reduced to correspond to the pressures shown in the left-hand box of Fig. 12 in order to bring the curves close together for comparison. The right-hand box gives the ratio of the observed counts for each gas at 12-mm pressure and 45° to the number of counts predicted by Mott's formula for pure hydrogen at the same pressure and angle, to give an indication of the amount of contaminating gas required to give the anomaly observed in the 45° counts.

The shape of the curve for the scattering of protons by 99 percent deuterium (similarly fed in through the palladium tube) is roughly that required to explain the observed hydrogen anomaly. However, the ratio of absolute magnitudes is such that about one-fifth of our tank hydrogen after passing through the palladium would have to be deuterium to explain the anomaly! Even allowing for the known fractionation factor due to passage through (relatively cold) palladium we must consider this unreasonable by a factor of at least 1000 (and a still larger factor if our tank hydrogen was electrolytic, as was probable).

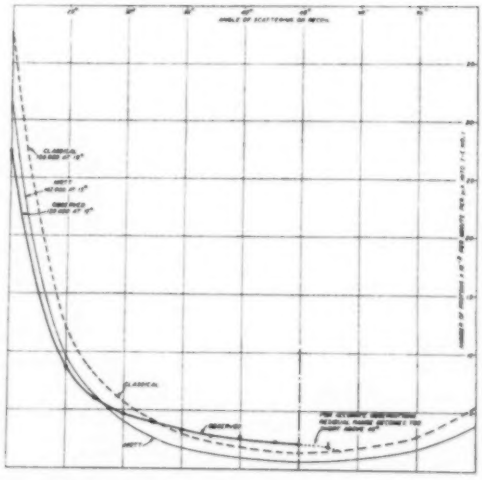

FIG. 11. Scattering of protons by protons at 800 kv, actual numbers of scattered particles as a function of angle.

Because of its possible usefulness in connection with other problems such as that of proton-neutron interaction we show in Fig. 13 the results of our two separate sets of observations on the scattering of protons by deuterons. It must be remembered in this case that at any one angle there are two groups of detectable particles, the scattered protons and the recoil deuterons (heavier recoil nuclei such as helium or nitrogen do not acquire sufficient energy to penetrate the ionization chamber window and give a detectable amplifier-pulse). Thus at 30° we may observe the protons scattered through an angle of 30° and the recoil deuterons resulting from protons which have been scattered through 90°. As the latter travel slower than protons for a given residual kinetic energy they give rise to larger kicks than those due to protons, which have exactly twice as sharply peaked a maximum in the curve for ionization per mm path against residual range. The two groups of kicks are easily distinguishable, in fact very obviously, on the cathode-ray screen. In recording, the bias of the thyratrons is

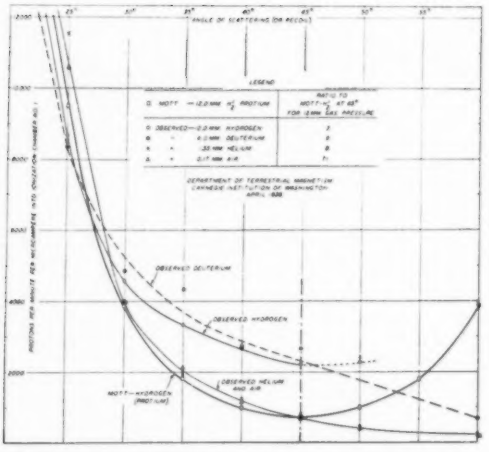

FIG. 12. Proton scattering in various gases, absolute values 800 kv.

set first to count all the particles and second to count only the large kicks, due to the recoil deuterons. The latter counts at various angles such as 15°, 20°, 25°, etc., serve to define the numbers of protons scattered through corresponding large angles (126°, 112°, 100°, etc.) and, again by subtraction of the deuteron counts, the proton scattering alone is obtained out to the point where the protons have lost too much energy to be accurately recorded further (about 50°; less proton energy is lost to a deuteron than in a proton-proton collision). The two sections of the curve so obtained are shown as curve *A* of Fig. 13, with the dots and circles indicating the agreement between the two separate days' observations. The ratio of the observed scattering to that predicted by the Rutherford-Darwin formula is shown as curve *B*.

(F) Results Based on Averages of Many Independent Observations

Having reached the conclusion that the excess scattering at high angles observed in the preliminary experiments did not arise from a contamination or other spurious cause, we were faced with the choice of interrupting the observations to build an apparatus capable of better observations than were obtained in our preliminary survey, or of continuing the observations with the original apparatus in the expectation that the errors involved were mainly statistical and could be reduced by an averaging process. The current changes, of the order of 15 percent, showed no systematic trend. Largely because of the important divergence from current theory indicated by the variation with voltage in our survey observations we chose the latter alternative.

Clearly the least satisfying element in the measurements was that of the proton current passing through the scattering volume. To reduce errors from this cause steps were taken to provide the second ionization chamber with its associated amplifier and thyratron counter, to serve as a "current monitor." Pending completion of this apparatus observations were continued as before but with the additional precaution that observations at 20° were frequently interspersed between

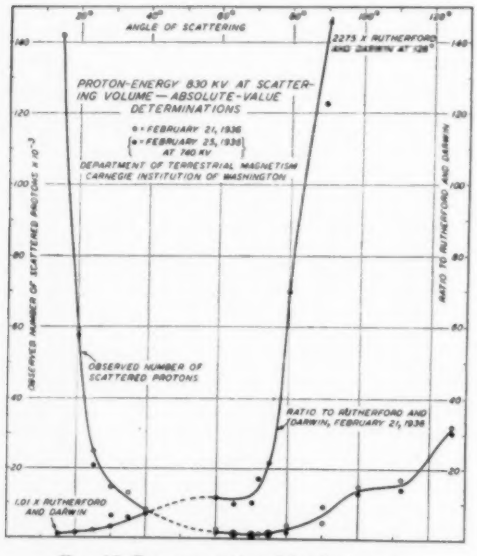
ANGLE OF SCATTERING
PROTON-ENERGY 830 KV AT SCATTERING VOLUME — ABSOLUTE-VALUE DETERMINATIONS
○ = FEBRUARY 21, 1936
● = FEBRUARY 25, 1936
AT 780 KV.
DEPARTMENT OF TERRESTRIAL MAGNETISM
CARNEGIE INSTITUTION OF WASHINGTON
2275 × RUTHERFORD AND DARWIN AT 126°
OBSERVED NUMBER OF SCATTERED PROTONS
RATIO TO RUTHERFORD AND DARWIN, FEBRUARY 21, 1936
1.01 × RUTHERFORD AND DARWIN
OBSERVED NUMBER OF SCATTERED PROTONS × 10⁻³
RATIO TO RUTHERFORD AND DARWIN

FIG. 13. Protons scattered by deuterons.

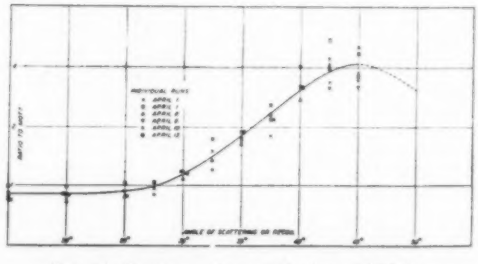

FIG. 14. Proton-proton scattering at 800 kv.

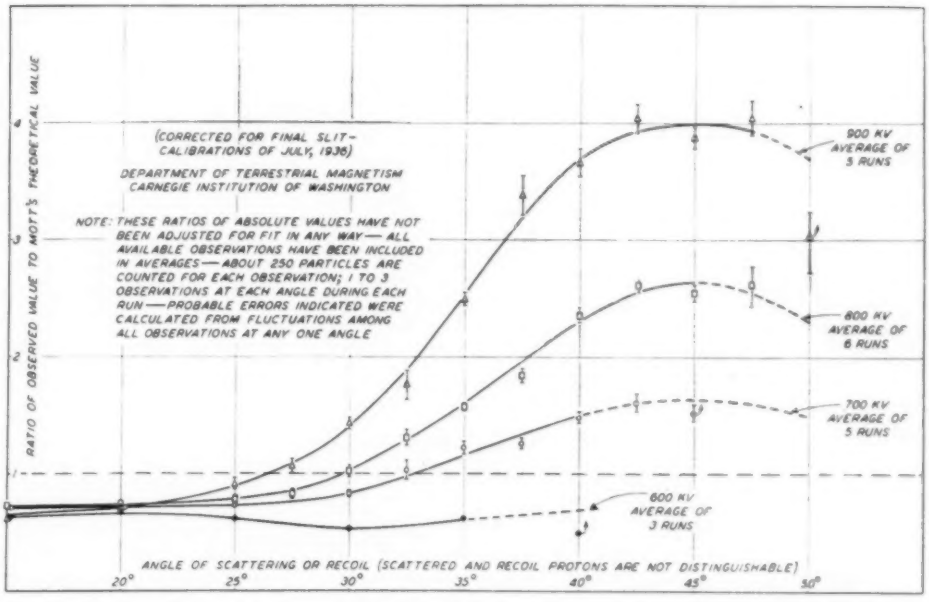
RATIO OF OBSERVED VALUE TO MOTT'S THEORETICAL VALUE
(CORRECTED FOR FINAL SLIT-CALIBRATIONS OF JULY, 1936)
DEPARTMENT OF TERRESTRIAL MAGNETISM
CARNEGIE INSTITUTION OF WASHINGTON
NOTE: THESE RATIOS OF ABSOLUTE VALUES HAVE NOT BEEN ADJUSTED FOR FIT IN ANY WAY — ALL AVAILABLE OBSERVATIONS HAVE BEEN INCLUDED IN AVERAGES — ABOUT 250 PARTICLES ARE COUNTED FOR EACH OBSERVATION; 1 TO 3 OBSERVATIONS AT EACH ANGLE DURING EACH RUN — PROBABLE ERRORS INDICATED WERE CALCULATED FROM FLUCTUATIONS AMONG ALL OBSERVATIONS AT ANY ONE ANGLE
900 KV AVERAGE OF 5 RUNS
800 KV AVERAGE OF 6 RUNS
700 KV AVERAGE OF 5 RUNS
600 KV AVERAGE OF 3 RUNS
ANGLE OF SCATTERING OR RECOIL (SCATTERED AND RECOIL PROTONS ARE NOT DISTINGUISHABLE)
20° 25° 30° 35° 40° 45° 50°

FIG. 15. Proton-proton scattering, curves obtained by averaging numerous independent observations at each angle for various voltages.

the observations at other angles in order to serve as a measure of the current variations. Fig. 14 shows a typical set of observations as obtained in this way involving six individual runs with independent fillings of hydrogen. Because of minor troubles with the second amplifier and "scale-of-eight" thyratron counter, observations at several voltages were completed before the "current monitor" was ready for use. The collected data for all the runs with the individual points averaged for each voltage is given in Fig. 15. The over-all error in the final Mott ratios, as indicated by the probable error calculated from the spread of all of the individual observations (shown by vertical bars through the points of Fig. 15) is two or three times the error to be expected from the number of counts alone and may be ascribed to current-fluctuations. Table II gives the data incorporated in these curves. Fig. 15 itself contains all essential information, although, in view of the fact that these results are much more nearly in agreement with a simple form of scattering theory than were our early survey results, it is not out of place to emphasize that *no selection of data has been made* for these final curves, all observations taken after April 15, 1936 (end of contamination studies) being included except for one or two cases where a breakdown interrupted a run. With the exception of the 700- and 600-kv curves of Fig. 15 and the final calibration of the detector slit system (see below) all of the data contained in this paper were presented and discussed at the Washington meeting of the Physical Society and at the Gibson Island (John Hopkins) and Ithaca (Cornell) conferences.

One particular feature of our curves disturbed us from the first, namely, an apparent lack of symmetry about 45°. Since this might constitute the best kind of evidence for a contamination of higher atomic number we examined carefully whether the discrepancy might arise from the rapid decrease in energy of the scattered (and recoil) protons above 45°. In checking over all of our numerical values before publication it was discovered, however, that most of the apparent dissymmetry in our curves was due to an error. The Mott values were originally calculated to 45° only and when it became obvious during the observations that the expected symmetry about 45° should be examined, the Mott numbers for 42.5° and 40° were taken offhand as applicable

TABLE II. *Summary of final averaged data.* The Mott values represent the numbers of protons per minute per microampere expected on the basis of Mott's formula to be scattered into ionization chamber 1 when pure H_2^1 at 12-mm pressure 20°C occupies the scattering volume; the Mott ratio is the observed counting rate divded by the Mott value; the probable errors are calculated from the spread of individual Mott ratios observed; the total number of observed counts, irrespective of rate, is given for each point as an indication of its statistical reliability.

Voltage	No. of runs	Item	Angle											
			15°	20°	25°	27.5°	30°	32.5°	35°	37.5°	40°	42.5°	45°	47.5°
kv														
900	5	Mott value	128700	28920	8570	5530	3530	2335	1610	1175	903	741	654	602
		Mott ratio	0.62	0.71	0.91	1.06	1.43	1.76	2.49	3.38	3.66	4.04	3.88	4.05
		Prob. error, ±	small	small	0.032	0.047	0.039	0.111	0.045	0.146	0.102	0.100	0.074	0.152
		Tot. obs. counts	2638	7640	880	408	1040	568	678	776	1488	1664	1152	648
800	6	Mott value	162700	36650	10850	7010	4470	2955	2036	1488	1143	939	828	762
		Mott ratio	0.73	0.73	0.78	0.83	1.02	1.31	1.57	1.84	2.36	2.59	2.55	2.62
		Prob. error, ±	0.018	0.016	0.028	0.029	0.042	0.066	0.023	0.043	0.049	0.048	0.054	..
		Tot. obs. counts	16360	7432	2104	1216	1248	920	1224	1432	1712	2208	1896	440
700	5	Mott value	212600	47780	14170	9170	5830	3860	2660	1942	1492	1224	1082	..
		Mott ratio	0.71	0.72	0.73	..	0.83	1.03	1.22	1.26	1.48	1.61	1.52	..
		Prob. error, ±	small	small	small	..	0.020	0.070	0.048	0.039	0.038	0.067	0.064	..
		Tot. obs. counts	3232	10800	992	..	1272	1000	1232	880	960	1432	936	..
600	3	Mott value	289200	65100	19270	..	7950	..	3620	..	2032	..	1473	..
		Mott ratio	0.64	0.68	0.61	..	0.53	..	0.61	..	0.57	..	..	..
		Prob. error, ±	small	small	0.020	..	0.017	..	0.027	..	0.114	..	..	..
		Tot. obs. counts	4904	7128	936	..	1776	..	664	..	28	..	..	..

for the symmetrical angles above 45°. Due to the motion of the center of mass of the two colliding protons the expected numbers of counts are not symmetrical, however. When this error was corrected the 47.5° values at 900 kv and 800 kv gave symmetry within the limits of experimental error, as shown in Fig. 15, although the value for 50° at 900 kv indicates that some counts are being missed, and from visual observation on the cathode-ray monitor the notation "missing counts" was recorded while this observation was being taken.

The data bearing on the angle at which counts begin to be missed by reason of having lost too much energy are shown in Fig. 16. A photographic record was made of the sizes of the deflections produced on the cathode-ray monitor by the scattered particles at various angles and at a voltage of 800 kv. At the same time a calibration was made to determine the cut-off point for the thyratrons, that is, the minimum size of deflection which would produce a count. Sizes of deflections are plotted to the right in Fig. 16. The left-hand margin corresponds to the zero position of the cathode-ray spot, and the shaded area corresponds to the zero noise of the amplifier, not as it looks on the photographic record, but defined by the maximum size of noise peak obtained during typical periods of two minutes, with the scattered particles prevented from entering the ionization chamber but with the high voltage and ion beam operating as usual. The frequency distributions of the sizes of the proton deflections recorded at the different angles are shown as the heavily shaded blocks. It is to be noted that at 40° the protons already are slowed down until their residual range just extends across the ionization chamber, giving the maximum size of kick. At 45° they fall short of crossing the chamber and at 47.5° they are on the average only two-thirds as large (total deflection) as at 45° and appear to straggle somewhat more in size. Bearing in mind that the ionization chamber itself corresponds to a depth of about 6 mm and that the variation of the ionization power per millimeter of path against the residual range is approximately as shown in Fig. 16, it is clear that those scattered particles which have only slightly less than the average residual range at 47.5° or 50°, due to an expected (slight) straggling in the two windows, will abruptly fail to be counted. There is further to be considered

here the spread in energies of the scattered particles due to the finite angular resolution of the slit systems (about 2°) and the fact that a failure to count, say, ten percent of the protons makes a very obvious dissymmetry. On the basis of the measurements of Fig. 16 one may say that a minimum residual range of 7.8 mm (normal air), corresponding to 45° at 800 kv, is necessary for accurate counting. At 900 kv this minimum is reached for 48°. Thus the dissymmetry should not be expected at 900 kv, 47.5°, and a dissymmetry is not indicated by the measurement for this point. This same residual range corresponds to 41° at 700 kv and 36° at 600 kv, hence one may say that the 45°-value at 700 kv and even the 40°-value at 600 kv, are definitely low, as indicated on Fig. 15.

It may be noted that the curves of Fig. 14 (800-kv curve alone) and Fig. 15 (all four final curves) disagree due to a change in the scale of ordinates (Mott ratios). This is intentional and arises from the fact that the curve of Fig. 14 (800 kv alone) shows the original data as obtained and without correcting for the final slit calibrations. As mentioned under section C above, as an extra precaution against personal bias in accepting or rejecting observations during an experiment we have made it a practice to carry out only rough calibrations of the critical parts of an apparatus at first, reserving the final calibrations until after all other experimental observations have been completed. The final calibration of the detector slit system, which together with the absolute measurement of the proton current through the scattering volume, determines the Mott ratios which form the final result, was made early in July after dismantling this original scattering apparatus to replace it with a more accurate unit. The "1 by 5 mm slit" indicated in Fig. 4 was found to be 1.10 mm wide (high), thereby showing that the size of the scattering volume actually observed was ten percent greater than originally supposed. Furthermore, the "0.55-mm hole" into the detecting chamber (drilled with a No. 74 drill) was found to measure actually 0.562 mm, an increase in area of four percent. These calibrations were made in terms of arbitrary microscope scale-readings, again avoiding any possibility of bias (the theoretical predictions by this time being known). Thus our original figure (see Section C) of 464 counts per minute per microampere as the "Mott standard" should have been 14 percent greater. This reduced all of our original Mott ratios (provisional until the final slit calibrations) by a similar percentage, with the resulting final curves of Fig. 15. None of the other curves in this paper have been corrected for these final slit values, it should be remarked.

The possible effects of certain errors not already considered remain to be discussed, together with the directions in which we hope to improve and extend the experiments using a new apparatus now under construction.

One such item is the constancy of the calibration of our voltmeter. The latter was carefully calibrated and used when new for the accurate location of the lithium and fluorine resonances (2 months). During the proton scattering ob-

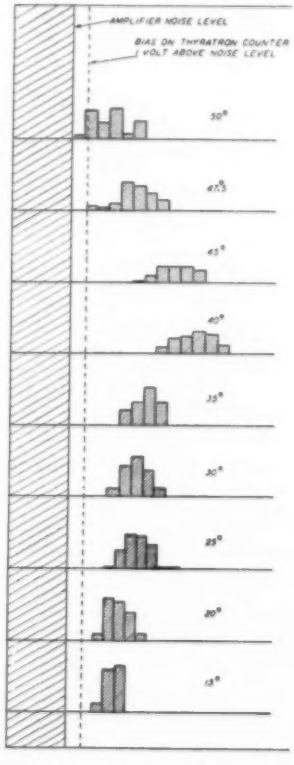

FIG. 16. Sizes of deflections produced by scattered particles entering ionization chamber at different angles of scattering. From photographic records using cathode-ray oscillograph. Proton-proton scattering 800 kv.

servations no check on the calibration was possible (only one target position was available on our apparatus until very recently). Although in May it was found that a "low voltage open circuit" had developed in the voltmeter (as measured using 100 volts), no other evidence of trouble was noticed. It is probable that one of the soldered joints between the 1000-ohm resistors broke open under the constant vibration of operation and the small meter-current easily bridged the gap with a voltage drop of five or ten kv. When the scattering apparatus was dismantled, the lithium evaporator was replaced and a new measurement made on the lithium resonance without any other changes and with the voltmeter still "defective." The 440-kv resonance in these measurements appeared at an apparent voltage of 435 ± 1 kv, thus showing that the voltmeter was indicating about one percent low, or possibly instead of a constant percentage error a nearly constant voltage error of five kv (low). This error is not large enough to affect any of our conclusions above.

The importance of a possible error as small as one-half degree in the zero position of the angular scale used with the movable scattering chamber was not fully realized until after the series of final runs at 900 to 600 kv had been completed and the scattering chamber taken down; the apparatus had been operated throughout this final series without opening it for regreasing the ground joint or any other purpose. Unfortunately, the arm carrying the ionization chamber was fastened to the core of the ground joint and to the ionization chamber itself by means of screws and without pins which would govern the precision of angles and positions in reassembly. Consequently, after once disturbing the instrument we were unable to reassemble it for a more accurate check on the zero position of the scale during our scattering measurements. The accuracy of setting at the individual angles for our measurements was probably within $\frac{1}{4}$ degree with respect to the zero of the scale itself. The maximum shift in angle permitted by all of the screw holes of the assembly corresponded to nearly $\pm$ one-half degree and although it is highly likely that the screws were nearly in the center of their proper holes when assembled as it was in use, the actual zero position of the scale cannot be said with certainty to have had an error less than three-fourths degree. This would not affect the measured Mott ratios for angles above 30° as the number of counts does not vary rapidly with angle at long angles, but at 15° it might account for a large part of the whole observed anomaly, or conversely might result in an apparent anomaly of roughly half of the true amount, since the number of counts varies so rapidly with angle in this region. Thus the observed Mott ratio at 800 kv and 20° is 0.73, and an error of three-fourths degree in the angular measurement would make this ratio 0.57 or 0.86. It is probable that our 15°-values are at neither one extreme nor the other, but absolute certainty on this point, which is of importance in determining whether phase shifts in the higher order de Broglie waves also come into account, must await measurements with an apparatus (such as we have under construction) giving an accuracy of the order of one-fifth degree in the angular measurements. In connection with these same measurements at 15° a second-order correction due to our angular spread of 2° might arise, the increased counts from the 14° to 15° zone more than balancing the decreased counts between 15° and 16°. This error has been examined and is not serious enough to warrant any correction of our present measurements.

As already mentioned, our new apparatus is being built to accommodate Geiger point-counters as detectors, primarily to extend the measurements to the region below 600 kv, where in a certain voltage region the scattering at 45° should approach or reach a small fraction of the Mott value, due to the compensating effects of the Coulomb repulsion and the attractive interaction for certain angles and "distances of approach."

(G) Discussion

A complete discussion of the theoretical significance of these results is given in the accompanying paper by Breit, Condon and Present. This may be summarized by the statement that these proton-scattering experiments demonstrate the existence of a proton-proton interaction which is violently different from the Coulomb repulsion for distances of separation of the order of 10^{-13} cm. The measurements are

quantitatively in agreement, as regards magnitudes, variation with angle, and variation with voltage, with a simple phase shift of the spherically symmetrical de Broglie wave ("S wave") due to the collision or scattering, corresponding to a new attractive force overpowering the Coulomb repulsion, and give a rather accurate measure of the "potential well" which is therefore permissible as representing the interaction. Interestingly enough, this potential well appears to be identical, within the limits of error of both determinations, with the potential well which represents the proton-neutron interaction as derived from the scattering and absorption of slow neutrons. Furthermore, the magnitude of interactions thus determined by scattering experiments is in very satisfactory agreement with that used successfully for calculations of mass defects of light nuclei.* It thus appears that a real beginning has been made toward an accurate and intimate knowledge of the forces which bind together the "primary particles" into the heavier nuclei so important in the structure and energetics of the material universe.

* A very readable discussion in this connection is given by Bethe in Rev. Mod. Phys. **8**, 82 (1936).

(H) ACKNOWLEDGMENTS

The writers are especially indebted to Professor G. Breit for stimulus and guidance in this problem in which he has been interested since the inception of the high voltage program in this department under his immediate supervision in 1926. We take pleasure also in expressing our indebtedness to Dr. J. A. Fleming for his courageous support of the whole program during the long period of development, and to Odd Dahl, our former colleague now in Norway, for construction of the scattering apparatus as well as for his numerous other ingenious contributions to our apparatus and technique.

NOVEMBER 1, 1936 PHYSICAL REVIEW VOLUME 50

Theory of Scattering of Protons by Protons*

G. BREIT, *University of Wisconsin, Madison, Wisconsin*, E. U. CONDON, *Princeton University, Princeton, New Jersey*, AND R. D. PRESENT, *Purdue University, Lafayette, Indiana*

(Received August 11, 1936)

The experiments of Tuve, Heydenburg and Hafstad and those of White are discussed by means of the standard theory of scattering in central fields. The theoretical formulas are presented in a form convenient for numerical computation and are supplemented by tables. These are arranged so as to enable an experimentalist to compute the effect of phase shifts due to angular momenta $L=0$, $\hbar$, $2\hbar$, and to infer these phase shifts from the experimental material (Tables I, II, III, IV, V, VI, VII, VIII, IX). Tables of necessary Coulomb wave functions are also given for zero angular momentum. By means of these the interaction energy can be computed from the experimental material (Tables X, XI, XII, XIII).

Statistical fluctuations make conclusions drawn from White's data somewhat uncertain. The experiments of Tuve, Heydenburg and Hafstad are comparatively free of statistical effects and their comparison with theory shows that (a) There is an unmistakable difference between the observed scattering and that to be expected according to Mott's formula which uses the inverse square law. (b) This difference can be explained by using practically entirely effects of the phase shift in the partial wave having $L=0$ (head on collisions; s wave distortions). The distortion of p and d waves ($L=\hbar$, $2\hbar$) is secondary and the experimental accuracy does not yet suffice to enable their quantitative determination. (c) The variation of the scattering anomaly with proton energy is in approximate agreement with that to be expected from an interaction potential independent of the energy. (d) For a given range of nuclear forces the interaction potential is accurately determined by the data. The values obtained are in good agreement with those found by Feenberg and Knipp and by Bethe from the mass defects of H^2, H^3, He^4 provided the mass defect calculations are made on the basis of a proton-neutron interaction which depends on the relative orientation of the spins of proton and neutron in accordance with Wigner's explanation of the large scattering of slow neutrons by hydrogen. Mass defect calculations based on a proton-neutron interaction indicated by the binding energy of H^2 without dependence on the spin orientation give a much lower value for the interaction between like particles than that obtained from the proton-proton scattering experiments. The "like-particle" interaction for a Gauss error potential is $39mc^2\epsilon^{-17r^2}$ with 8.97×10^{-13} cm as the unit of length and the interaction energy is 11.1 mev for a potential which is constant (except for its Coulombian part) within a distance

* A paper delivered at the Tercentary Conference of Arts and Sciences at Harvard University, September, 1936.

$e^2/mc^2 = 2.82 \times 10^{-13}$ cm. (e) The interaction between protons as derived from the scattering experiments is found to be very nearly equal to that between a proton and a neutron in the corresponding condition of relative spin orientation and angular momentum (^1S state). The proton-neutron values which come closest to being equal to the proton-proton values are those obtained by Fermi and Amaldi from the scattering and absorption of slow neutrons.

The close agreement between the empirical values of the proton-proton and proton-neutron interactions in ^1S states suggests that aside from Coulombian and spin effects the interactions between heavy particles are independent of their charge and that the apparent preference for equal numbers of protons and neutrons in the building up of nuclei is conditioned more by the operation of the exclusion principle than by the greater values of proton-neutron forces.

1. Introduction

OBSERVATIONS on the anomalous scattering of protons by protons have been made by Wells,[1] White[2] and Tuve, Heydenburg and Hafstad.[3] In the experiments of Wells a cloud chamber was used. On account of the small number of observed collisions the accuracy of his experiments was insufficient to make theoretical conclusions possible. White's experiments were made by the same method. A greater number of tracks was observed and White concluded that there is a large discrepancy between the actual scattering and that to be expected on the assumption of the inverse square law of force between protons. Such a discrepancy will be referred to below as a *scattering anomaly*. The theoretical interpretation of White's results has been considered in more detail by Present.[4] It was found impossible to account for White's angular distribution by any ordinary theory with a potential describing the interaction between protons. Nevertheless the order of magnitude of the scattering anomaly turned out to be in approximate agreement with the attractive potential which Feenberg and Knipp[5] found from the binding energies of H_1^2, He_2^3, He_2^4 by using a mixed Heisenberg-Majorana operator for the interaction between protons and neutrons. This operator gives an interaction between protons and neutrons in singlet states that is somewhat weaker than in triplet states, as has been suggested by Wigner from evidence on the scattering of slow neutrons by hydrogen.[6] The difficulties with the angular distribution and energy dependence in White's experiments make, however, conclusions about the interaction potential obtained from his data very uncertain.

The work of Tuve, Heydenburg, and Hafstad was done with electrical counters. Large numbers of scattered particles were observed and their data are comparatively free of statistical fluctuations due to an insufficiency of such particles. The scattering anomaly is smaller in their experiments than in those of White and it starts at a higher energy. It will be seen below that their final results are in reasonably good agreement with a simple form of scattering theory with respect to both the angular distribution and the energy dependence. There is no consistent evidence for the presence in the scattering of anything but an s wave (head-on collisions, $L=0$) which is in agreement with expectation for interaction forces confined to distances smaller than 10^{-12} cm. Although there were indications in the early experiments of THH of a too rapid variation of scattering anomaly with energy, later and more accurate data are in approximate agreement with theory also in this respect. The observations available at present are not yet precise enough to determine accurately the range of the proton-proton forces. Nevertheless, they appear to be good enough to eliminate strong long range forces. Thus interaction energies of constant magnitude through a distance of $3e^2/mc^2 = 8.5 \times 10^{-13}$ cm are in disagreement with the energy dependence of the

[1] W. H. Wells, Phys. Rev. **47**, 591 (1935).

[2] M. G. White, Phys. Rev. **47**, 573 (1935); **49**, 309 (1935). We are very grateful to Dr. White for communicating to us his complete data.

[3] M. A. Tuve, N. P. Heydenburg and L. R. Hafstad, Phys. Rev. **49**, 402 (1936); **50**, 806 (1936) (Preceding paper). We are very grateful to Messrs. Tuve, Heydenburg and Hafstad for making their results available to us before publication and for their wholehearted cooperation in answering by experiment the questions which came up in the interpretation of their earlier results.

[4] R. D. Present, Phys. Rev. **48**, 919 (1935).

[5] E. Feenberg and J. K. Knipp, Phys. Rev. **48**, 906 (1935).

[6] Dunning, Pegram, Fink and Mitchell, Phys. Rev. **47**, 970 (1935). Bjerge and Westcott, Proc. Roy. Soc. **A150**, 790 (1935). Fermi and Amaldi, La Ricerca Scientifica **1**, 1 (1936); Fermi, ibid., July, 1936. We are very grateful to Professor Fermi for informing us of his last results before publication. The value of 130 kv used for the position of the virtual level by us is too high. The effect of changing it to 110 kv is scarcely noticeable in Table XIV.

scattering anomaly while a constant interaction potential through $e^2/mc^2=2.8\times10^{-13}$ cm is in fair accord with observation. The magnitude of the interaction potential corresponds to $D=10.3$ mev through e^2/mc^2 if one uses square wells and to $A=39mc^2$ for the potential $Ae^{-\alpha r^2}$ with $\alpha=17$ and $\hbar(Mm)^{-\frac{1}{2}}c^{-1}=8.97\times10^{-13}$ cm as the unit of length. This value is in good agreement with the result of Feenberg and Knipp who obtain $A=41mc^2$ for the same α. The sensitivity of the expected scattering anomaly to the magnitude of the interaction potential is great and the above values of A and D are determinable to about $0.1mc^2$ from the scattering data at any given energy aside from uncertainties due to the possible effect of higher phase shifts.

In their present form the scattering experiments of THH give information about the force between two protons ($\pi-\pi$ force) when they collide head on (S state) and when they have antiparallel spins (^1S state). According to Wigner a similar state is of importance for the scattering of slow neutrons by hydrogen and the magnitude of the proton-neutron attraction in ^1S states ($\pi-\nu$ force) can be determined from scattering experiments combined with measurements of the absorption of slow neutrons in hydrogen. The $\pi-\pi$ and $\pi-\nu$ attractions will be compared for the ^1S states and it will be seen that the more careful experiments indicate a practically exact equality of the $\pi-\pi$ and $\pi-\nu$ forces. Although this comparison has been made only in the ^1S state the agreement is so striking as to suggest that the interactions between heavy particles are *universally equal*, i.e., that the only essential difference in the interactions between like and unlike particles is due to the exclusion principle. The magnetic moment of the proton is different from that of the neutron and, therefore, the force between protons cannot be expected to be exactly equal to that between neutrons or to that between protons and neutrons. The energy due to the magnetic interaction between two protons is, however, of the order $9(e\hbar/2Mc)^2/(e^2/mc^2)^3\sim0.012mc^2$ which is very much smaller than the main part of the interaction energy ($\sim20mc^2$). As a tentative hypothesis we may consider the interactions between heavy particles to be universally equal except for the Coulombian effects between protons and the spin effects between all the heavy particles. Whether this interaction has actually one of the forms used by Feenberg and Knipp and by Bethe still remains to be seen. Since the form

$$[(1-g)P^M+gP^H]J(r),$$

which has been used successfully by them (P^M = Majorana exchange operator, P^H = Heisenberg exchange operator) gives a value of the "like particle" interaction agreeing with that arrived at from the scattering experiments on protons, one may regard this form as the most likely. Since in H^3, He^3 and He^4 like particles can be considered as nearly in ^1S states the above operator would give for them the same effect as for the ^1S state of unlike particles. We should like to acknowledge our indebtedness to Dr. Feenberg who noticed independently that the above operator could be applied both to like and to unlike particles and kindly communicated his considerations to us. It is possible that the universal operator contains as a part of it a small Wignerian term.

The observations of Bjerge and Westcott and of Dunning[6] on the scattering of slow neutrons by hydrogen indicate that there is either a virtual or a stationary ^1S level of the deuteron at ±43 kv. If the level is stationary no agreement whatsoever is obtained between the $\pi-\pi$ and $\pi-\nu$ interactions. Assuming it to be virtual, the $\pi-\nu$ interaction as derived from these experiments corresponds to $A=42mc^2$ and is thus somewhat larger than the proton-proton interaction. The difference of $3mc^2$ is still too large to consider the interactions as the same because this difference will be seen to have significant and quite observable consequences for the scattering amounting to approximately a factor of 3 for neutrons. More recently improved measurements on neutrons were made by Fermi and Amaldi.[6] Their observations on the absorption of slow neutrons lead them to the conclusion that the level is virtual. Secondly the scattering cross section in hydrogen has been found by them to be 12×10^{-24} cm^2 instead of the previous larger values and the position of the virtual level has been raised to about 130 kv. *With these changes the difference between the interactions of like and unlike particles is insignificant and*

may be considered as lying within the limits of error of the experiments.

Recent experiments of Goldhaber[7] raised doubts concerning Wigner's explanation of the scattering of neutrons in hydrogen. According to Goldhaber the mean free path of 200 kv neutrons is about three times greater than that to be expected theoretically. If Goldhaber's result were correct all of the conclusions arrived at in this paper would have to be changed because the $\pi-\nu$ interaction would be modified and because Feenberg and Knipp's value of the like-particle interaction would be altered. In view of these radical implications of Goldhaber's experiment it was repeated by Tuve and his colleagues using carbon bombarded with deuterons as a source. The energy of the deuterons is between 600 kv and 1200 kv. Its precise value does not matter for the interpretation of the experiments. They find a mean free path in paraffin of 2.2 cm which is to be compared with a theoretical mean free path of 2.4 cm using 30 kv for the position of the virtual level and 600 kv for the neutron energy and 2.2 cm using 140 kv for the position of the virtual level and again 600 kv for the neutron energy. Their mean free path is smaller than Goldhaber's even though the energy of the neutrons is higher. Goldhaber's result thus implies a minimum in the scattering at about 200 kv of neutron energy and is improbable. We are very grateful to Dr. Tuve and his colleagues for permission to quote their experiments in this connection.

2. Phase Shift Analysis

The scattering of charged particles by an inverse square field of force has been considered by Gordon and Mott[8] while the effect of symmetry due to the identity of particles has been worked out by Mott.[9] The scattering anomaly due to deviations from an inverse square field has been discussed by Taylor[10] who applied the theory to the scattering of alpha-particles in helium and in hydrogen. The general form of the theory is well established in these papers, and its systematic presentation is given by Mott and Massey.[11] It will suffice here to suppose the methods as known and it will not be necessary to give the derivations of the formulas.

Notation

The following notation will be used:

M = mass of proton.
$\mu = M/2$ = reduced mass in the collision of two protons.
v = relative velocity of the two protons before the collision.
E = kinetic energy of incident protons $= \frac{1}{2}Mv^2$.
E' = energy in frame of center of gravity $= \frac{1}{2}E$
$\Lambda = \hbar/\mu v$ = de Broglie wave-length.
$k = 2\pi/\Lambda$.
$a = \hbar^2/\mu e^2$.
$\eta = 1/ka = (e^2/\hbar c)ZZ'c/v$.
r = distance between proton and neutron or proton and proton.
$\rho = kr$, $y = \rho\eta = r/a$.
$L\hbar$ = angular momentum of proton and neutron or proton and proton around common center of gravity.
P_L = Legendre function.

---

[7] M. Goldhaber, Nature **137**, 824 (1936). Cf. reference to M. A. Tuve in text. M. A. Tuve and L. R. Hafstad, Phys. Rev. **50**, 490 (1936).

[8] W. Gordon, Zeits. f. Physik **48**, 180 (1928). N. F. Mott, Proc. Roy. Soc. **A118**, 542 (1928).

[9] N. F. Mott, Proc. Roy. Soc. **A126**, 259 (1930). Cf. J. R. Oppenheimer, Phys. Rev. **32**, 361 (1928).

In applications of the solutions of Gordon and Mott the meaning of the physical condition represented by the solution is usually not clearly stated. This solution is given by Eqs. (1) (1′) in the text. It represents the wave inside a very large screening sphere of radius R. For $r>R$ there is supposed to be no field of force while for $r<R$ the field is given by the Coulombian potential. For elastic collisions between a proton and a hydrogen atom or between two hydrogen atoms one is interested in the state of the system before and after the atoms have collided, i.e. in the state in a force free region. Thus rigorously it is the solution "outside" the screening sphere ($r>R$) that matters. Such a solution is complicated and for ordinary applications it is not considered explicitly for the following reasons. According to the asymptotic expansion given by Eq. (3) in the text the solution inside the screening sphere is the sum of two parts represented by the two exponentials. The second of these is of special interest because it represents the scattered wave. Over a small area of the screening sphere the "spherical wave" represented by this term may be approximated by a plane wave which may be regarded as subject to reflection and refraction at $r=R$. Actually the screening is taking place through a region large compared with the wave-length and therefore the reflection may be neglected. There will also be no refraction as long as the wave may be considered as plane. For very small scattering angles, however, the wave cannot be considered as plane because the second term in the curly brackets in the spherical wave part of Eq. (3) is not negligible in comparison with unity. Thus at small angles one may expect the solutions used here to give incorrect results, in agreement with the Born method calculation of Coulomb scattering due to Wentzel. In order that the second term in curly brackets should become ~ 1 for 1 Mev protons at 0.53×10^{-8} cm it is necessary to have $2\Theta=\theta\sim1^\circ$. The magnitude of the term decreases with Θ^{-2} at small angles and therefore no serious effect due to this cause is expected in practical applications.

[10] H. M. Taylor, Proc. Roy. Soc. **A134**, 103 (1931); **A136**, 605 (1932).

[11] N. F. Mott and H. S. W. Massey, *The Theory of Atomic Collisions* (Oxford University Press).

θ = scattering angle in the reference system of center of gravity.
$\Theta = \theta/2$ = scattering angle in the reference system of the laboratory.
$\mathbf{c} = \cos\Theta$. $\mathbf{s} = \sin\Theta$.
Γ = the gamma function.
$\sigma_L = \arg\Gamma(L+1+i\eta)$.
F_L = regular solution of the differential equation for r times the radial wave function in a Coulomb field normalized so as to be asymptotic to a sine wave of unit amplitude at ∞. The asymptotic form is given by $F_L \sim \sin(\rho - \frac{1}{2}L\pi - \eta \ln 2\rho + \sigma_L)$ and the diff. eq. is $[d^2/d\rho^2 + 1 - 2\eta/\rho - L(L+1)/\rho^2]F_L = 0$.
G_L = irregular solution of the same differential equation normalized so that its asymptotic form is given by $G_L \sim \cos(\rho - \frac{1}{2}L\pi - \eta \ln 2\rho + \sigma_L)$.
K_L = phase shift defined by the asymptotic form of $\mathfrak{F}_L = r$ times the radial wave function in the actual field. This form shall be $\mathfrak{F}_L \sim e^{iK_L}\sin(\rho - \frac{1}{2}L\pi - \eta \ln 2\rho + \sigma_L + K_L)$.

The above notation for the Coulomb wave functions is the same as that used by Yost, Wheeler Breit[12] in tabulations of these wave functions.

The plane wave e^{ikz} is changed by the Coulomb field into

$$\psi^c = \sum_0^\infty i^L(2L+1)P_L(\cos\theta)e^{i\sigma_L}F_L/\rho. \tag{1}$$

An alternative form is

$$\psi^c = e^{-\frac{1}{2}\pi\eta + ikz}\Gamma(1+i\eta)\mathbf{F}(-i\eta; 1; ik(r-z)) \tag{1'}$$

where $\mathbf{F}$ is the confluent hypergeometric series. If the field is Coulombian at large distances but not at small ones then the same plane wave is changed into

$$\psi = \sum_0^\infty i^L(2L+1)P_L e^{i\sigma_L}\mathfrak{F}_L/\rho. \tag{2}$$

At large distances the asymptotic form of ψ^c is

$$\psi^c \sim \left\{1 + \frac{\eta^2}{ik(r-z)} + \cdots\right\}\exp\{i[kz + \eta\ln k(r-z)]\} - \frac{\eta}{k(r-z)}\left\{1 + \frac{(1+i\eta)^2}{ik(r-z)} + \cdots\right\}$$
$$\times \exp\{i[kr - \eta\ln k(r-z) + 2\sigma_0]\}. \tag{3}$$

The collision cross section per unit solid angle of the laboratory reference system is, on the classical theory, for Coulombian fields:

$$\sigma_{C1} = 4\mathbf{c}(\mathbf{s}^{-4} + \mathbf{c}^{-4})(e^2/2\mu v^2)^2. \tag{4}$$

The effect of taking into account the symmetry of the wave functions is according to Mott such as to change this into

$$\sigma_{\text{Mott}} = 4\mathbf{c}[\mathbf{s}^{-4} + \mathbf{c}^{-4} - \mathbf{s}^{-2}\mathbf{c}^{-2}\cos(\eta\ln\mathbf{s}^2\mathbf{c}^{-2})](e^2/2\mu v^2)^2. \tag{4'}$$

If the field deviates from the Coulombian the collision cross section per unit solid angle is

$$\sigma = 4\mathbf{c}\mathbf{P}, \tag{4''}$$

where

$$\mathbf{P} = \tfrac{1}{4}|f(\theta) + f(\pi-\theta)|^2 + \tfrac{3}{4}|f(\theta) - f(\pi-\theta)|^2$$

in the notation of Mott and Massey.[11] The quantity $\mathbf{P}$ and hence σ can be computed using

[12] F. L. Yost, John A. Wheeler and G. Breit, Phys. Rev. **49**, 174 (1936); Journal of Terrestrial Magnetism and Atmospheric Electricity, December, 1935, p. 443. See also T. Sexl, Zeits. f. Physik **56**, 62 (1929) for discussion of $L = 0$.

$$\mathbf{P}=(e^2/2\mu v^2)^2\Big\{\mathbf{s}^{-4}+\mathbf{c}^{-4}-\mathbf{s}^{-2}\mathbf{c}^{-2}\cos(\eta\ln\mathbf{s}^2\mathbf{c}^{-2})-\frac{2}{\eta}\sum{}_L g_L(2L+1)[\mathbf{s}^{-2}\cos\varphi_L{}^e+(-)^L\mathbf{c}^{-2}\cos\varphi_L{}^c]$$
$$+\frac{4}{\eta^2}\sum{}_L g_L(2L+1)^2P_L{}^2\sin^2K_L+\frac{8}{\eta^2}[\textstyle\sum_e+3\sum_o]_{L'>L}(2L+1)(2L'+1)P_LP_{L'}$$
$$\times\sin K_L\sin K_{L'}\cos(\varphi_L-\varphi_{L'})\Big\}, \quad (5)$$

where g_L has the value 1 for even L and 3 for odd L. The last term in braces contains two sums, the first referring to even L, as indicated by suffix e, and the second referring to odd L as indicated by suffix o. Both of these sums are taken over pairs of unequal values of L. No cross products between even and odd L occur. As before, the argument of the Legendre functions P_L is $\cos\theta$. The other quantities needed in this formula are:

$$\varphi_L=K_L+2(\sigma_L-\sigma_0);\quad \varphi_L{}^e=\varphi_L+\eta\ln\mathbf{s}^2;\quad \varphi_L{}^c=\varphi_L+\eta\ln\mathbf{c}^2, \quad (5.1)$$

$$\sigma_1-\sigma_0=\tan^{-1}\eta;\quad \sigma_2-\sigma_1=\tan^{-1}(\eta/2);\quad \sigma_L-\sigma_{L-1}=\tan^{-1}(\eta/L). \quad (5.2)$$

If all K_L beyond K_2 vanish

$$\mathbf{P}=\mathbf{P}_M+(\Delta\mathbf{P})_0+(\Delta\mathbf{P})_1+(\Delta\mathbf{P})_2, \quad (6)$$

with

$$(2\mu v^2/e^2)^2\mathbf{P}_M=\mathbf{s}^{-4}+\mathbf{c}^{-4}-\mathbf{s}^{-2}\mathbf{c}^{-2}\cos(\eta\ln\mathbf{s}^2\mathbf{c}^{-2}), \quad (6.1)$$

$$(2\mu v^2/e^2)^2(\Delta\mathbf{P})_0=-\frac{2}{\eta}(\mathbf{s}^{-2}\cos\varphi_0{}^e+\mathbf{c}^{-2}\cos\varphi_0{}^c)\sin K_0+\frac{4}{\eta^2}\sin^2K_0. \quad (6.2)$$

$$(2\mu v^2/e^2)^2(\Delta\mathbf{P})_1=-\frac{18}{\eta}(\mathbf{s}^{-2}\cos\varphi_1{}^e-\mathbf{c}^{-2}\cos\varphi_1{}^c)P_1\sin K_1+\frac{108}{\eta^2}P_1{}^2\sin^2K_1, \quad (6.3)$$

$$(2\mu v^2/e^2)^2(\Delta\mathbf{P})_2=-\frac{10}{\eta}(\mathbf{s}^{-2}\cos\varphi_2{}^e+\mathbf{c}^{-2}\cos\varphi_2{}^c)P_2\sin K_2+\frac{100}{\eta^2}P_2{}^2\sin^2K_2$$
$$+\frac{40}{\eta^2}\sin K_0\sin K_2\cos(\varphi_2-\varphi_0)P_2. \quad (6.4)$$

By means of (4″) and (6.1) one obtains Mott's value as is seen from (4′). The additions to $\mathbf{P}$ due to K_0, K_1, K_2 are given by (6.2), (6.3), (6.4), respectively. It will be noted that the effect of K_2 depends on K_0. The above formulas are convienent for computation if one is not interested in many values of the phase shifts. For such cases it is more convenient to expand (6.2), (6.3), (6.4) as follows

$$(2\mu v^2/e^2)^2(\Delta\mathbf{P})_0=-\frac{2}{\eta}\left(\frac{\cos\alpha_0}{\mathbf{s}^2}+\frac{\cos\beta_0}{\mathbf{c}^2}\right)\sin K_0\cos K_0+\left(\frac{4}{\eta^2}+\frac{2}{\eta}\frac{\sin\alpha_0}{\mathbf{s}^2}+\frac{2}{\eta}\frac{\sin\beta_0}{\mathbf{c}^2}\right)\sin^2K_0,$$
$$\alpha_0=\eta\ln\mathbf{s}^2,\quad \beta_0=\eta\ln\mathbf{c}^2, \quad (6.5)$$

$$(2\mu v^2/e^2)^2(\Delta\mathbf{P})_1=-\frac{18}{\eta}P_1\left(\frac{\cos\alpha_1}{\mathbf{s}^2}-\frac{\cos\beta_1}{\mathbf{c}^2}\right)\sin K_1\cos K_1+\left[\frac{108}{\eta^2}P_1{}^2+\frac{18}{\eta}\left(\frac{\sin\alpha_1}{\mathbf{s}^2}-\frac{\sin\beta_1}{\mathbf{c}^2}\right)P_1\right]\sin^2K_1,$$
$$\alpha_1=\alpha_0+2(\sigma_1-\sigma_0),\quad \beta_1=\beta_0+2(\sigma_1-\sigma_0), \quad (6.6)$$

$$(2\mu v^2/e^2)^2(\Delta\mathbf{P})_2=-\frac{10}{\eta}P_2\left(\frac{\cos\alpha_2}{\mathbf{s}^2}+\frac{\cos\beta_2}{\mathbf{c}^2}\right)\sin K_2\cos K_2+\left[\frac{100}{\eta^2}P_2{}^2+\frac{10}{\eta}P_2\left(\frac{\sin\alpha_2}{\mathbf{s}^2}+\frac{\sin\beta_2}{\mathbf{c}^2}\right)\right]\sin^2K_2$$
$$+\frac{40}{\eta^2}\sin K_0\sin K_2\cos[K_2-K_0+2\sigma_2-2\sigma_0],\quad \alpha_2=\alpha_0+2(\sigma_2-\sigma_0),\quad \beta_2=\beta_0+2(\sigma_2-\sigma_0). \quad (6.7)$$

TABLE I. *Values of* $(2\mu v^2/e^2)^2 P_M$.

η	E in kv	$\Theta=15°$	20°	25°	30°	35°	40°	45°
0.4775	108.8	219.1	68.84	27.74	13.15	7.19	4.694	4
.3821	170.0	215.4	67.42	27.14	12.90	7.10	4.673	4
.2867	302.4	212.3	66.25	26.65	12.70	7.02	4.657	4
.2069	580	210.3	65.52	26.35	12.58	6.98	4.648	4
.1751	810	209.7	65.27	26.25	12.53	6.97	4.644	4
.1591	981	209.4	65.18	26.21	12.52	6.96	4.644	4
.1017	2400	208.6	64.88	26.10	12.47	6.94	4.638	4

TABLE II. *Values of coefficients of* $-\sin K_0 \cos K_0$ *for* P/P_M.

η	E in kv	$\Theta=15°$	20°	25°	30°	35°	40°	45°
0.4775	108.8	0.0994	0.339	0.758	1.426	2.380	3.441	3.96
.3821	170.0	.212	.541	1.088	1.938	3.128	4.426	5.05
.2866	302.4	.385	.854	1.609	2.755	4.339	6.032	6.84
.1989	628	.665	1.376	2.484	4.15	6.42	8.84	9.95
.1830	741	.741	1.511	2.720	4.53	7.02	9.64	10.84
.1671	890	.830	1.679	3.004	4.99	7.69	10.53	11.88
.1512	1088	.936	1.873	3.350	5.54	8.54	11.69	13.16
.1432	1211	.995	1.990	3.54	5.86	9.06	12.34	13.88
.1332	1400	1.081	2.155	3.83	6.33	9.71	13.25	14.95
.1174	1800	1.244	2.468	4.37	7.21	11.04	15.06	16.98
.1017	2400	1.455	2.872	5.07	8.35	12.78	17.43	19.61

TABLE III. *Values of coefficients of* $\sin^2 K_0$ *for* P/P_M.

E in kv	$\Theta=15°$	20°	25°	30°	35°	40°	45°
108.8	−0.213	−0.194	−0.004(3)	0.493	1.380	2.469	3.025
170.0	−.185	−.0828	.332	1.244	2.769	4.579	5.48
302.4	−.117	.215	1.114	2.971	5.819	9.124	10.79
628	.114	1.000	3.11	7.12	13.37	20.5	23.9
741	.198	1.276	3.80	8.58	15.99	24.4	28.4
890	.309	1.643	4.71	10.49	19.42	29.6	34.4
1088	.460	2.130	5.94	13.07	24.02	36.4	42.4
1211	.565	2.438	6.71	14.68	26.96	40.6	47.4
1400	.700	2.907	7.87	17.11	31.3	47.3	55.0
1800	1.009	3.90	10.36	22.31	40.6	61.2	71.2
2400	1.471	5.40	14.07	30.07	54.6	82.1	95.3

In these equations, the coefficients of $\sin K_L \times \cos K_L$, $\sin^2 K_L$ are functions only of the energy and of the scattering angle. In formula (6.7) the cross product term in K_0, K_2 is conveniently computed directly. Values of the coefficients and other quantities for the computation of $\mathbf{P}$ are given in Tables I, II, ··· IX. In Table I are given values of $(2\mu v^2/e^2)^2 \mathbf{P}_M$. In the first column are listed values of η and the second column gives the approximate value of the energy of the incident proton for this η. The succeeding columns give the values of $(2\mu v^2/e^2)^2 \mathbf{P}_M$ for $\Theta=15°$, 20°, etc. as indicated at the top of each column. The values of $(2\mu v^2/e^2)^2 \mathbf{P}_M$ are seen to vary slowly with E and interpolation can be easily made in Table I. In Tables II, III are given values of the coefficients of $-\sin K_0 \cos K_0$ and $\sin^2 K_0$ for the calculation of $(\Delta \mathbf{P})_0/\mathbf{P}_M$.

The values of η listed in Table II were used in the computations of the coefficients for Tables II and III. The values of E are not as accurate as those of η because their calculation involves the somewhat uncertain values of the fundamental physical constants. The same applies to Table I and to Tables III, IV, V, VI. The numbers tabulated above, where they are plotted against E, form smooth curves. The graphs for the coefficient of $\sin^2 K_0$ are practically straight lines. By means of such graphs the coefficients can be easily obtained for the needed values of E. The

TABLE IV. *Values of coefficients of* $-\sin K_1 \cos K_1$ *for* P/P_M.

η	E in kv	$\Theta=15°$	20°	25°	30°	35°	40°	45°
0.4775	108.8	1.946	3.23	4.14	4.19	3.06	1.100	0
.2866	302.4	3.50	5.48	6.85	6.84	4.92	1.739	0
.1989	628	5.14	7.92	9.85	9.75	6.99	2.471	0
.1671	890	6.15	9.44	11.69	11.60	8.32	2.91	0
.1432	1211	7.19	10.98	13.60	13.52	9.70	3.39	0
.1174	1800	8.80	13.45	16.61	16.48	11.78	4.13	0
.1017	2400	10.17	15.54	19.18	19.02	13.59	4.77	0

TABLE V. *Values of coefficients of* $\sin^2 K_1$ *for* P/P_M.

E in kv	$\Theta=15°$	20°	25°	30°	35°	40°	45°
108.8	0.635	3.21	6.63	9.00	7.51	2.927	0
302.4	3.68	10.88	20.03	25.94	22.15	8.63	0
628	8.78	23.94	42.6	54.4	46.1	17.89	0
890	12.91	34.1	60.5	77.3	65.1	25.22	0
1211	17.93	46.8	82.7	105.2	88.9	34.3	0
1800	27.21	70.1	123.7	157.1	132.2	51.1	0
2400	36.6	93.7	165.1	209.5	176.4	68.0	0

TABLE VI. *Values of coefficients of* $-\sin K_2 \cos K_2$ *for* P/P_M.

E in kv	$\Theta=15°$	20°	25°	30°	35°	40°	45°
628	2.36	2.74	1.48	−2.48	−9.68	−18.36	−22.62
890	2.82	3.29	1.79	−3.02	−11.81	−22.48	−27.68
1211	3.32	3.88	2.10	−3.58	−14.10	−26.80	−33.02

TABLE VII. *Values of coefficients of* $\sin^2 K_2$ *for* P/P_M.

E in kv	$\Theta=15°$	20°	25°	30°	35°	40°	45°
628	4.90	6.17	1.840	2.19	34.0	104.0	147.0
890	6.89	8.54	2.426	3.50	49.9	150.8	214.3
1211	9.34	11.40	3.14	5.10	69.5	208.6	293.4

TABLE VIII. *Values of* $(40/\eta^2)P_2/[s^{-4}+c^{-4}-s^{-2}c^{-2}\cos(\eta \ln s^2 c^{-2})]$.

E in kv	$\Theta=15°$	20°	25°	30°	35°	40°	45°
628	3.00	5.88	4.60	−10.05	−47.0	−99.1	−126.3
890	4.27	8.35	6.54	−14.29	−66.7	−140.4	−179.0
1211	5.82	11.39	8.93	−19.48	−91.0	−191.2	−243.7

TABLE IX. *Values of* $2\sigma_2 - 2\sigma_0$.

E in kv	108.8	170.0	302.4	580	1088	1800	2400
$2\sigma_2-2\sigma_0$ =	77.9°	63.5°	48.3°	35.4°	25.8°	20.1°	17.4°

same applies to the coefficients for the effect of K_1 tabulated in Tables IV, V and the coefficients for the effect of K_2 tabulated in Tables VI, VII. In the computation of the cross product term in K_0, K_2 contained in (6.7) it is also convenient to have values of

$$(40/\eta^2)P_2/[\mathbf{s}^{-4}+\mathbf{c}^{-4}-\mathbf{s}^{-2}\mathbf{c}^{-2}\cos(\eta \ln \mathbf{s}^{-2}\mathbf{c}^{-2})]$$

which gives the coefficient of the trigonometric functions for $\mathbf{P}/\mathbf{P}_M$. These are given in Table VIII. Values of $2(\sigma_2-\sigma_0)$ for different E which are needed for the last trigonometric function in (6.7) can be computed by means of Eq. (5.2). Some values are given in Table IX. It will be noted that the coefficients of $\sin^2 K_1$, $\sin^2 K_2$ are practically linear functions of E for most of the energies covered here.

When the values of the energy and of the scattering angle are fixed $\mathbf{P}/\mathbf{P}_M$ turns out to be a smooth and almost linear function of K_0 and it is thus possible to interpolate for most values of K_0 having made calculations for a few of them.

Since it is probable that these scattering experiments will be repeated and since it is advisable for the experimentalists to have a ready means of testing their data for agreement with a possible analysis in terms of the phase shifts K_0, K_1, K_2 we summarize the procedure for using the above tables. From the experiments one obtains the collision cross section per unit solid angle. This is σ of Eq. (4''); it corresponds to the total number of protons observed and it thus includes the effect of recoil protons. Then $\mathbf{P}$ is obtained by means of Eq. (4''). By means of Table I one obtains $\mathbf{P}_M$ and hence $\mathbf{P}/\mathbf{P}_M$. Fixing the voltage the curve of $\mathbf{P}/\mathbf{P}_M$ against energy has to be fitted by means of K_0, K_1, K_2. The effect of K_0 is obtained by the following procedure. The coefficients given in Tables II, III are plotted for each scattering angle as a function of E. Using the graphs the coefficients for the needed voltage E are found. Usually no great accuracy is required in these coefficients. The coefficients of Table II are then multiplied by $-\sin K_0 \cos K_0$, those of Table III are multiplied by $\sin^2 K_0$ and the results are added. The result is the contribution to $\mathbf{P}/\mathbf{P}_M$ due to K_0. When added to unity it gives the expected $\mathbf{P}/\mathbf{P}_M$ for this K_0 if the other K are zero. These contributions are plotted as functions of K_0 keeping Θ fixed. The graphs give then the values of K_0 which are needed to fit the actual $\mathbf{P}/\mathbf{P}_M$ for any scattering angle as well as values of $\mathbf{P}/\mathbf{P}_M$ that correspond to this K_0 for other Θ. The same procedure may be used for the calculation of the effects of K_1 and K_2.

3. Calculation of Phase Shifts for Given Laws of Interaction

The nature of the forces between protons is not yet known. They may be partly describable by means of exchange potentials and partly by means of ordinary potentials. In spite of this apparent complication all kinds of interactions that have been seriously considered so far in nuclear theory give in effect a simple potential which is a function only of the distance r, at any fixed value of the relative angular momentum $L\hbar$. Thus exchange forces of the Majorana type give interaction potentials of the same absolute value but of opposite signs for states with odd and with even L. We will therefore suppose that there is some interaction potential for any L which may be different for different L. On account of the spins of the two protons they may be either in singlet or in triplet states. If the state is a singlet the orbital wave function is symmetric and therefore contains only terms with even L. If the state is a triplet the orbital wave function is antisymmetric and contains only odd L. Conversely the even L occur only in singlets and the odd only in triplets. For each L there is thus no necessity of considering interactions for singlets and triplets separately.

It will be supposed that for any L the potential is practically Coulombian beyond a certain distance r_0. The radial wave equation determines the function $\mathfrak{F}_L$ for $r<r_0$ to within a constant factor (see list of notation). In order to indicate that this solution involves only calculation inside r_0 it will be written as F_i. The suffix L will be omitted for the present so as not to complicate the formulas. The derivatives of F_i, F, G with respect to ρ will be written as F_i', F', G'. The relations between F'/F and K are

$$\tan K=(F'F_i-FF_i')/(GF_i'-F_iG')$$
$$=(F^2\delta)/(1-FG\delta), \quad (7.1)$$

$$\delta=F'/F-F_i'/F_i, \quad (7.2)$$

$$(F_i'/F_i)=(F'+G'\tan K)/(F+G\tan K). \quad (7.3)$$

Here all quantities are supposed to be taken at $r=r_0$. The calculation of F, G, F', G' can be made by means of the formulas given by Yost, Wheeler, Breit[12] in terms of the series Φ, Φ^*, Ψ, Ψ^*. The necessary relations are

$$F_L=C_L\rho^{L+1}\Phi_L;\quad \rho F_L'/F_L=\Phi_L^*/\Phi_L;$$
$$G_L=D_L\rho^{-L}\Theta_L;$$
$$\Theta_L=\Psi_L+\rho^{2L+1}(p_L\ln 2\rho+q_L)\Phi_L. \quad (7.4)$$

Using the last form in (7.1) one does not need G'. The tabulations of Yost, Wheeler, Breit do not cover the range of values needed here. The necessary numbers are given in Tables X, XI, XII, XIII. From the phase shifts determined by means of the angular distribution $\rho F_i'/F_i$ can be determined by means of (7.1) or (7.3). This is necessary for example if one wishes to determine the magnitude of the interaction when its shape as a function of distance is known. For small radii and $L=0$ the use of (7.1) is not advisable because the numerical accuracy is then poor. In such a case it is better to use

$$\frac{\rho F_i'}{F_i}=y\frac{X+(2\ln 2y+f)\Phi_0^*}{\Psi_0+y(2\ln 2y+f)\Phi_0}, \quad (7.5)$$

where $y=\rho\eta=r/a$;

$$f=-2\ln\eta+q_0/\eta+(C_0^2/\eta)\cot K_0. \quad (7.6)$$

$$X=(\Psi_0^*+2y\Phi_0)/y=2-\left(4+\frac{1}{\eta^2}\right)y-4y^2$$
$$+\left(\frac{1}{6\eta^4}+\frac{37}{27\eta^2}-\frac{32}{27}\right)y^3+\cdots,$$
$$\Phi_0=1+y+\left(\frac{1}{3}-\frac{1}{6\eta^2}\right)y^2+\left(\frac{1}{18}-\frac{1}{9\eta^2}\right)y^3+\cdots,$$
$$\Phi_0^*=1+2y+\left(1-\frac{1}{2\eta^2}\right)y^2+\left(\frac{2}{9}-\frac{4}{9\eta^2}\right)y^3+\cdots, \quad (7.7)$$
$$\Psi_0=1-\left(3+\frac{1}{2\eta^2}\right)y^2+\left(\frac{1}{9\eta^2}-\frac{14}{9}\right)y^3$$
$$+\left(\frac{1}{24\eta^4}+\frac{43}{108\eta^2}-\frac{35}{108}\right)y^4+\cdots,$$
$$q_0=2\eta\left[\gamma-\frac{1}{1+\eta^2}+(s_3-1)\eta^2-(s_5-1)\eta^4+\cdots\right],$$
$$s_3=1.2021;\quad s_5=1.0369;\quad s_7=1.00835.$$

If r_0 is not very small it is more convenient to use

$$\frac{\rho F_i'}{F_i}=\frac{\Phi_0^*}{\Phi_0}-\frac{1}{\Phi_0\Theta_0+C_0^2\rho\Phi_0^2\cot K_0}. \quad (7.8)$$

For $r=0$ it is found from Eqs. (7.1) and (7.5) that

$$\tan K_0=\frac{C_0^2/\eta}{(\bar{C}_0^2/\bar{\eta})\cot\bar{K}_0+2\ln\eta/\bar{\eta}+\bar{q}/\bar{\eta}-q/\eta}, \quad (7.9)$$

where the barred quantities refer to that energy at which $K_0=\bar{K}_0$. Some useful values are given in Tables X, XI. The values of η in Tables X, XI, XII, XIII correspond to those in Tables I, $\cdots$ VIII wherever the listed E are the same. As before η is the actual quantity used in the calculations while E was computed from η using values of the fundamental constants. Similarly the values of y given in the headings of the tables are accurate while the values of r_0 are approximate. The values tabulated are those needed for Eq. (7.8) in order to calculate $\rho F_i'/F_i$ from K_0 as well as for the calculation of K_0 from $\rho F_i'/F_i$ by means of the second form of Eq. (7.1).

The calculation of K_0 is now reduced to finding $\rho F_i'/F_i$. If the interaction potential is constant within r_0 the expression for $L=0$ is

$$\rho F_i'/F_i=z\cot z;\quad z=[2\mu\hbar^{-2}(D+E')]^{\frac{1}{2}}r_0$$
$$=0.439(rmc^2/e^2)(D+E')^{\frac{1}{2}}\text{ mv}. \quad (8)$$

Here D is the negative of the potential energy in $0<r<r_0$. For attractive forces D is positive. Estimates show that K_1, K_2, are probably very small if the range of the nuclear forces is of the order of magnitude arrived at from nuclear mass defects. However, nuclear mass defect calculations are not sensitive to small interactions at large distances. The magnitude of the expected phase shifts can be estimated using

$$K_L\leqq-\int(V/E')F_L^2d\rho. \quad (8.1)$$

Graphs of F_L for $L=0$, 1, 2 for energies $E=0.4$, 0.6, 0.8, 1.0 Mev are given in Figs. 1, 2. For 1 Mev these functions are compared with corresponding functions in the absence of a Coulomb field. The validity of the approximation implied in Eq. (8.1) was tested by an explicit numerical integration

TABLE X. *Coulomb functions for* $y=0.02445$; $r_0 \leqq e^2/2mc^2$.

$2\pi\eta$	$E \leqq$	Φ_0^*/Φ_0	$\Phi_0\Theta_0$	$C_0^2\rho\Phi_0^2$
0.95	1088	1.0156	0.9276	0.1008
1.00	981	1.0165	.9268	.0931
1.05	890	1.0172	.9258	.0862
1.10	810	1.0178	.9248	.0800
1.15	741	1.0184	.9237	.0743
1.20	681	1.0188	.9227	.0692
1.30	580	1.0197	.9206	.0602
1.50	436	1.0208	.9163	.0461

TABLE XI. *Coulomb functions for* $y=0.0489$; $r_0 \leqq e^2/mc^2$.

$2\pi\eta$	Φ_0^*/Φ_0	$\Phi_0\Theta_0$	$C_0^2\rho\Phi_0^2$
0.95	1.014	0.8847	0.2062
1.00	1.017	.8861	.1910
1.05	1.020	.8869	.1772
1.10	1.022	.8873	.1646
1.15	1.025	.8872	.1533
1.20	1.027	.8866	.1427
1.30	1.030	.8851	.1258
1.50	1.034	.8804	.0959

for $L=1$ using the Gauss error potential $Ae^{-\alpha r^2}$ with values of A and α that correspond to those found by Feenberg and Knipp. The agreement is good and the use of Eq. (8.1) appears to be justified for such estimates. If resonance is approached on account of a sufficiently large V the equation becomes unreliable. Direct calculation for K_1 using accurate formulas with a square well having a radius $2e^2/mc^2$ and a depth of 2 Mev gives $K_1 \leqq 0.3°$. Since this radius is too great one may expect the principal part of the interaction potential to give rise only to negligible higher phase shifts.

4. Discussion of Experiments

In Fig. 3 are given values of $\sigma \sin\Theta$ from White's experiments. Crosses mark the experimental points observed for energies of the incident protons ranging from 600–750 kv. The dotted curve was calculated for a pure Coulomb field from Mott's formula. The full curve was obtained by adjusting the phase shift K_0 for the distorted s wave so as to give agreement with experiment in the neighborhood of 45°. It is to be noticed that if the two points at 37.5° and 42.5° are rejected, there is surprisingly good agreement with exact Coulomb scattering. However, there is apparently no reason except for statistical fluctuations specially to doubt the reliability of these two points. If they are correct it becomes necessary to explain the strange deficiency at 30°. The effect of K_1 cannot reasonably explain this condition because it increases relatively to the effect of K_0 at smaller angles. Since this point is in contradiction with the observations of Tuve, Heydenburg, Hafstad it appears simplest to attribute it to statistical fluctuations in White's experiments. Conclusions about the magnitude of the interaction potential from his work appear to be somewhat unsafe in view of this erratic angular dependence. Nevertheless his values at 45° for the 600–750 kv range give an interaction potential which is in approximate agreement with that obtained from the experiments of THH. This happens essentially because the observed scattering anomaly is so large that its explanation calls for approximate *resonance*. In more detail the situation is as follows.

There are in general two values of K_0 that will account for the scattering at 45°. The smallest positive K_0 turns out to be the most probable. It can be explained in terms of an attractive potential agreeing closely with the calculation of Feenberg and Knipp. The other value would either require repulsive forces or a definitely stronger attraction than that obtained by Feenberg and Knipp with the mixed operator for neutron-proton interactions. Additional strong

TABLE XII. *Coulomb functions for* $y=0.0978$; $r_0 \leqq 2e^2/mc^2$.

$2\pi\eta$	Φ_0^*/Φ_0	$\Phi_0\Theta_0$	$C_0^2\rho\Phi_0^2$
0.95	0.9525	0.7663	0.4084
1.00	.9674	.7802	.3823
1.05	.9799	.7918	.3580
1.10	.9904	.8008	.3353
1.15	.9998	.8085	.3143
1.20	1.0079	.8139	.2945
1.30	1.0213	.8218	.2593
1.50	1.0400	.8277	.2025

TABLE XIII. *Coulomb functions for* $y=0.1467$; $r_0 \leqq 3e^2/mc^2$.

$2\pi\eta$	Φ_0^*/Φ_0	$\Phi_0\Theta_0$	$C_0^2\rho\Phi_0^2$
0.95	0.798	0.586	0.560
1.00	.837	.620	.535
1.05	.869	.649	.509
1.10	.896	.673	.484
1.15	.919	.694	.459
1.20	.939	.711	.435
1.30	.971	.738	.390
1.50	1.016	.769	.312

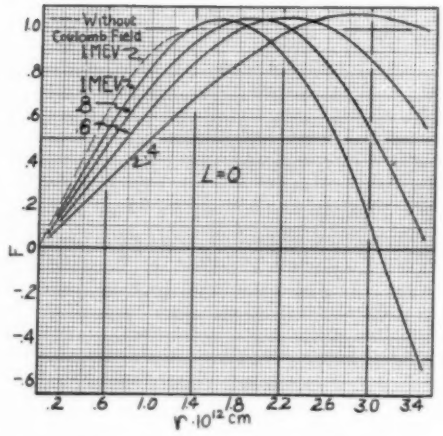

FIG. 1. Coulomb wave functions for $L=0$. Normalization is such as to give unit amplitude of sine wave at ∞.

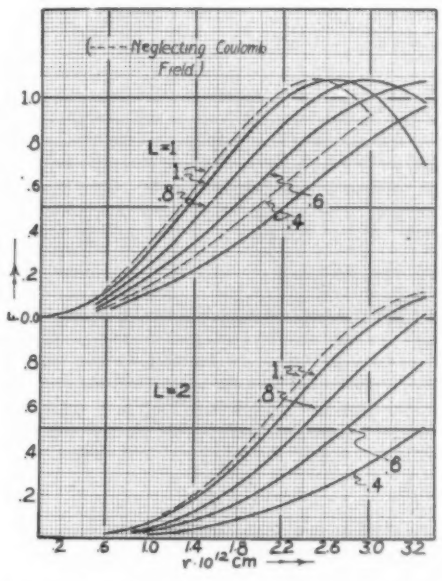

FIG. 2. Coulomb wave functions for $L=1$, 2. Normalization is such as to give unit amplitude of sine wave at ∞.

evidence against this K_0 will be seen to be contained in the experiments of THH. Combined evidence from all sources thus indicates only one of the two essentially different values of K_0 to be probable. In order to account for this value it becomes necessary to use approximate resonance of the s wave with the potential hole because the scattering anomaly is great. The expected scattering is then sensitive to the depth of the hole and nearly the same value of the depth is obtained for different values of scattering. By using the interaction energy $Ae^{-(r/a)^2}$ White's values are fitted with $A=45mc^2$ and $a=2.2\times10^{-13}$ cm. Between 450 and 600 kv his experiments show agreement with Coulomb scattering. The potential determined from the 600–750 kv range was used to calculate the scattering for energies between 450 and 600 kv. A value roughly six times Mott's was obtained. The disagreement between theory and experiment is here very definite and it is hard to account for it by any simple modification of the theory. Briefly White's angular distribution and voltage dependence of scattering do not allow of a simple theoretical explanation. The effects observed at a scattering angle of 45° for energies between 600 and 750 kv give nevertheless an interaction energy which is in approximate agreement with that found by THH, as will be seen presently.

The observations of THH will now be discussed and it will be seen that most of the scattering anomaly observed by them can be accounted for by the distortion of the s wave. At small scattering angles there are effects calling for p and perhaps d wave distortions. These effects are at present not decided enough to be regarded as definitely real. Nevertheless, they will be considered so as to give an idea of the reliability of the conclusions regarding the magnitude of the interaction potential. It will be seen that, aside from uncertainties having to do with the higher phases (p and d wave distortions), one can obtain very accurate values of the interaction energy from the experiments on the scattering of protons by hydrogen; the uncertainties due to higher phase shifts will be seen to be relatively small. The interaction energy derived from scattering experiments is in good agreement with that obtained from mass defect calculations.

The results of THH for $\mathbf{P}/\mathbf{P}_M$ at 900 kv are plotted in Fig. 4. The broken curve is drawn smoothly through their points. The full curves give the theoretical dependence of the scattering anomaly on the scattering angle when 30° and 31° are used for the phase shift K_0. Experiment and theory are seen to agree nicely at this energy.

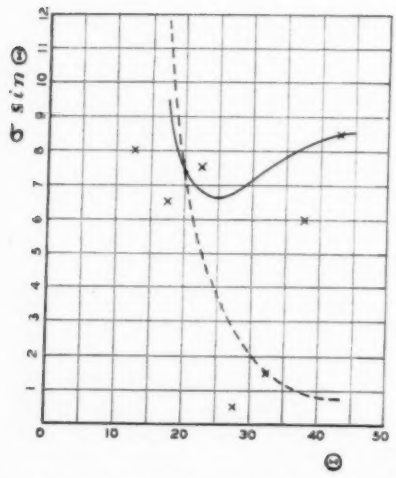

FIG. 3. White's data. Number of collisions of 600–750 kv protons within a 5° range plotted against angle. The experimental points are as communicated to us by Dr. White from his more complete data.

In Fig. 5 observations at 800 kv are compared with theory. It will be noted that here the agreement is less satisfactory if one uses only the s wave phase-shift K_0. At small angles there is relatively too much scattering. Thus if the experimental data are fitted in the neighborhood of 45° then one expects about 15 percent less scattering at 25° than is actually observed. It will be noted that this discrepancy is independent of the precise value which is used for $\mathbf{P}/\mathbf{P}_M$ at $\Theta=45°$. Thus at $\Theta=20°$ and 15° the curves for $K_0=26°$ and 28° give nearly the same $\mathbf{P}/\mathbf{P}_M$ while at $\Theta=45°$ the values of $\mathbf{P}/\mathbf{P}_M$ which correspond to these K_0 differ by about 0.6 in a total of 3. The estimated error of the observations is shown on the same graph for some of the points. It is at the most 0.1 in the neighborhood of $\Theta=45°$. There is also an uncertain error in the measurement of the scattering angle which is important for small Θ. It is not clear, however, why this error should matter at 800 kv and not at 900 kv. Curves for $K_0=30°$ and $K_0=35°$ are drawn in in order to show what happens when one attempts to fit the data at small Θ. There is then no indication of agreement between theory and experiment from $\Theta=30°$ on to higher values. At the bottom of the graph is shown the contribution to $\mathbf{P}/\mathbf{P}_M$ which may be expected on account of a distortion of the p wave by a phase shift $K_1=-1°$. This has a relatively insignificant effect for values of Θ between 35° and 45° and it raises the theoretically expected values by the necessary amount to agree with experiment from $\Theta=15°$ to 30°. The data in their present form thus indicate $K_0=26°$ and $K_1=-1°$ at 800 kv. Similarly in Fig. 6 comparisons between theory and experiment are made for 700 kv and 600 kv. At these energies and at high scattering angles the observations are supposedly more difficult on account of the increased importance of the stopping power of the window in the electrical counter. Thus at 600 kv and $\Theta=40°$ the experimental point is known to be definitely too low and for this reason the experimental curve is drawn in by THH somewhat higher than the number of observed particles at this angle would indicate. It is difficult to be sure of the angular distribution curves sufficiently to make a definite phase angle analysis possible. The difference between the experimental and theoretical $\mathbf{P}/\mathbf{P}_M$ at 800 kv amounts to roughly 0.1 at $\Theta=20°$ which when attributed to the distortion of the p wave gives roughly $-\frac{1}{2}°$ for K_1. There is thus an indication that the phase shift K_1 is present from 600 kv to 800 kv and that it is negligible at 900 kv. Such a variation of K_1 is contrary to all expectation for forces of such spatial extension as is usually assumed in theories of nuclear structure. Thus according to Fig. 2 and Eq. (8.1) the distortion of the p wave would have to be attributed to potentials extending to 3×10^{-12} cm. Otherwise Fig. 2 shows that F_1^2 will increase with E much too rapidly to make such a behavior of K_1 possible. In order to account for $K_1=-1°$ at 1 mev one would need roughly an interaction energy of 10 kv extending through a distance of 10^{-12} cm. The Coulomb energy at 3×10^{-12} cm is about 50 kv. There appears to be at present no other evidence of such long range forces that is at all definite.

Quantitative conclusions about K_0 and K_1 are sensitive to possible effects of K_2. If K_1 is due to an interaction extending as far out as the above estimates would indicate then appreciable values of K_2 would also be expected. This is seen again from Fig. 2 by comparing the wave functions for $L=2$ with those for $L=1$. Fig. 7 shows qualitatively the effect of combining the effects of $K_0=35°$ and $K_2=2.2°$. This curve should be

compared with that representing the effect of $K_0=29°$ and $K_2=0$ shown in the same figure. The difference in shape is seen to be relatively slight and it will be noted that it corresponds to the difference in shape between the experimental curves for 900 kv and 800 kv and the corresponding theoretical curves in Fig. 4 and Fig. 5 in that slightly higher values of $\mathbf{P}/\mathbf{P}_M$ are obtained in the region of 30–35°. The same applies to Fig. 6 for 700 kv while at 600 kv the angular distribution is well represented by K_0 alone. Less weight should be given to 600 kv because the number of observations is smaller and none were possible at 45°. The present data are seen to agree better with a combination of K_0, K_1, K_2 than with K_0 alone. To some extent this is doubtless due to the larger number of available parameters. The signs of K_1, K_2 suggested by the above discussion of the experiments are such as to correspond to attractive forces for $L=2$ and to repulsive forces for $L=1$. These are the signs which would be expected if the interaction were representable by a pure Majorana exchange operator or by the linear combination of Wigner and Majorana potentials which is expressible as a spin-spin interaction.[5, 13] Agreement in sign between the empirical and the expected phase shifts is an argument in favor of their reality. This argument is not very strong because the interaction potential for $L=0$ may change sign between the long range region of 3×10^{-12} cm and the short range region 3×10^{-13} cm. The value of K_0 derived from scattering at 45° does not depend on K_1 but is quite sensitive

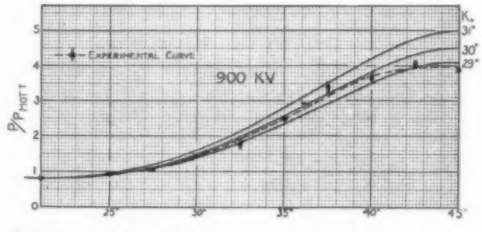

FIG. 4. Angular distribution of scattering anomaly at 900 kv according to THH. Statistical error as estimated in the observations is indicated where it exceeds size of dot. Points at small angles may be in error on account of difficult angle measurement. Some points in this and in Figs. 5 and 6 do not correspond to latest revision of data from which they differ by amounts insignificant for interpretation.

[12] J. H. Van Vleck, Phys. Rev. **48**, 367 (1935).

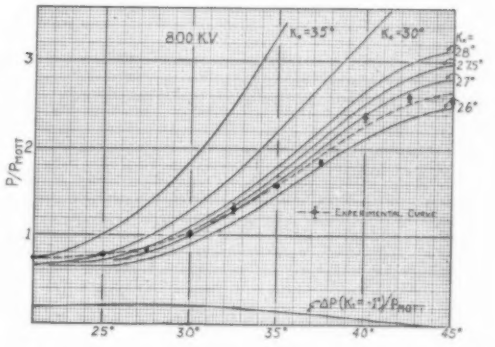

FIG. 5. Same as Fig. 4 but for 800 kv. Curve at bottom gives effect of K_1.

to the presence of small amounts of K_2. It is seen from Fig. 7 that inclusion of $K_2=2.2°$ in the theoretical analysis makes it necessary to change K_0 from 29° to about 36°. Such a change in K_0 will be seen to have serious consequences on the possible interpretation of the change of K_0 with energy as well as on the comparison of the proton-proton with proton-neutron interactions.

In the above discussion it was supposed that the main effect is due to K_0 which is a reasonable hypothesis on present views regarding the range of nuclear forces. As has been already noted in connection with White's experiments there are for any scattering angle essentially two values of K_0 which account for a given experimental value of $\mathbf{P}$. In the discussion of angular distributions due to K_0 alone the effect of an addition of π to K_0 cannot be noticed. To every K_0 in the first quadrant there corresponds another possible K_0 in the third and to every K_0 in the second quadrant there corresponds another possible K_0 in the fourth. For the present purpose one can consider values of K_0 differing by π as equivalent. They are also equivalent for the purpose of drawing conclusions about the interaction potential for $L=0$ using K_0, because only $\tan K_0$ enters into the expression for $\rho F_i'/F_i$. Aside from this duplicity it is possible to fit the experimental values by means of K_0 lying either in the first or in the fourth quadrant. The possibilities in the fourth quadrant were not considered above. For such K_0 the values of $\mathbf{P}/\mathbf{P}_M$ remain consistently above unity while according to the experimental points presented in Figs. 4, 5, 6 the actual $\mathbf{P}/\mathbf{P}_M$ drop below unity for small scattering angles in

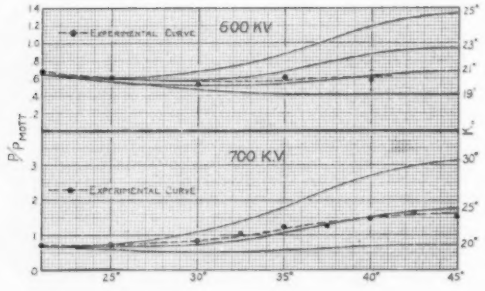

FIG. 6. Same as Fig. 4 for 600 kv and 700 kv.

all cases. At 600 kv $\mathbf{P}/\mathbf{P}_M$ remains in fact below 1 for all angles at which observations were made. In addition the dependence of $\mathbf{P}/\mathbf{P}_M$ on the scattering angle for all voltages experimentally examined is represented poorly by means of such K_0 even for those angles for which $\mathbf{P}/\mathbf{P}_M<1$. If values of K_0 in the fourth quadrant were to be seriously considered one would need to use large values of the phase shifts for higher L in order to bring about agreement with the observed angular distributions. The difference between the first and fourth quadrant for K_0 can be understood qualitatively as follows. The interaction potential which exists in addition to that representing the inverse square law may be imagined to be either increased or decreased by small amounts starting with zero. If it is increased one gets repulsive forces and values of K_0 in the fourth quadrant; if it is decreased the forces are attractive and K_0 is positive. In the first case the repulsive forces reinforce the Coulombian effect and a larger scattering is to be expected. For attractive forces the Coulombian effect is partly counteracted and a smaller scattering should be found. If, however, the attractive force is made sufficiently great then the Coulombian effect may be practically entirely overcome and the scattering will become nearly zero. As the attractive force is increased further the scattering becomes due primarily to the attraction and may exceed that which would exist if only the Coulombian force were acting. Qualitatively this corresponds to the condition of the theoretical curves shown for 900 kv in Fig. 4 for most of the scattering angles. At small scattering angles the effect of the inverse square field on the wave function becomes great and is sufficient to partly neutralize the effect of attraction so that $\mathbf{P}/\mathbf{P}_M$ again becomes <1. As the energy of the incident protons decreases the effect of the attraction becomes less pronounced since the proton penetrates into the attractive region with greater difficulty. The region of $\mathbf{P}/\mathbf{P}_M<1$ thus moves towards higher scattering angles. These qualitative features of the attractive potentials which correspond to the values of K_0 in the first quadrant are in good agreement with the data which appear to give very *direct evidence against repulsions and for attraction inside the nucleus*. Further evidence in favor of this view will be found in a quantitative discussion of the variation of the scattering anomaly with energy.

In Figs. 8, 9, 10, 11 calculations with "square wells" are compared with experiment. The interaction potential is here constant for $0<r<r_0$ and its value will be referred to as $-D$. For $r>r_0$ the potential is supposed to be Coulombian. The curves represent the theoretical dependence of K on the energy. In Fig. 8, r_0 was taken to be $e^2/2mc^2 \leqq 1.4\times10^{-13}$ cm. The three curves correspond to $D=47.9$, 47.0, 46.3 mev. The ovals mark the values of K_0 derived from the data of Figs. 4, 5, 6 using scattering close to 45° and neglecting possible effects of K_2. The dotted curve gives the theoretical dependence of K_0 on the energy when $r_0=0$. This curve may be raised or lowered by approaching the limit of $r_0=0$ in different ways. Its shape does not vary greatly when this is done. The same curve is reproduced in Figs. 9, 10, 11 so as to give a standard of comparison. No relativistic corrections and no spin forces were taken into account in the calculation of the curves. The experimental

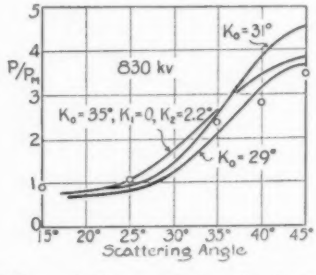

FIG. 7. Effect of K_2 on angular distribution. Circles represent experimental points as obtained by THH in their first set of experiments. These points should be lowered by 13 percent on account of a geometrical correction.

points are seen to be in good agreement with $D=47.0$ Mev. It will be noted from the figure that D is determined by this fit with an apparent accuracy of about 0.2 Mev. In order to illustrate this sensitivity the differences in the values of D were used accurately even though the absolute values are perhaps not quite accurate for each r_0. These depend on the correctness of numerical conversion factors such as that occurring in Eq. (8). (Comparisons with neutron-proton forces will be made without demanding great accuracy of the conversion factors and the absolute values of D.) The heavy straight line cutting obliquely across the three curves gives an average of the dependence of K_0 on E in an earlier set of data taken by THH. This is drawn in because it illustrates how hard it would be to fit these earlier data by means of a simple theory. It should be noted that with the plausible potentials used here such steepness cannot be attained and that, therefore, the rate at which K_0 varies with the energy can be used to rule out some kinds of interactions. Fortunately the newer data represented by ovals are free of this troublesome feature. In Figs. 9, 10, 11 similar comparisons of empirical and theoretical calculations for K_0 are made for $r_0=e^2/mc^2$, $2e^2/mc^2$, $3e^2/mc^2$, respectively. The theoretical dependence for $r_0=3e^2/mc^2$ is seen to fit experiment poorly.

The theoretical curves for $r_0=0$, $e^2/2mc^2$, e^2/mc^2, $2e^2/mc^2$ are seen to be in fair agreement with observation. The interval from $E=700$ kv to 900 kv appears to be too small to make it possible to determine r_0 to a higher accuracy. Inspection of the curves shows that *in a larger energy interval more precise information about r_0 should be obtainable.* It should be noted that the interaction energy $-D$ is determinable with great accuracy in all the cases considered as is obvious from the graphs. It would nevertheless be premature to claim at present an absolutely precise determination of the depth of the potential well because the question of the possible presence of the higher phase shifts has not been settled. Although it appears probable that K_2 is not the largest phase shift it is seen that a small positive K_2 of less than 2° would necessitate using a K_0 larger than what has been used by about 5°. The whole difference between the curves corresponding to $D=-47.9$ and 47.0

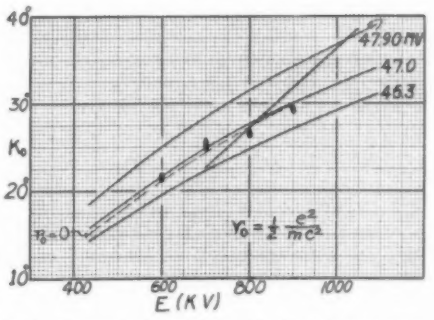

FIG. 8. Theoretical variation of K_0 with proton energy for an interaction energy constant within $r_0=e^2/2mc^2=1.4\times10^{-13}$ cm. Coulombian potential is supposed to be inoperative for $r<r_0$. Ovals represent values of K_0 derived from the newer experiments of THH using data near $\Theta=45°$. Straight line gives average of the first set of data of THH. Dashed line represents theoretical behavior for $r_0=0$. Numbers like 47.0 refer to negative of interaction energy in mev.

Mev amounts to roughly 4° in K_0. The graphs of Figs. 8, 9, 10, 11 thus give an exaggerated impression of accuracy if K_2 is of importance, i.e., if the forces extend to large distances, even to a small degree.

In Fig. 12 are given theoretical and experimental values of $\mathbf{P}/\mathbf{P}_M$ as a function of E for scattering at 45°. The experimental values are indicated by ovals. The full lines refer to $r_0=0$ and $r_0=e^2/2mc^2$. All of the theoretical curves are labeled by means of two numbers such as 1, 10.03. The first of these gives the radius r_0 in units of e^2/mc^2. The second gives the depth in mev. For $r_0=0$ the graph is extended to low energies. It will be noted that around 400 kv the scattering at 45° should become very small as a consequence of dealing with an attractive potential. As the energy is decreased towards 100 kv the penetration through the Coulombian barrier becomes small and the attractive potential ceases to be effective. From 100 kv down one may expect the scattering to obey Mott's formula closely, in agreement with the experiments of Gerthsen.[14] However, even the relatively low energy of 200 kv is definitely of interest in drawing conclusions about forces between protons, since the scattering can be expected to be roughly ½ of Mott's value in this region. The sensitivity of $\mathbf{P}/\mathbf{P}_M$ to the magnitude of the interaction energy is even more striking than the

[14] C. Gerthsen, Ann. d. Physik **9**, 769 (1931).

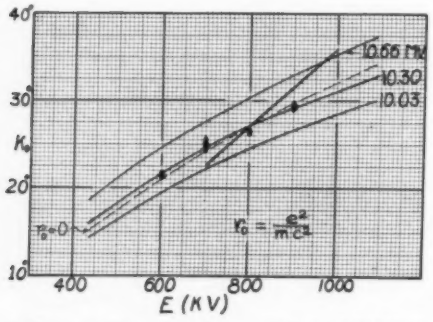

FIG. 9. Same as Fig. 8 but for $r_0=e^2/mc^2=2.8\times10^{-13}$ cm.

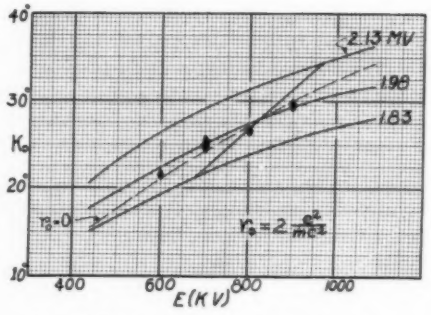

FIG. 10. Same as Fig. 8 but for $r_0=2e^2/mc^2$.

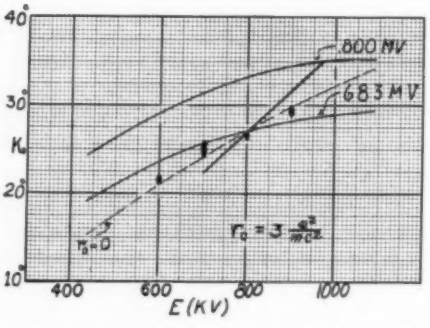

FIG. 11. Same as Fig. 8 but for $r_0=3e^2/mc^2$. Note insufficient slope of theoretical curve.

sensitivity of K_0. Thus the difference between $r_0=e^2/mc^2$, $D=10.30$ Mev and $r_0=e^2/mc^2$, $D=10.03$ Mev is quite unmistakable, and the latter value is seen to be definitely excluded by comparison with experiment. Comparison of observation at 800 kv with that at 900 kv favors values of $r_0<e^2/mc^2$ while comparison of 700 kv with 800 kv is in better agreement with somewhat larger ranges. This comparison is of course theoretically equivalent to that made in Figs. 8, 9, 10, 11, but it puts relatively more emphasis on the 900 kv point on account of the sensitivity of $\mathbf{P}/\mathbf{P}_M$ to K_0 in this region. As before, the apparent precision in the determination of the depth of interaction may be deceptive on account of the possible presence of higher phase shifts.

Dr. J. A. Wheeler in his work on the scattering of alpha-particles has developed a criterion which makes it possible to eliminate certain kinds of potentials. This criterion will now be used to give an additional argument against the second possibility for K_0 which is due to the fact that it is related to $\mathbf{P}$ by an equation having two roots. The point of Wheeler's criterion is that the quantity $\rho F_i'/F_i$ must decrease with energy as a consequence of Green's theorem. According to Figs. 8, 9, 10, 11, 12, the K_0 which was used varies approximately as would be expected. For the other possible K_0 the following numbers are obtained at $r_0=2e^2/mc^2$ using Eq. (7.8). At 700 kv, $K_0=-4.1°$, $\rho F_i'/F_i=1.30$; at 800 kv, $K_0=-7.3°$, $\rho F_i'/F_i=1.54$; at 900 kv, $K_0=-11.3°$, $\rho F_i'/F_i=1.97$. These numbers show that $\rho F_i'/F_i$ would have to increase with energy if these K_0's were true. In the light of this, combined with the angular dependence as well as the presence in the experimental data of regions in which $\mathbf{P}/\mathbf{P}_M<1$ *one must consider the choice of* K_0 *made here as correct* provided higher phase shifts do not interfere with the analysis. If there were even an infinite repulsive interaction through e^2/mc^2 one would expect K_0 to be approximately $-11.3°$ and it is thus *impossible to use repulsive interactions* in s states for the explanation of the data both on account of the wrong energy dependence and on account of the difficulty of obtaining a sufficiently large scattering anomaly. In addition the angular dependence of the scattering anomaly would be wrong. It is satisfactory to have the data point so definitely to one rather than two possibilities of interpretation.

In Fig. 13 graphical comparisons are made between the observed scattering and the Gauss error potential $-Ae^{-ar^2}$. This potential is supposed to be present in addition to the potential e^2/r which represents the Coulombian interaction. With mc^2 as the unit of energy and $\hbar(Mm)^{-\frac{1}{2}}c^{-1}=8.97\times10^{-13}$ cm as the unit of length the

equation for $\mathfrak{F}$ is

$$\left[\frac{d^2}{dr^2}+E'-\frac{0.312}{r}+Ae^{-\alpha r^2}\right]\mathfrak{F}=0.$$

By introducing $x=\alpha^{\frac{1}{2}}r$ and letting α, A have the probable values 17, 40 this becomes

$$\left[\frac{d^2}{dx^2}+\frac{E'}{17}-\frac{0.075(7)}{x}+2.35(4)e^{-x^2}\right]\mathfrak{F}=0. \quad (9)$$

The quantity $-0.0757/x+2.354e^{-x^2}$ can be regarded as the negative of the potential energy in units of 17 mc^2. It is plotted against x in the figure. The quantity $-0.0757/x$ corresponds to the Coulombian potential and is also plotted for comparison in the same figure. The potential is seen to be very nearly Coulombian at $x=2.6$ which corresponds to $r_0 \leqq 2e^2/mc^2$. There are three curves in the figure going through the origin which represent wave functions. Two of them are marked $E'=0$, $2E'=800$ kv. They are regular solutions of Eq. (9) corresponding to these values of E'. The third is marked f and is a regular solution of

$$d^2f/dx^2+2.66e^{-x^2}f=0. \quad (9.1)$$

This equation corresponds approximately to the condition of having $df/dx=0$ at large distances which makes the stationary level of the two particles in each other's field fall at $E'=0$. The function f will be used later in order to obtain the value of A for the proton-neutron interaction as well as in order to check on calculations using Eq. (9). The value of the constant multiplying factor for $\mathfrak{F}$ was not determined here by joining to the Coulomb wave functions. This factor cancels out in the applications. Corresponding to these three curves there are three other graphs starting from the point 2.0 on the axis of ordinates which represent $xd\mathfrak{F}/\mathfrak{F}dx$ and xdf/fdx. The uppermost of these carries the label $E=0$ at its right-hand end. It corresponds to the solution of Eq. (9) for $E=0$. The lowest gives values of xdf/fdx and is labeled by Eq. (9.1) at its lowest right-hand end. The intermediate curve of the set corresponds to $E=2E'=800$ kv. It should be compared with the curve marked 800 kv among the three pointed out as "experimental values of $rd\mathfrak{F}/\mathfrak{F}dr$" on the figure. These "experimental values of $rd\mathfrak{F}/\mathfrak{F}dr$" are obtained from empirical values of K_0 by means of Eq. (7.8), neglecting higher phase shifts, for the energies of 680 kv, 800 kv, 980 kv, respectively. For any r these curves give the value of $rd\mathfrak{F}/\mathfrak{F}dr$ which corresponds to an experimental K_0 provided the field is Coulombian at all distances greater than this r.

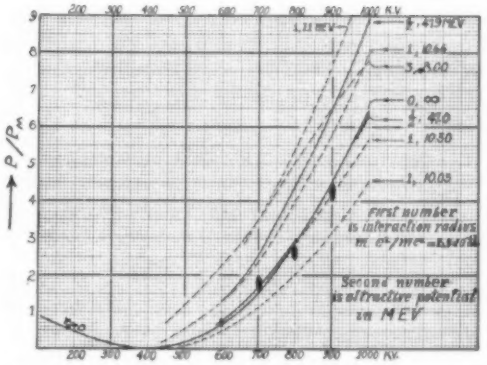

FIG. 12. Theoretical variation of $\mathbf{P}/\mathbf{P}_M$ with energy at a scattering angle of 45°. Curves are labeled by two numbers. First number gives the interaction radius of square well (r_0) in units of $e^2/mc^2=2.82\times10^{-13}$ cm. Second number gives the negative of interaction potential in mv. The ovals are obtained from the second set of data of THH using theoretical angular distribution curves fitted to experiment at higher scattering angles.

Comparison of the theoretical and experimental curves for $rd\mathfrak{F}/\mathfrak{F}dr=xd\mathfrak{F}/\mathfrak{F}dx$ at 800 kv shows, as is clear from the graph, that the two curves are very nearly the same for $x=2.6$ on towards larger r and that therefore the values of A and α used here are nearly right. The values of Feenberg and Knipp are $\alpha=17$, $A=41$ and the agreement is seen to be satisfactory. It is to be noted that Feenberg and Knipp considered two possibilities. In one of these the neutron-proton interaction was taken to be represented by a Majorana exchange operator. It gave $A\sim26$ for the proton-proton and neutron-neutron interactions using the same α. In the other possibility Wigner's suggestion of using different interactions in the singlet and triplet states of the deuteron was used by regarding the proton-neutron interaction as a linear combination of a Majorana and a Heisenberg exchange operator. This view gave rise to the proton-proton and neutron-neutron interactions being represented by the Gauss error potential with $A=41$ and $\alpha=17$. There is on the

whole a remarkable qualitative consistency in the way in which the proton-neutron scattering, the mass defects of H^2, He^3, H^3, He^4 and the proton-proton scattering fit in with each other. *The data on the scattering of protons in hydrogen are seen to speak definitely in favor of using different neutron-proton interactions in singlet and triplet states and make a pure Majorana force between neutrons and protons improbable.*

5. More Accurate Determinations and Comparisons with the Neutron-Proton Potential

It has been pointed out that, once definite values are assigned to the higher phases and to the range of the forces then accurate information can be obtained about the magnitude of the interaction potential. This is due to the fact that the experimental scattering anomaly is rather large and requires for its explanation interaction energies giving rise to approximate resonance. Thus the depth of the "square well" which was used to fit the data for $r_0=e^2/mc^2$ is 10.3 Mev while the depth of the "square well" required to give a virtual level at $E=0$ is 12.8 Mev. Qualitatively this condition is similar to that in the interaction of a proton and neutron in their singlet S state. In order to account for the large scattering of slow neutrons in hydrogen it is necessary to suppose that there is either a virtual or a stationary ^1S level of the proton and neutron in their mutual field. Evidence as to whether the level is stationary or virtual is very scant. It appears of interest to see whether it is possible to consider the proton-proton and proton-neutron interactions to be identical in the ^1S states. We are indebted to Dr. L. A. Young, who made estimates analogous to and qualitatively agreeing with those presented here, for pointing out to us that one should not neglect to correct the depth of the "well" for the position of the stationary or virtual level in the neutron-proton potential.

In addition one must consider with greater care the possible effect of a Coulomb potential within the "square well." If it is supposed that the Coulombian force acts everywhere, a closer agreement is obtained between proton-proton and proton-neutron potentials than on the assumption that it acts only outside the square

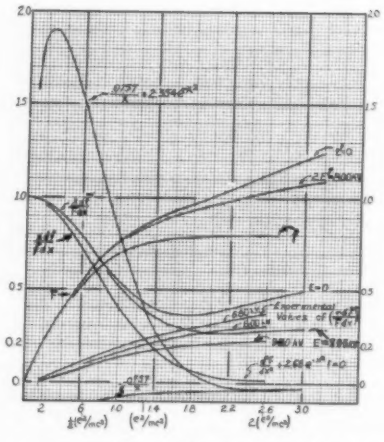

Fig. 13. Comparison of observation with the potential Ae^{-ar^2}. Curve marked $-0.0757/x+2.354e^{-x^2}$ represents negative of potential energy in units of $17mc^2$. Coulombian part is shown by $-0.0757/x$. Note approximate agreement of experimental value of $rd\mathfrak{F}/\mathfrak{F}dr$ for 800 kv with corresponding theoretical curve for $xd\mathfrak{F}/\mathfrak{F}dx$. In the figure $\mathfrak{F}$ is written as F with a bar over it.

well ($r>r_0$). Since the range of interaction is not definitely determined by either the proton-proton or the proton-neutron scattering experiments, comparisons are listed below in Table XIV, for three values of the interaction radius r_0. The depth of the square well is given in Mev. The first row in the table gives the radius in units of e^2/mc^2. The second row $D_{\pi\pi}$ gives the depth that is obtained if the Coulomb potential does not act inside the well. The third row gives similarly the depth, if the potential inside the well is taken to be $-D_{\pi\pi}{}^c+e^2/r$. In order to counterbalance the effect of the repulsion the depth has to be increased by roughly mc^2. The fourth row gives the depth required to give a virtual or stationary level at $E=0$ taking the potential energy to be $-D$ inside the well and zero outside. In the fifth row $D_{\pi p}$ gives the depth for the proton-neutron interaction required to give a virtual level at 43 kv

Table XIV. *Comparison of proton-proton and proton-neutron singlet S interactions.*

$r_0mc^2/e^2=$	1/2	1	2
$D_{\pi\pi}$ =	47.0	10.3	1.98
$D_{\pi\pi}{}^c$ =	48.7	11.1	2.42
$(D)_{E=0}$ =	51.2	12.8	3.20
$(D_{\pi p})_{43}$ =	49.3	11.9	2.73
$(D_{\pi p})_{130}$ =	48.0	11.2	2.38

which corresponds to a collision cross section of 30×10^{-24} cm^2 for slow neutrons scattered by protons. The sixth row gives D_{tt} using 130 kv for the position of the virtual level. The third and fifth rows agree fairly well indicating that the proton-proton force acting in addition to the Coulombian may be equal to the proton-neutron force in states with antiparallel spins. The third and sixth rows agree still better.

Although the numbers in the above comparison suggest very strongly that they are actually the same, caution in drawing this conclusion should be exercised for the following reasons: (a) It was not known until recently whether the neutron-proton interaction should be taken so as to give a virtual or a stationary level. If the level were stationary rather than virtual the depth for $r_0=e^2/mc^2$ would be 13.7 Mev and there would be then no agreement between D_{tt} and $D_{tt}{}^c$ for this r_0. However, the recent experiments of Fermi and Amaldi[6] show that the level is virtual and indicate that $D_{tt}=D_{tt}{}^c$. (b) The theoretical value of the neutron-proton scattering cross section is in disagreement with the experiments of Goldhaber.[7] Goldhaber's experiments are, however, contradicted by those of Tuve and may be considered as probably incorrect. (c) The values of D_{tt} and $D_{tt}{}^c$ are sensitive to the value of K_2 which is used in the interpretation of proton-proton scattering experiments. (d) The numbers given in the third row of Table XIV for $D_{tt}{}^c$ would give a smaller scattering cross section of slow neutrons in hydrogen than 30×10^{-24} cm^2 by roughly a factor of four and the values of D_{tt} given in the fifth row would give larger cross sections for proton-proton scattering at 45° by roughly a factor of 1.3. The sixth row in Table XIV corresponds to the measurements of Fermi and Amaldi and indicates a practically perfect agreement with D_{tt} for reasonably large values of r_0. The agreement is poorer for $rmc^2/e^2=\frac{1}{2}$ but this is a smaller range of force than is usually considered probable.

In order to be sure of the differences $\delta D=D_{tt}{}^c-D_{tt}$ the calculations were carried out by two methods one of which is a direct calculation using Coulomb wave functions inside the "well." The other is a perturbation calculation using D_{tt} as a starting point. For the direct calculation only the regular wave function inside the "well" need be known. The main part of this function is the same as though there were no Coulomb field and it is convenient to arrange the series so as to take this into account. The functions Φ_0, $\Phi_0{}^*$ of Eq. (7.4) can be expressed as

$$\begin{aligned}\Phi_0&=\sin z/z+c_1y+c_2y^2+\cdots;\\ \Phi_0{}^*&=\cos z+2c_1y+3c_2y^2+\cdots,\end{aligned}\tag{10}$$

where z is given by Eq. (8) and the coefficients are

$$c_1=1,\quad c_2=\frac{1}{3},\quad c_3=\frac{1}{18}-\frac{1}{9\eta^2},\quad c_4=\frac{1}{180}-\frac{1}{36\eta^2},$$

$$c_5=\frac{1}{2700}-\frac{1}{270\eta^2}+\frac{23}{5400\eta^4},$$

$$c_6=\frac{1}{56700}-\frac{1}{3240\eta^2}+\frac{7}{8100\eta^4}.$$

The perturbation calculations were made using the formula

$$\delta D=\frac{e^2}{r_0}\frac{z\int_0^z(\sin^2 z/z)dz}{\int_0^z\sin^2 z\,dz}=\frac{e^2z}{r_0}\frac{\ln 2z+0.5772-Ci(2z)}{z-\sin z\cos z}\tag{10.1}$$

with $$Cix=-\int_x^\infty\frac{\cos u}{u}du.$$

The two methods of calculation agree to the desired accuracy. This fact is of practical interest if exact calculations are more difficult to perform than those with "square wells." Use of the validity of the perturbation method will now be made for an improvement on calculations with the Gauss error potential. The general relations needed for extensions of the perturbation method are as follows. A given differential equation

$$[(d^2/dr^2)-E'+\lambda\chi(r)+A\varphi(r)]\mathfrak{F}=0\tag{10.2}$$

of the type considered here has, to within an arbitrary constant factor, one and only one solution which is regular at $r=0$. For such a solution $rd\mathfrak{F}/\mathfrak{F}dr$ is, therefore, uniquely defined. It may be considered as a function of E', A and λ.

Using Green's theorem one obtains

$$\mathfrak{F}_1\mathfrak{F}_2\left[\frac{1}{\mathfrak{F}_1}\frac{d\mathfrak{F}_1}{dr}-\frac{1}{\mathfrak{F}_2}\frac{d\mathfrak{F}_2}{dr}\right]+(A_1-A_2)\int_0^r\varphi\mathfrak{F}_1\mathfrak{F}_2dr=0$$

and similar equations with E' and λ. In the limiting cases $A_1=A_2$, $\lambda_1=\lambda_2$, $E_1'=E_2'$ they become:

$$\begin{aligned}\frac{\partial}{\partial\lambda}\left(\frac{\partial\mathfrak{F}}{\mathfrak{F}\partial r}\right)&=-\frac{1}{\mathfrak{F}^2}\int_0^r\mathfrak{F}^2\chi dr;\\ \frac{\partial}{\partial A}\left(\frac{\partial\mathfrak{F}}{\mathfrak{F}\partial r}\right)&=-\frac{1}{\mathfrak{F}^2}\int_0^r\mathfrak{F}^2\varphi dr;\\ \frac{\partial}{\partial E'}\left(\frac{\partial\mathfrak{F}}{\mathfrak{F}\partial r}\right)&=\frac{1}{\mathfrak{F}^2}\int_0^r\mathfrak{F}^2dr.\end{aligned}\qquad(10.3)$$

These formulas are useful for the following applications: (a) The determination of the change which must be made in A in order to compensate for a given change in λ so as to leave the phase shift unaltered. This is possible by means of Eqs. (10.3) as long as the rates of change of $\partial\mathfrak{F}/\mathfrak{F}\partial r$ with λ and A are nearly constant. For all that is required is to leave $\partial\mathfrak{F}/\mathfrak{F}\partial r$ unchanged at the boundary of the "well." Eq. (10.1) can be obtained by this procedure by regarding $\chi(r)$ as arising from the Coulombian energy. (b) From the values of the phase shift K_0 one can obtain $\partial\mathfrak{F}/\mathfrak{F}\partial r$ for definite energies and hence from the last Eq. (10.3) the quantity $(1/r\mathfrak{F}^2)\int_0^r\mathfrak{F}^2dr$ can be determined. It may be considered as a rough form factor of the wave function. By means of the form factor information can also be obtained about the character of the interaction potential. Thus the first set of data of THH indicated a variation of K_0 such as is shown by the straight line in Figs. 8, 9, 10, 11. Computing $(1/r\mathfrak{F}^2)\int_0^r\mathfrak{F}^2dr$ from the variation of $\partial\mathfrak{F}/\mathfrak{F}\partial r$ with energy gives then values >1 for the form factor which cannot be explained by the simple potentials used here but would have required other less probable possibilities. This is in agreement with the fact that the older data of THH and the data of White gave a more rapid variation of K_0 with energy than would be expected for $r_0=0$. The same effect is shown by the two curves for "experimental values of $r\partial\mathfrak{F}/\mathfrak{F}\partial r$" of Fig. 13 which are marked by 680 kv and 980 kv. These were computed for the old data of THH which were represented by straight lines in Figs. 8, 9, 10, 11. Comparing them with the theoretical curves for $E=0$ and $E=800$ kv the experimental variation of $r\partial\mathfrak{F}/\mathfrak{F}\partial r$ is found to be too great. It will be seen presently, however, that the newer data which were taken at 900, 800, 700 and 600 kv give an energy dependence of K_0 and of $r\partial\mathfrak{F}/\mathfrak{F}\partial r$ which is in approximate agreement with expectation for the Gauss error potential used for Fig. 13.

In order to improve the comparison of the Gauss error potential obtainable from proton-proton scattering with those derivable from mass defects and from neutron-proton scattering, calculations were made in which the field was supposed to become Coulombian for $r>2e^2/mc^2$ while for $r<2e^2/mc^2$ the potential was taken as in Eq. (9). By means of Eq. (10.3) the value of A used in Eq. (9) was then corrected so as to give the experimental value of $r\partial\mathfrak{F}/\mathfrak{F}\partial r$ at $r=2e^2/mc^2$ for $E=800$ kv. This calculation gave $A=38.5$ in units of mc^2 which is slightly lower than Feenberg and Knipp's value of $A=41$. It should be noted that if a small positive K_2 is present this value of A should be raised and that therefore the agreement with Feenberg and Knipp may be better than $A=38.5$ would indicate. For comparison with neutron-proton interactions it is desirable to eliminate cumulative errors which might be present in the numerical integration. This was done by using the solution for a stationary level at $E=0$ in the absence of a Coulomb field as a starting point for the determination of both the $\pi\pi$ and the $\pi\nu$ potentials. For $A_{\pi\pi}$ this method of calculation is not very accurate because the shape of the wave function changes appreciably between the initial condition and the final one. The value of A obtained for a stationary level at $E=0$ is 45.7. The result of applying the perturbation method using the wave function in this state (see curve marked f in Fig. 13) is to give $A_{\pi\pi}=40.9$. Using the wave function in the final state (marked 2 $E'=800$ kv in Fig. 13) we get $A_{\pi\pi}=37.8$. The mean from the two perturbation calculations is 39.3 which is somewhat higher than that obtained by direct calculation. The mean of the direct determination and the perturbation method is $A_{\pi\pi}=38.9$.

For the $\pi\nu$ interaction the perturbation calcu-

lation should be much more accurate. With the solution f as a starting point and by solving for $A_{\pi\nu}$ so as to have a virtual level at 43 kv. $A_{\pi\nu}=42.0$. The difference $A_{\pi\nu}-A_{\pi\pi}$ is seen to be positive just as $D_{\pi\nu}-D_{\pi\pi}$ and it is of the same order of magnitude. Use of $A_{\pi\nu}$ for calculations on $\pi\pi$ scattering gives too high values and use of $A_{\pi\pi}$ for $\pi\nu$ scattering gives values too small by approximately the same amounts as for square wells with $r_0=e^2/mc^2$. As expected, this feature of the comparison does not depend critically on the shape of the "well." Use of Fermi and Amaldi's position of the virtual level (130 kv), lowers the value of $A_{\pi\nu}$ to 39.2 which is in practically perfect agreement with $A_{\pi\pi}=38.9$.

The rate of change of $\partial\tilde{\gamma}/\tilde{\gamma}\partial r$ with energy was calculated for $\alpha=17$ by means of Eq. (10.3) and hence also the rate of change with energy of K_0. It was found that K_0 varies approximately in the same way at 800 kv as for a square well with $D=10.3$ Mev and $r_0=e^2/mc^2$. It definitely varies more rapidly than for $D=1.98$ Mev and $r_0=2e^2/mc^2$.

Measurements at voltages below and above those used so far will be valuable in determining the range of nuclear forces as is clear from Figs. 8, 9, 10, 11 and they should be helpful in establishing the effects due to higher angular momenta. For an attractive interaction energy of 10 Mev through 2.8×10^{-13} cm the phase shift K_1 should be 0.2° and 1.5° at incident energies of 2 and 9 Mev, respectively; K_1 is roughly twice as great for $D=2$ Mev, $r_0=5.6\times10^{-13}$ cm as for $D=10$ Mev, $r_0=2.8\times10^{-13}$ cm at 2 Mev of incident proton energy. Attractive and repulsive potentials for $L=1$ can be distinguished by the sign of K_1.

Summary. The experiments of THH indicate an interaction potential between protons equivalent to -11.1 Mev in a distance of 2.82×10^{-13} cm acting in addition to the Coulombian repulsion. The potential agrees closely with that obtained from mass defect calculations which use a neutron-proton interaction depending on spin orientation. Higher phase shifts than those for $L=0$ are not called for sufficiently definitely to make their existence certain.

The magnitude of the interaction between like particles in ^1S states is arrived at here with a relatively high precision. It is compared with the proton-neutron interaction in the corresponding state as derived from the experiments of Fermi and Amaldi. The proton-proton and proton-neutron interactions in ^1S states are found to be equal within the experimental error. This suggests that interactions between heavy particles are equal also in other states.

In addition to our indebtedness to Messrs. Tuve, Heydenburg, Hafstad, Wheeler and Young which was mentioned in the text and footnotes we should like to acknowledge our gratitude to Mr. L. R. Eisenbud for conscientious help in checking the numerical calculations.

On Nuclear Forces

B. CASSEN AND E. U. CONDON, *Harper Hospital, Detroit and Palmer Physical Laboratory, Princeton, N. J.*

(Received August 10, 1936)

The various types of exchange forces that are being used in current discussions of nuclear structure may all be simply expressed in terms of a formalism which attributes five coordinates to each "heavy" particle and applies the Pauli exclusion principle to all the particles in the system. The simplest assumption for the interaction law is that which implies equality of proton-proton and neutron-neutron forces and also equality with the proton-neutron forces of corresponding symmetry. This is in accord with the empirical knowledge of these interactions at present.

IN this paper we show how the use of a coordinate having two proper values which tells whether a particle is a proton or a neutron, together with the assumption of the Pauli exclusion principle for all the particles, gives a unified description of the various types of exchange forces used in nuclear structure theories. Such a coordinate was first introduced by Heisenberg[1] and also plays a role in the Fermi-Konopinski-Uhlenbeck[2] theory of beta disintegration.

We suppose that each heavy particle (proton or neutron) is described by five coordinates. These are three for its position in space, a spin coordinate σ giving the component of its angular momentum along some direction in space, and a fifth coordinate, τ, which can have the values ± 1. If τ has the value $+1$ the particle is a proton, while the value -1 indicates that it is a neutron.

The spin angular momentum is a vector equal to $\frac{1}{2}\hbar$ times the vector, $\boldsymbol{\sigma}$, which is represented by

$$\boldsymbol{\sigma}=\begin{pmatrix}\mathbf{k} & \mathbf{i}-i\mathbf{j}\\ \mathbf{i}+i\mathbf{j} & -\mathbf{k}\end{pmatrix},$$

the rows and columns referring to states which are labeled by precise values of the z component of $\boldsymbol{\sigma}$. This nonrelativistic description of the spin was introduced by Pauli and by Darwin.

In the same way τ can be considered purely formally like the z component of a vector. The analogy is purely formal in that the three "components" of $\boldsymbol{\tau}$ do not refer to directions in space. Formally we may write

$$\boldsymbol{\tau}=\begin{pmatrix}\mathbf{n} & \mathbf{l}-i\mathbf{m}\\ \mathbf{l}+i\mathbf{m} & -\mathbf{n}\end{pmatrix},$$

where $\mathbf{l}$, $\mathbf{m}$ and $\mathbf{n}$ behave algebraically like the three unit vectors $\mathbf{i}$, $\mathbf{j}$ and $\mathbf{k}$. The third component of $\boldsymbol{\tau}$ may be called the character coordinate and the whole expression $\boldsymbol{\tau}$ the character vector.

We postulate that in an assembly of heavy particles the wave function has to be antisymmetric in all particles with regard to exchange of all five of their coordinates. We want to show that this gives a convenient formalism for working with nuclear problems.

Let us first consider any attribute of a single heavy particle such as its mass, its charge or its magnetic moment. If A is the arithmetic mean of the two values for proton and neutron and B is half the difference, proton value minus neutron value, then that attribute will appear in the equations as a term involving,

$$(A+B\tau).$$

For example, the electrostatic charge will appear as $\frac{1}{2}e(1+\tau)$ where e is the electronic charge.

Next, let us consider the scalar product $\boldsymbol{\tau}_1\cdot\boldsymbol{\tau}_2$ of the character vectors associated with two particles. We have

$$(\boldsymbol{\tau}_1+\boldsymbol{\tau}_2)^2=\boldsymbol{\tau}_1^2+\boldsymbol{\tau}_2^2+2\boldsymbol{\tau}_1\cdot\boldsymbol{\tau}_2,$$

since the operators for two different particles commute. Now as defined $\boldsymbol{\tau}$ is formally like twice an angular momentum vector of magnitude $\frac{1}{2}$. Therefore, the possible values of the vector sum are twice 1 and zero. Letting $2T$ stand for the magnitude of the resultant we have

$$4T(T+1)=3+3+2\boldsymbol{\tau}_1\cdot\boldsymbol{\tau}_2,$$

so the allowed values of $\boldsymbol{\tau}_1\cdot\boldsymbol{\tau}_2$ are $+1$ and -3. The value $+1$ corresponds to the case of parallel character vectors and so to a wave function that is symmetric in τ_1 and τ_2 while the value -3

[1] Heisenberg, Zeits. f. Physik **77**, 1 (1932).
[2] Fermi, Zeits. f. Physik **88**, 161 (1934); Konopinski and Uhlenbeck, Phys. Rev. **48**, 7 (1935).

corresponds to resultant zero of the two character vectors and hence to an antisymmetric dependence of the wave function on τ_1 and τ_2.

Therefore, the expression

$$\tfrac{1}{2}(1+\boldsymbol{\tau}_1\cdot\boldsymbol{\tau}_2)$$

has the allowed values $+1$ and -1, the positive value going with wave functions symmetric in τ_1 and τ_2, while the negative value has for its proper function a wave function antisymmetric in these two character coordinates.

These results are, of course, exactly analogous to the well-known results for the vector sum of two spin angular momenta and their connection with the symmetry properties of the wave function with regard to exchange of σ_1 and σ_2.

The applicability of the Pauli exclusion principle to a dynamical system requires that the Hamiltonian function for the system be a symmetric function of the coordinates of the particles. In looking for possible interaction laws we therefore have to confine ourselves to symmetric functions.

So far, four types of exchange forces have been proposed for description of the interaction between heavy particles. These are:

1. Ordinary (Wigner) potential.[3] This is the familiar kind and is simply a function of the distance between the two particles.

2. Heisenberg potential.[4] This is of the form of a function of the distance multiplied by an operator H. This operator is defined as having the value $+1$ when applied to a wave function that is symmetric with regard to exchange of both position and spin coordinates of the two particles whose interaction is being considered, and the value -1 for the antisymmetric case.

3. Bartlett potential.[5] This is a function of the distance multiplied by an operator B. This operator is defined as having the value $+1$ when applied to a wave function that is symmetric in the spin coordinates alone and -1 for the antisymmetric case.

4. Majorana potential.[6] This is a function of the distance multiplied by an operator M. This operator is defined as having the value $+1$ when applied to a wave function that is symmetric with regard to exchange of the positional coordinates only of the two particles in question, and -1 when applied to an antisymmetric function in the positional coordinates.

Evidently the Majorana type can be expressed in terms of the preceding two:

$$M=HB=BH.$$

Since the operator H exchanges both position and spin, and the Bartlett operator B exchanges spin only, the product will be equivalent to an exchange of position only, for the double exchange of spin provided by the combined action of H and B cancels out and is the same as no exchange of spin.

We now point out that the four operators, 1, H, B and M are readily expressible in terms of the spin and character vectors, $\boldsymbol{\sigma}$ and $\boldsymbol{\tau}$ of the two particles. This follows from the requirement of over-all antisymmetry of the wave functions in the five coordinates of each of the particles. Let the letters a, b, c, d $\cdots$ stand for the different particles and consider a general wave function ψ that is a function of all five of the coordinates of each particle. More explicitly

$$\psi=\psi(\mathbf{r}_a, \tau_a, \sigma_a;\ \mathbf{r}_b, \tau_b, \sigma_b;\ \mathbf{r}_c, \tau_c, \sigma_c;\ \cdots).$$

Whatever the functional form of ψ this can be written

$$\begin{aligned}\psi=\tfrac{1}{2}[&\psi(\mathbf{r}_a, \tau_a, \sigma_a;\ \mathbf{r}_b, \tau_b, \sigma_b;\ \cdots)\\ &+\psi(\mathbf{r}_b, \tau_a, \sigma_b;\ \mathbf{r}_a, \tau_b, \sigma_a;\ \cdots)]\\ &+\tfrac{1}{2}[\psi(\mathbf{r}_a, \tau_a, \sigma_a;\ \mathbf{r}_b, \tau_b, \sigma_b;\ \cdots)\\ &\quad-\psi(\mathbf{r}_b, \tau_a, \sigma_b;\ \mathbf{r}_a, \tau_b, \sigma_a;\ \cdots)],\end{aligned}$$

that is, as the sum of a function symmetric in the position and spin coordinates of particles a and b and one antisymmetric in these same coordinates. As we require ψ to be antisymmetric in all five coordinates of a and b we know that the first term here must be antisymmetric in τ_a and τ_b and the second term must be symmetric in τ_a and τ_b. Therefore the operator H has the value -1 for symmetry in τ_a and τ_b, and $+1$ for antisymmetry in τ_a and τ_b. Using the earlier calculation of $\boldsymbol{\tau}_1\cdot\boldsymbol{\tau}_2$ we have

$$H_{ab}=-\tfrac{1}{2}(1+\boldsymbol{\tau}_a\cdot\boldsymbol{\tau}_b)$$

which expresses the Heisenberg exchange operator in terms of the two character vectors.

[3] Wigner, Phys. Rev. **43**, 252 (1933).
[4] Heisenberg, Zeits. f. Physik **77**, 1 (1932).
[5] Bartlett, Phys. Rev. **49**, 102 (1936).
[6] Majorana, Zeits. f. Physik **82**, 137 (1933).

Similarly it is easy to see that

$$B_{ab}=+\tfrac{1}{2}(1+\boldsymbol{\sigma}_a\cdot\boldsymbol{\sigma}_b)$$

and therefore, in view of the relation, $M=HB$, we have

$$M_{ab}=-\tfrac{1}{4}(1+\boldsymbol{\sigma}_a\cdot\boldsymbol{\sigma}_b)(1+\boldsymbol{\tau}_a\cdot\boldsymbol{\tau}_b),$$

which completes the expression of each of the exchange operators in terms of symmetric functions of the coordinates of the two particles.

With the different types of exchange operators written in this simple way it suggests itself that the general law of interaction for the specifically nuclear forces can be written in the form:

$$U=V+V_hH+V_bB+V_mM.$$

Here the four V's may be quite different functions of the separation distance but the simplest assumption is that the entire dependence of the interaction on $\boldsymbol{\sigma}$ and $\boldsymbol{\tau}$ is contained in the operators 1, H, B and M.

Of course, this simple result is not required by the formalism. It is simply the simplest form for the exchange operators. The mere requirement of a symmetric function would be met if any one or all of the V's were replaced by

$$A+B(\tau_1+\tau_2)+C\tau_1\tau_2,$$

where A, B and C are functions of the distance of separation. In fact, this more general form is necessary even for the description of the Coulomb interaction between the particles which for two particles is expressed as

$$\tfrac{1}{4}(e^2/r)(1+\tau_1)(1+\tau_2).$$

The expression above, involving A, B and C, has the value $(A+2B+C)$ for two protons, the value $(A-C)$ for a proton and a neutron, and the value $(A-2B+C)$ for two neutrons. If proton-proton forces are the same as neutron-neutron forces we may conclude that $B=0$, and if like-particle forces are the same as proton-neutron forces in states of corresponding symmetry then we can conclude that $C=0$. With both B and C equal to zero the dependence on the components τ_1 and τ_2 is gone and we are reduced to the simpler original form.

The assumption that B and C are zero seems to be in accord with the facts about nuclear interactions as far as these are known.* The assumption makes the unification that there are only four different force laws, corresponding to the four possible types of symmetry in σ and τ. These four types are describable in terms of more usual notation by giving the symmetry in position and spin, since this determines the symmetry in character. A state that is symmetric in spin is called a triplet, one antisymmetric a singlet. Symmetry for exchange of position will be denoted by S and antisymmetry by P, since these are the standard notations for states of least orbital angular momentum in the two-body problem which have these positional symmetry properties. Here, however, we use S and P in a more general sense.

The distinct laws of interaction are given in Table I. Using the values of the operators 1, H, B and M we can write for the four interaction laws:

$$\begin{aligned}U(^3S)&=V+V_h+V_b+V_m,\\ U(^1S)&=V-V_h-V_b-V_m,\\ U(^3P)&=V-V_h+V_b-V_m,\\ U(^1P)&=V+V_h-V_b-V_m.\end{aligned}$$

These are readily solved for explicit expressions for each V in terms of the four empirically occurring combinations.

We shall only make a few brief remarks about the empirical facts as they are known as these have been recently reviewed by Bethe and Bacher.[7] Ideally one would like to learn all eight force laws (there are eight if we do not make the simple formal assumption of the previous section) from studies based wholly on the two-body problem. So far this is not possible.

The situation with regard to the two-body problems is this:

Proton-Neutron

$U(^3S)$: Normal state of deuteron. Observed binding energy gives a relation between depth and width of a potential well.

Scattering of neutrons by protons: This involves all four laws in principle, but in fact owing

* The consequences of assuming equality of the various specifically nuclear forces for like and unlike particles are considered in detail in a paper by Feenberg and Breit in this issue which we had the pleasure of seeing in manuscript after this paper was sent in.

[7] Bethe and Bacher, Rev. Mod. Phys. **8**, 82 (1936).

to short range of the forces only the two S laws enter in an important way for neutron energies less than some tens of millions of volts. Slow neutron scattering cross section indicates a ^1S level of deuteron near to zero binding energy, according to Wigner.

Photodissociation of the deuteron: Electric dipole effect involves transitions from bound ^3S normal state to continuum of ^3P, hence these two laws. In addition to Bethe and Bacher, the problem is discussed by Breit and Condon.[8] Magnetic dipole effect produces transitions from ^3S normal state to ^1S continuum. This is important near the photoelectric threshold.

Radiative capture of neutrons by protons: Here the important effect is for slow neutrons principally by action of magnetic dipole radiation from ^1S continuum to ^3S normal state, according to Fermi.[9]

None of these involve the ^1P law in an essential way. Apparently this can only be studied by scattering very high energy neutrons with protons.

Proton-Proton

Here a little evidence comes from the probable nonexistence of He^2. But mainly the knowledge comes from the recent work of Tuve, Heydenburg and Hafstad as analyzed by Breit, Condon and Present.[10] The analysis indicates that up to 1 Mev the departures from coulomb scattering may be described entirely in terms of effects of the ^1S law and gives strong indication that this is the same as the ^1S law in the deuteron.

Neutron-Neutron

No positive evidence from two-body interactions. Absence of a double neutron is in accord with assumption of the same ^1S law as in proton-neutron since the ^1S level is now supposed to be virtual (see reference 10 for details).

All other knowledge of the force laws comes from approximate calculations of binding energies of many-body nuclei as fully reviewed by Bethe and Bacher. These are in accord with assumption of equality of the interaction laws for various kinds of particles so far as specifically nuclear forces are concerned.

This paper grew out of association at the 1936 summer symposium on theoretical physics of the University of Michigan. We wish to express here to Professor H. M. Randall our deep appreciation of the opportunity of working in the stimulating atmosphere of the Michigan laboratory.

Table I.

Symmetry in			Notation	Occurrence
Position	Spin	Character		
s	s	a	^3S	proton-neutron
s	a	s	^1S	proton-neutron proton-proton neutron-neutron
a	s	s	^3P	proton-neutron proton-proton neutron-neutron
a	a	a	^1P	proton-neutron

[8] Breit and Condon, Phys. Rev. **49**, 904 (1936). See also Morse, Fisk and Schiff, Phys. Rev. **50**, 748 (1936).
[9] Fermi, Phys. Rev. **48**, 570 (1935).
[10] Breit, Condon and Present, Phys. Rev. this issue.

The Possibility of the Same Form of Specific Interaction for All Nuclear Particles

G. BREIT AND E. FEENBERG,* *University of Wisconsin, Madison Wisconsin*

(Received August 19, 1936)

Experimental evidence pointing to a universal form of interaction for all nuclear particles is summarized. The form given by Eq. (1) is discussed. It is found to be satisfactory for H^3, He^3, He^4 considered together with proton and neutron scattering. In order that heavy nuclei should not be too stable it is necessary to require the inequality (7.2) and in order that there be no very heavy and electrically neutral nuclei the inequality (7) has to be satisfied. The form of the interaction energy restricted by these conditions is as satisfactory as nuclear theories postulating different forms for like and unlike particles. The simplest form, satisfying all present requirements is obtained from Eq. (1) by letting $g_1=g_2=0$.

THE interaction between protons and protons which acts in addition to the Coulombian repulsion is generally supposed to be the same as that between neutrons and neutrons. The evidence for this lies in the fact[1] that the mass defect of He^3 is smaller than that of H^3 by approximately the amount required by the Coulombian repulsion between the protons in He^3. Further strong support for regarding the specific like-particle interaction as the same for protons and neutrons is found in the close agreement[2] of the values obtained for its magnitude from experiments on the scattering of protons in hydrogen[3] with that derived from the mass defect of H^3.

The accuracy of the determination of the like-particle interaction from the proton-proton scattering experiments is great. Numerical comparison of its magnitude with that which follows from experiments on the scattering and recombination of slow neutrons in hydrogen shows that in ^1S states the specific interaction between all nuclear particles are the same to within the accuracy of present experiments. The equality of the interactions is obtained independently of what range is used for the spacial extension of the force within wide limits and is, therefore, probably real rather than accidental. It thus becomes reasonable to attempt to regard the specific nuclear forces as the same between all nuclear particles independently of whether they are neutrons or protons. In the present note the qualitative consequences of this view are discussed.

In the early development of nuclear theory it was supposed that the principal interactions within the nucleus take place between neutrons and protons because by doing so the approximate equality of the number of neutrons with the number of protons automatically received a simple explanation. According to present evidence, mentioned above, this explanation does not apply and a new one must be made. This is offered by the exclusion principle which favors the addition of unlike particles analogously to the way in which the building up of electronic shells in an atom proceeds by adding electrons with opposite spin directions. In addition it is favorable for stability to have proton-neutron pairs in symmetrical (S, D, G, $\cdots$) triplet states because the attraction is then greater than in symmetrical singlet states. For like particles the exclusion principle rules out the symmetrical triplet state. This circumstance is important in the building up of the first shell up to He^4.

The universal interaction energy between any pair of heavy elementary particles will be assumed to be of the form

$$V_{ij}=\{(1-g-g_1-g_2)P_{ij}^M+gP_{ij}^H+g_1\cdot 1+g_2P_{ij}^S\}J(r_{ij}), \quad (1)$$

where g, g_1, g_2 are constants and P^M, P^H are the Majorana and Heisenberg exchange operators while $P^S = P^MP^H$ is the operator proposed by Bartlett which exchanges the spins without affecting the coordinates.[4] For this interaction

* Now at the Institute for Advanced Study.

[1] E. Feenberg and J. Knipp, Phys. Rev. **48**, 906 (1935); S. S. Share, Phys. Rev. **50**, 488 (1936).

[2] G. Breit, E. U. Condon and R. D. Present, Phys. Rev. this issue; Fermi and Amaldi, Ricerca Scient. **1**, 1 (1936); Fermi, ibid., July (1936).

[3] M. A. Tuve, N. P. Heydenburg and L. R. Hafstad, Phys. Rev. this issue.

[4] Another formulation of the symmetrical Hamiltonian using a fifth "character" variable is given by Condon and Cassen in this issue.

TABLE I. *Two-particle systems.*

Even L		Odd L	
triplets $^3S, ^3D, \cdots$ $J(r)$ Absent for equivalent like particles	singlets $^1S, ^1D, \cdots$ $(1-2g-2g_2)J(r)$	triplets $^3P, ^3F, \cdots$ $(-1+2g_1+2g_2)J(r)$	singlets $^1P, ^1F, \cdots$ $(-1+2g+2g_1)J(r)$ Absent for equivalent like particles

the potential energies in different states are as in Table I where L is the orbital angular momentum in units of $\hbar$. Two isolated like particles moving in each other's field cannot have different principal quantum numbers and are in equivalent states if L is even and the spins are parallel or when L is odd and the spins are antiparallel. Triplets of even L and singlets of odd L are thus ruled out by the exclusion principle. In proton-proton scattering experiments only states with $L=0$ matter and, therefore, the effective interaction energy is that corresponding to ^1S namely $(1-2g-2g_2)J(r)$. In the scattering of slow neutrons by hydrogen a similar ^1S state is responsible for the large collision cross section according to Wigner's hypothesis. Both sets of scattering experiments thus have to do with $(1-2g-2g_2)J(r)$ while $J(r)$ determines the binding energy of the deuteron.

LIGHT NUCLEI

In H^3, He^3, He^4 like particles are in nearly spacially symmetric states with respect to each other and the effective interaction potential is thus again $(1-2g-2g_2)J(r)$. This is consistent with the agreement between the values of the like particle interaction energy as obtained from the mass defects of the isotopes of hydrogen and helium with that derived from the scattering of protons in hydrogen. Unlike particles are partly in triplet and partly in singlet states with respect to each other. However, the space wave function is nearly symmetric and thus the effective interaction potential between protons and neutrons is $[1-\frac{1}{2}(g+g_2)]J(r)$ which is the weighted mean of the potentials in singlets and triplets with statistical weights $\frac{1}{4}$ and $\frac{3}{4}$. In these questions the sum of $g+g_2$ occurs as a whole and one cannot distinguish between g and g_2 separately. The calculations on mass defects that have been made without using g_1, g_2 thus apply directly to (1) and are consistent with it. The way in which this comes about may be seen for H^3 as follows. The wave equation is

$$(T+\Sigma_{i>j}V_{ij})\psi=E\psi,$$

where T is the operator representing the sum of kinetic energies of the three particles. Since ψ is antisymmetric in the neutrons it is of the form

$$\psi=u((12_+),3)S^0((12_-),3)+v((12_-),3)S'((12_+),3),$$

where the two neutrons are denoted by 1, 2 and a plus suffix indicates that the function is symmetric in the particles while a minus suffix similarly indicates antisymmetry. The functions u, v contain only the Cartesian coordinates while the functions S^0, S' contain only the spin coordinates. Considering the state with total spin angular momentum $\frac{1}{2}$ in the z direction one may use

$$S^0=2^{-\frac{1}{2}}[(+-+)-(-++)],$$
$$S'=6^{-\frac{1}{2}}[(+-+)+(-++)-2(++-)],$$

where the + and − signs correspond to positive and negative orientations of the spin axis in an arbitrary fixed direction. Each ( ) stands for a product of spin functions referring to the particles in the order 1, 2, 3. One obtains

$$(H_0+H'-E)\begin{pmatrix}u\\v\end{pmatrix}=0, \tag{2}$$

where

$$H_0=T+\begin{pmatrix}1-2g-2g_2, & 0\\ 0, & -1+2g_1+2g_2\end{pmatrix}J_{12}+\begin{pmatrix}1-\frac{1}{2}(g+g_2), & 0\\ 0, & 1-(3/2)(g+g_2)\end{pmatrix}(J_{13}+J_{23}), \tag{2.1}$$

$$H'=\begin{pmatrix}X, & Y\\ Y, & Z\end{pmatrix}, \tag{2.2}$$

$$X=(1-\tfrac{1}{2}g-g_1-g_2)[J_{23}(P_{23}{}^M-1)+J_{13}(P_{13}{}^M-1)], \tag{2.3}$$

$$Y=3^{\frac{1}{2}}2^{-1}[(gP_{13}{}^M+g_2)J_{13}-(gP_{23}{}^M+g_2)J_{23}], \tag{2.4}$$

$$Z=(1-(3/2)g-g_1-g_2)[J_{23}(P_{23}{}^M-1)+J_{13}(P_{13}{}^M-1)]. \tag{2.5}$$

Neglecting H' one obtains an approximation to ψ,

$$\psi_0=\begin{pmatrix}u\\0\end{pmatrix}, \tag{3}$$

with u defined by

$$\{T+(1-2g-2g_2)J_{12}+(1-\tfrac{1}{2}g-\tfrac{1}{2}g_2)(J_{13}+J_{23})-E\}u=0. \tag{3.1}$$

In the approximation of using ψ_0 the energy can be calculated without exchange operators by using $(1-2g-2g_2)J$, $(1-\frac{1}{2}g-\frac{1}{2}g_2)J$, respectively, for the potential energies between like and unlike particles. The function u is symmetric in the neutrons but has, in general, no symmetry property for interchange of a proton and a neutron. If, however, $g+g_2$ is small then u becomes symmetric in all three particles. In this case the first-order perturbation due to H' vanishes as is obvious from (2.3). The second-order perturbation may be estimated as $-(\psi_0|H'^2|\psi_0)/E_m$ where E_m is an average energy of perturbing levels above that of the normal state. According to (2.2) and (3)

$$(\psi_0|H'^2|\psi_0)=(u|X^2+Y^2|u).$$

The calculation of this matrix element is readily made using (2.3) and (2.4) and gives for a completely symmetric u

$$(\psi_0|H'^2|\psi_0)=(3/2)(g+g_2)^2\int u^2(J_{13}^2-J_{13}J_{23})d\tau_1 d\tau_2. \tag{3.2}$$

Thus the estimate of the second-order perturbation energy depends only on $g+g_2$ and one may expect the energy to depend on $g-g_2$, g_1 only in a secondary way. Since $g+g_2$ is the only combination of the g's which matters for the mass defect of the deuteron and the present proton-proton and proton-neutron scattering experiments the inclusion of g_1 and g_2 makes little practical difference in the comparison of the mass defect of H^3, H^2, He^3 with the scattering experiments.

Similarly in He^4

$$H_0=T+\begin{pmatrix}1-2g-2g_2,\ 0\\ 0,\ -1+2g_1+2g_2\end{pmatrix}(J_{12}+J_{34})+\begin{pmatrix}1-\frac{1}{2}g-\frac{1}{2}g_2,\ 0\\ 0,\ 1-(3/2)g-(3/2)g_2\end{pmatrix}(J_{13}+J_{23}+J_{14}+J_{24}), \tag{4.0}$$

$$H'=\begin{pmatrix}X,\ Y\\ Y,\ Z\end{pmatrix}, \tag{4.1}$$

$$\begin{aligned}X&=[J_{12}(P_{13}^M-1)+J_{14}(P_{14}^M-1)+J_{23}(P_{23}^M-1)+J_{24}(P_{24}^M-1)](1-\tfrac{1}{2}g-g_1-g_2),\\ Y&=3^{\frac{1}{2}}2^{-1}[J_{23}(gP_{23}^M+g_2)+J_{14}(gP_{14}^M+g_2)-J_{13}(gP_{13}^M+g_2)-J_{24}(gP_{24}^M+g_2)],\\ Z&=(1-(3/2)g-g_1-g_2)X/(1-\tfrac{1}{2}g-g_1-g_2).\end{aligned} \tag{4.2}$$

These equations differ from Eqs. (2.1) to (2.5) essentially only through the presence of more terms in sums over like and unlike particles. The wave Eq. (2) is the same in form but now

$$\begin{aligned}S^0&=\tfrac{1}{2}[(+-+-)+(-+-+)-(+--+)-(-++-)],\\ S'&=12^{-1}[2(++--)+2(--++)-(+-+-)-(-+-+)-(-++-)-(+--+)].\end{aligned}$$

Particles 1 and 2 are alike and so are 3 and 4. With a completely symmetric u

$$(\psi_0|H'^2|\psi_0)=3(g+g_2)^2(u|J_{13}^2+J_{13}J_{24}-2J_{13}J_{23}|u). \tag{4.3}$$

Thus here also only $g+g_2$ enters in the calculation of the normal state. With wave functions

$u=\exp\{-(\nu/2)(r_{12}^2+r_{13}^2+r_{23}^2)\}$ for H^3 and $\exp\{-(\nu/2)(r_{12}^2+r_{13}^2+r_{14}^2+r_{23}^2+r_{24}^2+r_{34}^2)\}$ for He^4 and with

$$J(r)=Ae^{-\alpha r^2} \tag{4.4}$$

one obtains for H^3

$$(\psi_0|H''|\psi_0)=\frac{3}{2}(g+g_2)^2A^2\left[\left(\frac{3\nu}{3\nu+4\alpha}\right)^{\frac{3}{2}}-\left(\frac{\nu}{\nu+\alpha}\right)^{\frac{3}{2}}\left(\frac{3\nu}{3\nu+\alpha}\right)^{\frac{3}{2}}\right] \tag{4.5}$$

and for He^4

$$(\psi_0|H''|\psi_0)=3(g+g_2)^2A^2\left\{\left(\frac{\nu}{\nu+\alpha}\right)^{\frac{3}{2}}+\left(\frac{2\nu}{2\nu+\alpha}\right)^{3}-\frac{128\nu^3}{[3(\nu+\alpha)^2+10\nu(\nu+\alpha)+3\nu^2]^{\frac{3}{2}}}\right\}. \tag{4.6}$$

The contributions to (3.2) and (4.3) in the present approximation are due entirely to Y^2 and thus, according to (2.4) and (4.2) originate in interactions between unlike particles. They are thus present even if the form of the interaction is not made to be the same for like and unlike particles. Formulas (4.5) and (4.6) are then correct provided for A the value corresponding to the neutron-proton potential in the ^3S state is used. The magnitude of the perturbation can be estimated using the approximation

$$\Delta E=-(\psi_0|H''|\psi_0)/E_m, \tag{5}$$

where E_m is a properly taken mean of the perturbing energy levels. For lack of better knowledge of the relative importance of different levels one may use the binding energy for E_m and thus obtain most probably an overestimate of the absolute value of ΔE. Using the units $\hbar(mM)^{-\frac{1}{2}}c^{-1}$ for length and mc^2 for energy and letting $\alpha=16$ the values of ν which minimize $(0|H_0|0)$ are $\nu\sim 10$ for both H^3 and He^4. Eq. (5) gives then $\Delta E\sim -mc^2$ for H^3 and $-0.4mc^2$ for He^4. It should be noted that these estimates refer only to the effect of Y and do not represent the total effect of terms in $(g+g_2)^2$ in an expansion of the energy starting from a value corresponding to a symmetric wave function. Thus if the Hamiltonians

$$T+(1-g-g_2)(J_{12}+J_{13}+J_{23}),$$

$$T+(1-g-g_2)(J_{12}+J_{13}+J_{23}+J_{24}+J_{34}),$$

are used respectively for H^3 and He^4 in order to define unperturbed energy values and wave functions then the values of $(\psi_0|H''|\psi_0)$ given by Eqs. (4.5) and (4.6) should be multiplied by 2.

Calculations have already been made for Hamiltonians having different symmetries.[5] According to these the difference in energy values of H^3 corresponding to

$$H=T+J^*_{23}+J^*_{13}$$

and

$$H=T+\tfrac{2}{3}(J^*_{12}+J^*_{13}+J^*_{23})$$

is about $-2mc^2$. The quantity $\frac{2}{3}J^*_{12}-\frac{1}{3}J^*_{23}-\frac{1}{3}J^*_{13}=H''$ may be considered as a perturbation which when applied to the symmetric form gives the unsymmetric form. For a symmetric initial wave function

$$(0|H''^2|0)=\tfrac{2}{3}(0|J^*_{13}{}^2-J^*_{13}J^*_{23}|0).$$

Equating $2mc^2$ and $(0|H''^2|0)/E_m'$ it is found that $E_m'\sim 100mc^2$. The energy levels which matter in this connection are those corresponding to pure singlet states in neutrons while the effect of Y is concerned with perturbations by states in which the neutrons are in a triplet condition. Nevertheless it is probable that there is a qualitative similarity between E_m and E_m'. Using $E_m=E_m'$ the estimate of perturbations due to triplet neutron states in H^3 drops to $0.14mc^2$. It is thus seen that the second-order perturbations which depend essentially only on $(g+g_2)^2$ are themselves likely to be small. Ordinarily the effect of these perturbations is neglected and the calculations are made using $(1-\frac{1}{2}g)A_{\tau\tau}e^{-\alpha r^2}$ for the average neutron-proton interaction and $A_{\tau\tau}e^{-\alpha r^2}$ for the interaction between like particles. The value obtained for $A_{\tau\tau}$ agrees with that from proton-proton scattering experiments and is equal to $(1-2g)A_{\tau\tau}$. The mass defects of the

[5] E. Feenberg and S. S. Share, Phys. Rev. **50**, 253 (1936); E. Feenberg, Phys. Rev. **49**, 273 (1936).

isotopes of hydrogen and helium are thus in agreement with the interaction energy (1), but give at present practically no information about g, g_1, g_2 except for determining $g+g_2$.

Heavy Nuclei

Calculations of any exactness are difficult for heavy nuclei. It is, however, possible to establish some inequalities which are necessary for stability of existing nuclei by means of the statistical model. The density matrices for protons and neutrons will be written $\rho_\pi(x, x')$ and $\rho_\nu(x, x')$. These functions are supposed to involve only the space coordinates. For simplicity it will be supposed that each space state is filled by two like particles having opposite spin directions. The density matrix contains therefore two identical terms for each occupied space state. For diagonal elements the abbreviations

$$\rho_\pi(x)=\rho_\pi(x, x), \quad \rho_\nu(x)=\rho_\nu(x, x)$$

will be used.

For the estimates made below the wave function is approximated by a product of two determinants, one for the neutrons and the other for the protons. Substitution of such a wave function into the variational integral gives an upper limit to the energy. The expression thus obtained is

$$E=T+W^\nu+W^\pi+W^{\pi\nu} \tag{6}$$

where T is the average value of the kinetic energy operator (a sum of the kinetic energies of the individual particles). The quantities W represent the contributions due to (1). The interactions between neutrons give W^ν, those between protons give W^π, and those between neutrons and protons give $W^{\pi\nu}$. It is found that

$$W^\nu=(1-\tfrac{1}{2}g-(3/2)g_1-2g_2)E_{\rm ex}{}^\nu + (1-\tfrac{1}{2}-\tfrac{1}{2}g+(3/2)g_1+g_2)E^\nu, \tag{6.1}$$

$$W^\pi=(1-\tfrac{1}{2}g-(3/2)g_1-2g_2)E_{\rm ex}{}^\pi + (-\tfrac{1}{2}-\tfrac{1}{2}g+(3/2)g_1+g_2)E^\pi, \tag{6.2}$$

$$W^{\pi\nu}=(2-g-2g_1-2g_2)E_{\rm ex}{}^{\pi\nu} + (2g_1+g_2)E^{\pi\nu}, \tag{6.3}$$

where

$$E^{\alpha\beta}=\tfrac{1}{2}\int \rho_\alpha(x)J(x-x')\rho_\beta(x')dxdx';$$
$$E_{\rm ex}{}^{\alpha\beta}=\tfrac{1}{2}\int \rho_\alpha(xx')J(x-x')\rho_\beta(x'x)dxdx', \tag{6.4}$$
$$E^{\alpha\alpha}=E^\alpha; \quad E_{\rm ex}{}^{\alpha\alpha}=E_{\rm ex}{}^\alpha; \quad \alpha, \beta=\mu \text{ or } \nu.$$

If the density of particles is so high that a large number of them are on the average within the range of J then the quantities $E_{\rm ex}$ show saturation while the quantities E are proportional to the square of the number of particles. This circumstance may lead to instability. Thus consider W^ν. If the coefficient of E^ν in it is positive, the nuclear energy can be lowered by increasing the number of neutrons N. In particular it would be possible to have nuclei consisting entirely of large numbers of neutrons. For such nuclei the kinetic energy would be proportional to $N^{5/3}r_0^{-2}$ where r_0 is the nuclear radius while the potential energy would vary as N^2 and would be independent of r_0, if r_0 is sufficiently smaller than the range of force. Keeping r_0 constant the kinetic energy varies more slowly with N for high N than the potential energy and therefore a negative potential energy will lead to infinite stability for very high N. A positive coefficient of E^ν in Eq. (6.1) would require, therefore, the existence of infinitely heavy nuclei of high stability. This is contrary to experience and hence[6]

$$1+g\geqq 3g_1+2g_2. \tag{7}$$

For a nucleus in which the number of neutrons N is equal to the number of protons Z the density matrices ρ_ν, ρ_π may be taken to be equal. Then

$$W=W^{\pi\nu}+2W^{\nu\nu}=4(1-\tfrac{1}{2}g-(5/4)g_1 - (3/2)g_2)E_{\rm ex}+(-1-g+5g_1+3g_2)E, \tag{7.1}$$

where the superscripts π, ν on the E's are dropped. The trial wave function can be made to correspond to an r_0 smaller than the range of J. By increasing N and Z simultaneously, the governing term in W becomes that due to E which varies as N^2. The only other term which varies as rapidly is that due to the Coulomb energy. Since in the present case $N=Z$ the whole energy expression can be considered as a

[6] Condition (7) is equivalent to requiring that for like particles the interaction be of the form $(a+bP^M)J$ where $b\geqq 2a$ as is clear from the fact that Eq. (1) is equivalent to an interaction energy $(1-g-g_1-2g_2)P^MJ+(g_1-g)J$ for like particles.

function of N. In order that it be impossible to have stable nuclei of this type with very high N and Z it is necessary to require that the coefficient of N^2 in the energy expression be positive. This condition is

$$1+g+\frac{6e^2}{5r_0|J(0)|}\geqq 5g_1+3g_2. \tag{7.2}$$

The nuclear radius r_0 must be chosen smaller than the range of nuclear forces which is of the order e^2/mc^2. If r_0 is made equal to e^2/mc^2 the last term on the left side of (7.2) is 1/58 for $|J(0)|=70mc^2$. Since r_0 must be made still somewhat smaller in order to bring about the full activity of $J(0)$ this term should be considered as somewhat greater than 1/58, say 1/20. It is nevertheless numerically insignificant. The conditions (7.1) and (7.2) may be summarized, using the empirical value of $g+g_2=0.2$, as

$$\begin{aligned} 1.2&=1+g+g_2\geqq 3(g_1+g_2)\,;\\ 1.2&=1+g+g_2\geqq 5g_1+4g_2. \end{aligned} \tag{7.3}$$

On these grounds therefore the interaction in triplet states of odd L can be expected to lie between $-0.2J$ and $-J$ for $g+g_2=0.20$ and between $-0.1J$ and $-J$ for $g+g_2=0.25$ (provided that g_1+g_2 is not negative). It is these states that matter in the photoelectric disintegration of the deuteron by high energy γ-rays. For high particle densities with $N>Z$ the value of the variational integral is

$$\begin{aligned} E=T&-N(1-\tfrac{1}{2}g-(3/2)g_1-2g_2)|J(0)|\\ &-Z(3-(3/2)g-(7/2)g_1-4g_2)|J(0)|\\ &+\tfrac{1}{4}(N^2+Z^2)(1+g-3g_1-2g_2)|J(0)|\\ &-NZ(g_1+\tfrac{1}{2}g_2)|J(0)|+\frac{3}{5}\frac{Z^2e^2}{r_0}. \end{aligned} \tag{7.4}$$

In order that it be impossible to obtain in this expression contributions varying quadratically with N and Z for a given ratio N/Z it is necessary to require that

$$\begin{aligned} 1+g\geqq 3g_1+2g_2+\frac{2NZ}{N^2+Z^2}(2g_1+g_2)\\ -\frac{12}{5}\frac{Z^2}{Z^2+N^2}\frac{e^2}{r_0|J(0)|}. \end{aligned} \tag{7.5}$$

For $Z=0$ this gives (7) and for $Z=N$ it gives (7.2). Neglecting the relatively insignificant Coulomb energy all conditions implied by (7.4) are contained in (7.3). These conditions are obtained above by considering a higher particle density than that which exists in actual nuclei. This circumstance does not formally spoil the argument because the energy is lower than the value of the variational integral. The above discussion does not say much about the reaction rate or the values of N and Z at which transformations would occur. It does not make much difference, however, if the possibility of very heavy neutral nuclei is allowed but instead it is required that there should be no neutral nuclei of mass 200 having a greater stability than a collection of equal numbers of protons and neutrons in the form of alpha-particles. The kinetic energy is statistically $11.3mc^2N^{5/3}(e^2/mc^2r_0)^2$. The requirement is then

$$\begin{aligned} 1+g-3g_1-2g_2\geqq -\frac{45e^4N^{-1}}{|J(0)|r_0^2mc^2}\\ +\frac{4}{N}(1-\tfrac{1}{2}g-(3/2)g_1-2g_2)-\frac{54mc^2}{N|J(0)|}. \end{aligned} \tag{7.6}$$

By using $|J(0)|=70mc^2$ and $r_0=e^2/mc^2$ the right side is -0.09. This condition differs very little from (7). If instead of requiring a smaller stability than that corresponding to groups of alpha-particles one requires a smaller stability than that corresponding to $17mc^2$ mass defect per particle the right-hand side of the last inequality is changed only by -0.001. Similarly if instead of (7.2) it is required that a nucleus with $N=Z$ should not have a greater stability than that corresponding to a mass defect of $17mc^2$ per particle, which corresponds to the stablest nuclei, one obtains

$$\begin{aligned} 1+g-5g_1-3g_2\geqq -\frac{45e^4N^{-1}}{|J(0)|r_0^2mc^2}+\frac{8}{N}\Big(1-\frac{1}{2}g\\ -\frac{5}{4}g_1-\frac{3}{2}g_2\Big)-\frac{6e^2}{5r_0|J(0)|}-\frac{68mc^2}{N|J(0)|}. \end{aligned} \tag{7.7}$$

For nuclei with $Z=N=100$ this condition is only slightly weaker than (7.2) since the right side of the last inequality is -0.09 using the

same constants as previously. The inequality (7.2) is thus also nearly the condition for not having too much stability in nuclei with ordinary numbers of particles.

Actual heavy nuclei are far from being in a state of high particle density such as was just used. For Hg^{200} $E^r/E_{ex}{}^r$ can be estimated to be approximately 4 using the statistical model and $r_0=0.8\times10^{-12}$ cm with $\alpha^{-\frac{1}{2}}=2.2\times10^{-13}$ cm. For a very high particle density this ratio would be $N/2=60$. Eq. (7.4) is thus not a guide for the actual energy dependence. A too large numerical value of a negative coefficient of E in (7.1) would be harmful to stability but it is impossible to tell without further calculation whether higher approximations reduce the energy sufficiently to allow appreciable positive values of $1+g-5g_1-3g_2$. If $g_1=g_2=0$ and if $E/E_{ex}=4$ the potential energy occurring in (7.1) is $-6gE_{ex}$ and is positive. Nevertheless this does not exclude the possibility of a simple theory with $g_1=g_2=0$ because (1) the energy corresponding to an assumed interaction is lower than the value of the variational integral with an approximate wave function; (2) $E^r/E_{ex}{}^r$ is <4; (3) exact values of E/E_{ex} are hard to obtain since the uncertain nuclear radius is involved.

In all of the above discussion it was supposed that $J(r)$ has the same sign throughout and complications arising from a reversal of sign near $r=0$ were not taken up. In proton-proton scattering experiments the kinetic energy is of the order of 1 Mev while in the nucleus the kinetic energy of individual particles is of the order of 30 Mev. The kinetic energy inside the "potential well" representing the interaction of two particles is changed, however, only from $\sim$20 Mev to $\sim$35 Mev or perhaps $\sim$50 Mev in the comparison of scattering experiments with conditions inside the nucleus. This corresponds to a decrease of the wave-length inside the deep part of the "well" by a factor of about 1.3 which means that roughly the same features of $J(r)$ come into consideration in existing heavy nuclei as in proton-proton scattering experiments. In the deduction of the inequalities (7.3), however, the size of the nucleus was taken to be smaller than that of an actual nucleus and, therefore, the kinetic energy per particle was increased to a maximum of about $(8\times10^{-13}/2.8\times10^{-13})^2$ 30 Mev$\sim$200 Mev for $N=100$. Since some of the nuclear particles collide while traveling in opposite directions the relative kinetic energy is changed by a factor of about 10 in the deep part of the "well" which corresponds to a factor 3 in the wave-length. A reversal of sign of J within about $\frac{1}{3}$ of e^2/mc^2 will thus begin to affect the conditions (7.6) and (7.7) without seriously affecting the scattering experiments and the mass defect calculations of light nuclei. The conditions (7.3) for infinite N and Z are changed to their opposites for such a reversal.

Although it appears from the above that there is nothing against considering the main part of the interaction of nuclear particles as being the same in form for all particles it is not likely that the interaction law is identical in all approximations. Spin-orbit interactions and spin-spin interactions involve the magnetic moments which are different for protons and neutrons. In such, essentially relativistic approximations it appears necessary to consider the interactions to be different between different kinds of nuclear particles. It is also unlikely that the Coulombian interaction which already destroys the symmetry has no more intimate connection with the specific forces than that given by an additive term in the Hamiltonian.

For the sake of simplicity the same form of $J(r)$ was used in Eq. (1) for P^M, P^H, 1, P^S. It is obviously possible to use different space functions as multipliers of these operators. There appears to be at present no call for such a generalization.

We are very grateful to Professor E. Wigner for discussions of nuclear stability questions related to the conditions (7).

A Theory of Orbital Neutrons

GILBERT N. LEWIS, *Department of Chemistry, University of California, Berkeley, California*

(Received April 28, 1936)

As an alternative to present theories of the capture of slow neutrons by atoms, it is suggested that such capture is not primarily a phenomenon affecting the interior of the nucleus, but rather that, owing to the interaction between the spin of the nucleus and the spin of the neutron, there is a field outside the nucleus in which neutrons can be held in quantized "orbits." The fall from one of these orbits into the center of the nucleus is regarded as a second phenomenon not immediately related to the first. The probability of capture in a particular orbit is assumed to depend (1) upon a relationship between the energy of the approaching neutron and the kinetic energy in this orbit, and (2) upon the presence in the same neighborhood of occupied electronic orbits. Some consequences are drawn from these assumptions and compared with the results of experiment.

IN the study of slow neutrons, begun by Fermi and his associates, and since continued in many laboratories, it has been found that many elements absorb these slow neutrons to a remarkable extent. The absorption of fast electrons indicates the same small nuclear cross section that is obtained by other experimental methods, but with slow neutrons the effective cross section is frequently many times, and in one case over ten thousand times, as great. This fact does not necessarily imply that there is associated with the nucleus any physical entity which has these large dimensions. If we extend Rayleigh's theory of the absorption of sound and of light to the absorption of material particles, the absorber, no matter how small, should be capable of capturing the particle over an area of approximately λ^2, where λ is the de Broglie wave-length of the oncoming particle. However, this theory, while it gives an estimate of the maximum possible absorption, does not aid in predicting the actual absorption. It may be more naïve, but also may be more useful, to assume that, associated with the atom, there is some definable entity which has dimensions of the order of magnitude of the cross sections deduced from the absorption coefficients of these slow neutrons.

At first these absorption coefficients were supposed to vary inversely with the velocity of the neutron. Now, however, it is known that the absorption is no simple function of the energy of the neutron and that frequently an element absorbs selectively in one or more energy ranges. In the case of lithium and boron the absorption has so far shown no maximum and seems to be nearly proportional to the inverse velocity. To the group exemplified by lithium and boron we must add hydrogen, which absorbs neutrons to produce deuterium far more effectively when the neutrons pass through paraffin at the temperature of liquid air.[1]

An explanation of the selective absorption has recently been presented by Bohr,[2] and by Breit and Wigner.[3] This explanation rests upon two main assumptions. The first assumption is that there is a series of energy levels in the system nucleus+neutron, rising through the enormous range of approximately ten million electron volts to the dissociation potential, and continuing above this potential. The second assumption is that the nucleus has sufficient complexity so that the different parts of the nucleus+neutron system may possess, for a certain time, an energy greater than that required to disrupt the system, if all the energy were possessed by one neutron. According to this second assumption the more complex nuclei possess a mechanism of absorption which would be lacking in so simple a nucleus as that of hydrogen.

At first sight it would seem unlikely that remote control from a state so distant in energy as the ground state of the system nucleus +neutron could account for the fineness, and the highly specific nature of the absorption phenomena. Nevertheless the mathematical analysis

[1] Moon and Tillman, Proc. Roy. Soc. **A153**, 476 (1936).
[2] Bohr, Nature **137**, 344 (1936).
[3] Breit and Wigner, Phys. Rev. **49**, 519 (1936).

of Breit and Wigner shows that it is possible, without the aid of any unreasonable assumptions, to account for existing experimental facts by a consideration of nuclear energy levels alone. They retain the view of an absorption coefficient inversely proportional to the neutron velocity in the low energy range but superpose additional resonance bands in the range of higher energies. This view seems to be in accord with the main body of experimental facts regarding neutron absorption which has so far been obtained.

Furthermore, at the end of their paper Breit and Wigner attempt to show that no mechanism except the one that they suggest can account for the facts of neutron absorption. Here of course their task is a more difficult one, for it would seem impossible in the present state of our knowledge to predict all the possible interactions between nuclei, electrons and neutrons. Yet the ideas of all mathematical physicists are so nearly in accord on this subject that it might appear superfluous to offer at this time an alternative view of the phenomenon of neutron capture. Nevertheless there are some experiments, especially one of von Halban and Preiswerk, to which later reference will be made, which suggest that the capture of slow neutrons may not be a pure nuclear phenomenon, but may be due rather to phenomena occurring in the atom and molecule at a considerable distance from the nucleus. For this reason a rough sketch of such an alternative explanation will be offered in the present paper.

If we had before us only the experimental results regarding the absorption of slow neutrons without any of the theories which have developed, we would be tempted to regard the absorption as analogous to the absorption of light, where we ordinarily find a number of resonance bands with little absorption at energies which are either very much larger or very much smaller than the resonance energies. According to this analogy the absorption which is peculiar to slow neutrons would be regarded as all of one type, and in the case even of those elements which at present show only an absorption which is approximately inversely proportional to the neutron velocity, we might expect, at lower velocities than have yet been investigated, a maximum of absorption, followed at still lower energies by a diminution of absorption with diminishing velocities. This is in fact the picture of the absorption of slow neutrons which follows from the hypothesis that we are now to consider.

While it is probably not permissible to assume any large field of force operating on the neutron at large distances from the nucleus, we may, however, assume a field near the nucleus which becomes faint but not entirely negligible at interatomic distances. Our hypothesis will be that a neutron may be held in such a field and travel in what we may for brevity call orbits. Knowing little of the nature of the field we can only say with certainty that these orbits must be quantized with respect to angular momentum. If, as suggested by the absorption experiments, the kinetic energy of the neutron in its innermost orbit is of the order of a few volts, and if the angular momentum is $h/2\pi$, then the radius of this first orbit will be of the order of 10^{-10} cm.

It seems natural to assume that the field we are speaking of is due to an interaction between the spin of the nucleus and the spin of the neutron. In the first place we know of no other property of the neutron to which this effect could reasonably be attributed, and in the second place, no elements so far investigated have a large absorption coefficient for slow neutrons except those that have at least one prominent isotope which possesses a spin. Atoms with zero spin such as C^{12} and O^{16} do not show this effect, although a neutron entering these nuclei to produce C^{13} and O^{17}, respectively, would release energy of the order of five million electron volts.

Regarding the probability of the capture of a neutron in one of its orbits, we can make use only of the roughest analogies. We might assume that the probability of the neutron capture is highest, either when the kinetic energy of the approaching neutron is of the same order of magnitude as the kinetic energy of the neutron in its orbit, or when the diameter of the neutron orbit bears some definite ratio to the de Broglie wave-length of the approaching neutron. By either assumption we may expect neutrons of larger energy to be captured in the lower orbits and those of smaller kinetic energy in the higher neutron orbits. This will be our first postulate.

At first sight it is hard to imagine how a

neutron falling into an orbit, or falling from one orbit to a lower orbit, can get rid of its energy. It is not likely that a transition involving an uncharged particle like the neutron could lead directly to the emission of a photon. However, in our picture of neutron orbits, beginning at something like 10^{-10} cm from the nucleus, and proceeding outward, some of these outer orbits will lie in the region of occupied electronic orbits, and here the amount of interaction between neutron and electrons may well be sufficient to permit the energy lost by the neutrons to be given off as light, or soft x-rays. We thus arrive at our second postulate: a neutron has a larger probability of capture into a neutron orbit which is in the neighborhood of occupied electronic orbits. According to this view, capture is due to simultaneous interaction between nucleus, neutron and electrons, resulting in a peculiar kind of molecule.

From these two postulates we are able to draw a conclusion for which there seems already to be good experimental evidence. Since the electronic orbits or shells move toward the nucleus as the atomic number increases, we may expect, in the main, that regions of large selective absorption will occur at relatively high energies only in the case of heavier atoms. It is already evident that while many of the heavy elements have absorption bands far above the thermal range, the three light elements, hydrogen, lithium and boron, are powerful absorbers, but only in the range of very small energies. As far as I am aware this striking fact is not predictable by any other proposed theory of neutron capture.

The problem of neutron scattering is a difficult one. The neutrons that are captured and have lost their excess energy by the emission of a photon can no longer be ejected from the atom, but one would expect in the neighborhood of the absorption bands many reversible collisions between neutron and atom which would result in scattering. In the case of cadmium, which has a high absorption coefficient for neutrons of thermal energy, and which apparently does very little scattering,[4] it may be necessary to assume that the neutron falls into the nucleus almost simultaneously with its capture. This would result in a broadening of the absorbing levels, with an increase in the probability of absorption and a diminution in the probability of scattering.

When the neutron is captured to form a radioactive element of measurable life, there seems at present no direct way of ascertaining whether the neutron falls into the nucleus soon after its capture, or whether it remains in the atomic orbit for a time which may even determine the apparent life of the new element. It is to be noted that the latter assumption would enable us to account for the long life of certain artificially radioactive elements which emit β-rays of great energy, and seem therefore hard to reconcile with Sargent's rules for β-emission. If in any case the probability of falling into the nucleus should happen to be of the same order of magnitude as the probability of decomposition of the resulting nucleus, an interesting type of decay curve would be obtained.

A further consequence of the theory of neutron orbits is that the absorption coefficient of an element, depending, as we have assumed, upon the positions of electrons with respect to the nucleus, should vary with the type of chemical binding. This would be especially true of hydrogen. We should, therefore, expect that hydrogen in paraffin, where the electrons are presumably nearer to the hydrogen than in other hydrogenous substances such as water, would be the most efficient in capturing neutrons of thermal energy.

The only experiments that I know which have a bearing on this question are those of von Halban and Preiswerk.[5] They studied the number of slow neutrons emerging when a neutron source is placed in the center of spheres of different size containing different hydrogenous substances. They found that the number of slow neutrons coming through the surface of the sphere depended not only upon the number of hydrogen atoms lying between source and target, but also upon the particular compound containing these hydrogen atoms. They interpreted their results as due to the difference in the rate at which the neutrons are slowed down by the different types of hydrogen atom. More recent experiments on the slowing of neutrons by very cold paraffin, and the fact that hydrogen pre-

[4] Dunning, Pegram, Fink and Mitchell, Phys. Rev. **48**, 265 (1935).

[5] von Halban and Preiswerk, Nature **136**, 951 (1935).

sumably does not absorb efficiently except when the neutron velocities have become small, makes it seem as likely that their results actually indicate a greater absorption coefficient for paraffin than for the other substances which they studied. There are, however, so many factors involved, the slowing down, the scattering, and the capture of neutrons, that it is highly desirable that new experiments be made to ascertain the actual absorption coefficient of hydrogen in its various compounds. These experiments are crucial for, if the capture of neutrons by hydrogen is determined solely by energy levels in the deuterium nucleus, it could in no way depend upon the particular chemical compound in which the hydrogen is bound.

Note added August 14. In experiments which have just been carried out in this laboratory by W. F. Libby and E. A. Long, two remarkable results have been obtained, first, at 20°K there is a great increase either in the slowing of neutrons, or their absorption, or both, when liquid hydrogen is replaced by paraffin. Second, the slowing of neutrons by cold paraffin continues down to temperatures at which there is no mechanism now known to account for this phenomenon. These experiments indicate very strongly that there are processes involved which concern the molecule as a whole and not merely the nucleus.

NOVEMBER 1, 1936 PHYSICAL REVIEW VOLUME 50

The Magnetic Anisotropy of Copper Sulphate Pentahydrate, $CuSO_4 \cdot 5H_2O$, in Relation to Its Crystal Structure. Part I

K. S. KRISHNAN AND ASUTOSH MOOKHERJI, *Indian Association for the Cultivation of Science, Calcutta*

(Received July 6, 1936)

The magnetic anisotropy of the triclinic crystal $CuSO_4 \cdot 5H_2O$ has been measured. The crystal is found to be nearly uniaxial magnetically, i.e., has an axis of approximate magnetic symmetry, the susceptibility along the axis being less than that along perpendicular directions by about 300×10^{-6} c.g.s. e.m.u. per gram molecule at 26°C. The above axis is inclined at 156°, 65°, and 52°, respectively, to the '*a*', '*b*' and '*c*' axes of the crystal. These results are discussed in relation to the known arrangement of the water molecules and oxygens round the Cu^{++} ions and the resulting crystalline electric fields acting on the latter.

1. INTRODUCTION

IN some recent papers Van Vleck and his collaborators[1] have discussed theoretically the magnetic behavior of some of the Tutton salts of the iron group of metals, particularly in relation to the influence of the strong internal electric fields which are acting on the paramagnetic ions in the crystals. The two copper salts $CuSO_4 \cdot K_2SO_4 \cdot 6H_2O$ and $CuSO_4 \cdot (NH_4)_2SO_4 \cdot 6H_2O$ have been studied in detail by Jordahl[2] and by Janes,[3] and they conclude from the magnetic data that the crystalline electric field acting on the Cu^{++} ion in these crystals has monoclinic symmetry. The field can be split up into two parts, one with cubic symmetry, which is found to be very predominant, and the other with rhombic symmetry, which is much feebler; the over-all Stark separations of the energy levels of Cu^{++} produced by these two fields are about 18,000 cm^{-1} and 350 cm^{-1}, respectively. This predominantly cubic symmetry of the field is a natural consequence of the octohedral arrangement[4] of the six water molecules in the crystal round each Cu^{++} ion, the disposition of the SO_4^{--} and the K^+ or NH_4^+ ions, which are at a greater distance from Cu^{++}, probably producing the feeble rhombic field.

The magnetic susceptibility of the triclinic crystal $CuSO_4 \cdot 5H_2O$ has been measured in the *powder state* over an extensive range of temperatures by de Haas and Gorter,[5] and from these susceptibility data, both Jordahl and Janes concluded that in this crystal also, the crystalline

[1] See Van Vleck, *Theory of Electric and Magnetic Susceptibilities*, Oxford (1932), Chapter XI.
[2] Jordahl, Phys. Rev. **45**, 87 (1934).
[3] Janes, Phys. Rev. **48**, 78 (1935).
[4] Regarding the structure of the Tutton salts see Hofmann, Zeits. f. Krist. **78**, 319 (1931).
[5] de Haas and Gorter, Leiden Comm. 210 d (1930).

fields acting on Cu^{++} should be predominantly cubic. This result too has recently been shown to be in conformity with the structure of the crystal, by Beevers and Lipson;[6] they find that each Cu^{++} ion in the crystal is at the center of an approximate octohedron formed by four water molecules and two oxygens.

Whether this crystalline field is wholly cubic, or whether there is also a feeble rhombic component, as in the Tutton salts, it is not possible to decide, since the mean susceptibility of the crystal, for which alone experimental data are at present available, is not sensitive to such feeble superposed fields. Measurements on the magnetic anisotropy of the crystal will however give us much information on this point. We have therefore made measurements on the anisotropy of this crystal at different temperatures. In Part I of this paper we give an account of the measurements at room temperature, and discuss the results in relation to the structure of the crystal. Measurements at low temperatures will be dealt with in Part II.

2. Experimental

Copper sulphate pentahydrate crystallizes in the triclinic system, in the space group C_i^1. An x-ray analysis of the crystal has recently been made by Beevers and Lipson.[7] The unit cell has the dimensions

$a = 6.12$A,	$\alpha = 82° 16'$,
$b = 10.7$,	$\beta = 107° 26'$,
$c = 5.97$,	$\gamma = 102° 40'$,

and it contains 2 molecules of $CuSO_4 \cdot 5H_2O$.

As the crystal is triclinic, the direction of none of its magnetic axes is known directly from considerations of symmetry, as in the other crystal systems. We have therefore to determine experimentally these directions as well.

The experimental procedure adopted is as follows. The crystal is suspended at the end of a calibrated quartz fiber, in a uniform horizontal magnetic field, with some natural face of the crystal horizontal, or some edge in it vertical. The upper end of the fiber is attached axially to a graduated torsion-head. The movements of the crystal are watched through a telemicroscope, whose axis has been adjusted to be horizontal and normal to the direction of the field.

In the first place the torsion-head is rotated suitably so as to make the torsion on the fiber nothing when the crystal takes up its equilibrium orientation in the magnetic field. We shall call this position of the torsion-head as its zero position. We require now to determine (1) the directions of the maximum and minimum susceptibilities of the crystal in the horizontal plane, i.e., the directions which set themselves along and perpendicular to the magnetic field; (2) the difference between the maximum and minimum susceptibilities in the horizontal plane, i.e., the anisotropy in the horizontal plane. The latter is determined by finding the angle α_0 through which the torsion-head has to be rotated from its zero position in order to make the crystal *just* to turn round in the field.[8] The anisotropy $\Delta\chi$ per gram molecule is then given by the relation

$$\Delta\chi = (2Mc/mH^2)(\alpha_0 - \pi/4), \qquad (1)$$

where c is the torsional constant of the fiber, H is the magnetic field, m is the mass of the crystal and M is the gram molecular weight.

To determine the directions of the magnetic axes in the horizontal plane we proceed as follows. When the crystal has taken up its equilibrium orientation in the field under zero torsion of the fiber, let some horizontal edge, or some vertical face of the crystal make a small angle $\varphi(<\pi/4)$ with the direction of observation, i.e., with the direction of the normal to the field. Let α be the angle through which the torsion-head has to be rotated from its zero position in order to bring the above edge or face exactly along the direction of observation. Evidently

$$\sin 2\varphi = (\alpha - \varphi)/(\alpha_0 - \pi/4), \qquad (2)$$

from which φ is known. By finding the inclination φ of two such edges or faces, to the normal to the field, the two magnetic axes in the horizontal plane are fixed uniquely.

The crystal is resuspended so as to make other convenient crystal directions successively vertical, and for each suspension the directions of the

[6] Beevers and Lipson, Proc. Roy. Soc. **A146**, 570 (1934).
[7] See reference 6. See also Tutton, *Crystallography and Practical Crystal Measurement*, Vol. 1 (Macmillan, 1927), p. 297.
[8] See Phil. Trans. **A234**, 265 (1935).

TABLE I. *Magnetic anisotropy of $CuSO_4 \cdot 5H_2O$ at 26°C.*

Serial number	Mode of suspension	Orientation in the field	$\Delta\chi$ ($\times 10^6$)	θ	$\Delta\chi/\sin^2\theta$ ($\times 10^6$)
1	'c' ax. vert.	($\bar{1}00$) at 25° to the field and ($\bar{1}\bar{1}0$) at 51° to it.	183	52°	295
2	'a' ax. vert.	(011) at 2½° to field and (021) at 17½° to it.	55	24½°	320
3	($\bar{1}00$) and ($\bar{1}11$) vert.	($\bar{1}00$) at 45¼° to field and ($\bar{1}11$) at 14° to it.	261	86°	262
4	($\bar{1}\bar{1}0$) and ($\bar{1}11$) vert.	($\bar{1}\bar{1}0$) at 60° to field and ($\bar{1}11$) at 12° to it.	263	79°	273
5	(100) horiz.	'c' ax. at 59½° to field and intersection of ($\bar{1}00$) and ($\bar{1}11$) at 7½° to it.	163	45°	326
6	(110) horiz.	'c' ax. at 44° to field, and intersection of ($\bar{1}\bar{1}0$) and ($\bar{1}11$) at 12° to it.	220	61°	288
7	($\bar{1}10$) horiz.	'c' ax. at 90° to field and intersection of ($\bar{1}10$) and ($\bar{1}11$) at 2½° to it.	113	38°	298
8	($\bar{1}11$) horiz.	Intersection of ($\bar{1}11$) and ($\bar{1}00$) at 22° to field, and intersection of ($\bar{1}11$) and ($\bar{1}\bar{1}0$) at 47° to it.	26	16°	342

magnetic axes in the horizontal plane, and the corresponding anisotropy $\Delta\chi$, are determined in the above manner.

3. RESULTS

The experimental results obtained at room temperature are collected together in Table I. The second column gives the manner of suspension of the crystal, and the third the observed orientation of the crystal in the magnetic field; the fourth column gives the value of the anisotropy. The room temperature fluctuated about a mean value of 26°C by a few degrees, and all the values of $\Delta\chi$ have been reduced for uniformity to this temperature by assuming that $\Delta\chi$ varies inversely as the square of the temperature. This temperature correction is small. The last two columns in the table will be explained in the next section.

4. THE MAGNETIC AXES AND THE ANISOTROPY OF THE CRYSTAL

It is convenient to study the experimental data obtained in the previous section with the help of the stereographic projection. For any given suspension of the crystal, there is one plane which is horizontal (which need not necessarily be a natural or a possible crystallographic plane). In Table I we have numbered the different crystal suspensions for which we have made magnetic observations, serially from (1) to (8). In the stereographic projection (see Fig. 1) the poles of the corresponding horizontal planes are denoted by the same numbers. Thus point 1 in the figure is the pole of the plane which would be horizontal when the crystal suspension is 1; and so on.

From each of these poles a great circle is drawn to represent the direction of maximum susceptibility in the particular plane, i.e., the direction which sets itself along the field in the corresponding suspension of Table I. (To be more precise, this great circle is the locus of the poles of all the tautozonal planes which have the above direction of maximum susceptibility as the zone axis.) Only relevant portions of these great circles are shown in the figure.

As will be seen from the figure, all these great circles pass very close to a certain point M which we have marked by a small circle with a central dot. This indicates (1) that the crystal has an axis of approximate magnetic symmetry, namely along the normal to the plane which has M as its pole; this axis is found to make with the a, b and c axes of the crystal the angles 156°, 65° and 52°, respectively: (2) that the susceptibility of the crystal along the above axis is less than that along perpendicular directions; denoting the two susceptibilities by $\chi_{\parallel}$ and $\chi_{\perp}$, respectively, $\chi_{\parallel}$ should be less than $\chi_{\perp}$.

If the above conclusion regarding the approximate uniaxial symmetry of magnetism of the

crystal is correct, then the anisotropy $\Delta\chi$ for a given plane should be given by the relation

$$\Delta\chi=(\chi_\perp-\chi_{II})\sin^2\theta, \qquad (3)$$

where θ is the angle between the normal to the plane and the axis of symmetry; in other words, $\Delta\chi/\sin^2\theta$ should be nearly constant.

The value of θ corresponding to any given suspension can be directly read from the stereographic projection. The values entered in Table I were obtained in this manner. It will be seen from the last column of the table that except for suspension (8), for which θ is very small (16°), the values of $\Delta\chi/\sin^2\theta$ are near about 300×10^{-6}.

The variations of the individual values of $\Delta\chi/\sin^2\theta$ from the mean offer a rough estimate of the deviation from perfect axial magnetic symmetry. On close examination we find that the values of $\Delta\chi/\sin^2\theta$ are largest for the suspensions (2) and (5), and smallest for (3) and (4), which suggests that the direction of the greater of the two almost equal susceptibilities in the plane M is nearly perpendicular to the planes (3) and (4).

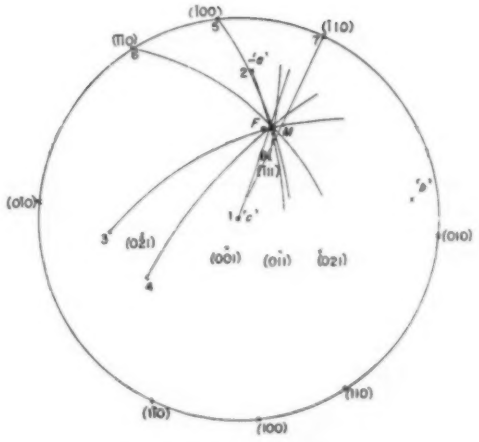

FIG. 1. Stereographic projection.

5. THE CRYSTALLINE FIELD AND ITS AXES

The above value for the magnetic anisotropy of $CuSO_4\cdot5H_2O$, namely $\chi_\perp-\chi_{II}=300\times10^{-6}$ c.g.s. e.m.u. per gram molecule, points definitely to the existence of a rhombic component in the crystalline field, of nearly the same magnitude as in the Tutton salts of copper.

This small rhombic field is indeed to be expected from the disposition of the water molecules and the oxygens round the Cu^{++} ions in the crystal. From the x-ray analysis by Beevers and Lipson it is found that though each copper ion is at the center of an octohedron formed by four water molecules and two oxygens, the octohedron is only an approximate one; the four water molecules being much closer to Cu^{++} than the two oxygens. The crystalline field acting on Cu^{++} along directions in the plane of the water molecules, should therefore differ slightly from that along the normal to the plane of the water molecules.

There are two Cu^{++} ions in the unit cell, which we shall differentiate by the subscripts I and II. On calculating the orientations of the square of water molecules surrounding Cu_I and that surrounding Cu_{II}, from the parameters given by Beevers and Lipson, we find that the two squares are nearly perpendicular to each other (actually at 82°), and that they are both parallel to a direction F which makes with the a, b and c axes of the crystal the angles 155°, 68° and 50°, respectively. This direction F, as will be seen from the stereographic projection, is very close to the magnetic symmetry axis M, which is inclined at 156°, 65° and 52°, respectively, to the same crystallographic axes.

This coincidence of the magnetic and the crystalline field axes is significant; it points to the asymmetry of the crystalline field acting on the paramagnetic ion as the ultimate cause of the magnetic anisotropy of the crystal, as contemplated in Van Vleck's theory.

The New Relativity

D. G. BOURGIN, *Mathematics Department, University of Illinois, Urbana, Illinois*

(Received May 15, 1936)

The Page-Milne relativity theories are shown to imply the continuous group concept in connection with the conditions of equivalence and the one-dimensional problem is studied. Motional invariants are determined. A quadratic form left invariant under permissible motions is found. The expression determined is a proper one for the quadratics given in noninvariant form by Milne and Page. A tentative suggestion is made to extend the theory by making this quadratic form central for correlating observations and the consequences are studied. The form is invariant under a three parameter continuous group though one of the new groups introduced this way seems difficult to interpret physically. The Lorentz transformation is not necessarily part of the group and even when admitted it must be used with care. Nevertheless, another relation similar to that of the Lorentz transformation always exists between coordinate assignments made by two observers, moving in a permissible way, on the set of particles moving with constant velocity relative to one of them. This generalizes a result given by Page. A fairly extensive category of motions is taken up in some detail and the motional equations found.

RECENTLY Page[1] has presented a new relativity theory. As Page himself has remarked, there is a marked formal resemblance to the researches of E. A. Milne.[2] These authors have obtained, from the new viewpoint, coordinate transformations between observers who are (a) at rest relatively to each other, (b) moving with constant relative velocity, (c) moving with constant acceleration (Page alone). We shall not be concerned here with the subsidiary cosmological specifications of these investigators. Their results are readily generalized[3] and completed once we establish that "equivalence" is connected with the group property. Furthermore, a plausible extension of the theory based on a central invariant quadratic form is taken up though most of the results are independent of this salient. The method used is that of the Lie theory of groups.[4] For the convenience of the reader not very conversant with this discipline, the theorems of group theory made use of in this paper are indicated in an appendix.

As a preliminary, we summarize briefly the basic argument of the new relativity. Consider two observers I and II, where II's observations will hereafter be differentiated from those of I by primes. Both observers are assumed time conscious of "later" and "earlier" and are equipped with devices called "clocks" which give T readings increasing monotonically with time. Both assign coordinates to other points supposed equipped with observers, according to the conventions

$$x=c(T_3-T_1)/2$$
$$t=(T_3+T_1)/2 \qquad (1)$$

the value of the arbitrary constant c is agreed on by all observers. T_1 and T_3 represent the clock reading of I when a light signal is sent to II and the reading when this outgoing signal, reflected back by II, returns to I. II defines x' and t' similarly. If the clocks are adjusted so that all observations made by I on II are the same as those of II on I the observers and clocks are equivalent. If besides this $t=t'$ the clocks are also isochronous. Page and Milne have given a method[5] by which this equivalence may be experimentally established in principle though the natural question of uniqueness is left open.

We introduce the symbol $\sim_A$ to indicate equivalence of two observers established with respect to the somewhat vague concept (at the moment) of motion of type A. It would seem that the theory of such motions must require: Postulate α: If $\text{II}\sim_A\text{I}$ and $\text{III}\sim_A\text{I}$ then $\text{III}\sim_A\text{II}$ (in the sense of clock equivalence). Page's procedure is to take particular motions (a), (b) (c) and actually show that the property de-

[1] Leigh Page, Phys. Rev. **49**, 254, 466 (1936). These will be referred to as P. I and P. II, respectively.

[2] E. A. Milne, *Relativity, Gravitation and World Structure*. All page references to Milne's work will refer to this book.

[3] Thus fulfilling the expectations of Page I, p. 258, "in all probability there are many other such categories as yet unsuspected."

[4] T. Y. Thomas, *Differential Invariants of Generalized Spaces* (Cambridge Press), may be consulted for elucidation of the group theory. However, the paper may be readily comprehended without a group theory background if the reader take the theorems of the appendix on faith.

[5] P. I, pp. 255, 256. Milne, P. II.

manded in postulate α is implied. Our attitude is in a sense the converse: Starting with postulate α we find the class of motions permitted.

If I$\sim_A$II Milne has shown that the observations carried out by I and II on III are such that with $x_1=x$, $x_2=ct$, $p=x_2-x_1$, $q=x_2+x_1$, $p'=z_1(p)$ $q'=z_2(q)$, $z_1=z_2^{-1}$, where the functional form z_1 is *determined* by the motion type alone and contains parameters specifying the magnitude of the motion of II relative to I. We may therefore write $z_1(p, \lambda)$; $z_2(q, \lambda)$. Postulate α implies that from

$$\begin{aligned} p''&=z_1(p', \lambda_a), \quad q''=z_2(q', \lambda_a), \\ p'&=z_1(p, \lambda_b), \quad q'=z_2(q, \lambda_b) \end{aligned} \tag{2}$$

there follows $p''=z_1(p, \lambda_c)$, $q''=z_2(q, \lambda_c)$, where $\lambda_c=\varphi(\lambda_a, \lambda_b)$. This, however, is the main group property[6] (cf. Appendix).

This group property enables us, then, to write any one parameter group in p and q of the form given above as the finite transformation equations for a motion type in the new relativity. The various motional invariants are then immediate.

The derivation of an invariant quadratic form is a simple matter. The exposition is perhaps clarified by the introduction of a preliminary lemma.

Lemma: If the coordinate x^i alone enters into $f^i(x^i, \cdots x^n; \lambda)$ and if the transformations $x^{i'}=f^i(x^i, \lambda)$ form a one-parameter continuous group, where λ is a canonical parameter (Appendix), then $\partial x^{i'}/\partial x^i=X^i(x^{i'})/X^i(x^i)$ $i=1, \cdots n$.

From the group property

$$x^{i''}=f^i(x^{i'}, \lambda_2)=f^i(x^i, \lambda_1, \lambda_2)=f^i(x^i, \lambda_3)$$
$$\text{if} \quad x^{i'}=f^i(x^i, \lambda_1). \tag{3}$$

Suppose the variables x^i, λ_1, λ_2, λ_3 independent and the others dependent, then from the second relation of Eq. (3) there follows

$$\frac{\partial x^{i''}}{\partial \lambda_1}=\frac{\partial f^i(x^i, \lambda_3)}{\partial \lambda_1}=0=\frac{\partial f^i(x^{i'}, \lambda_2)}{\partial x^{i'}}\frac{\partial x^{i'}}{\partial \lambda_1}$$
$$+\frac{\partial f^i(x^{i'}, \lambda_2)}{\partial \lambda_2}\frac{\partial \lambda_2}{\partial \lambda_1}. \tag{3.1}$$

[6] For ease in manipulation we assume that the other axioms are also satisfied and that the derivatives and integrals introduced during the course of this work, exist.

Hence $$\frac{\partial x^{i''}}{\partial x^{i'}}=-\frac{\partial x^{i''}}{\partial \lambda_2}\frac{\partial \lambda_2}{\partial \lambda_1}\Big/\frac{\partial x^{i'}}{\partial \lambda_1}.$$

Since λ is a canonical parameter $\lambda_3=\lambda_1+\lambda_2$ and $\partial\lambda_2/\partial\lambda_1=-1$. Th. (1) (Appendix) implies

$$\partial x^{i''}/\partial \lambda_2=X^i(x^{i''}), \quad \partial x^{i''}/\partial \lambda_1=X^i(x^{i''})$$

for canonical parameters. Hence

$$\partial x^{i''}/\partial x^{i'}=X^i(x^{i''})/X^i(x^{i'})$$

which is equivalent to the conclusion of the theorem stated. An extension to r-parameter groups is possible, but is omitted here.

We are in position to derive the general quadratic form invariant under the condition of equivalence of observers. The discussion will be restricted to one-parameter transformations.

$$dp'=\frac{\partial p'}{\partial p}\Big|_\lambda dp, \quad dq'=\frac{\partial q'}{\partial q}\Big|_\lambda dq, \tag{4}$$

$$\therefore \quad dp'dq'=\frac{\partial p'}{\partial p}\frac{\partial q'}{\partial q}dpdq. \tag{4.1}$$

According to the lemma

$$\partial p'/\partial p=\bar{F}(p')/\bar{F}(p); \quad \partial q'/\partial q=F(q')/F(q)$$

where $$\bar{F}(p)=\partial p/\partial\lambda, \quad F(q)=\partial q/\partial\lambda$$

and $$p'=z_1(p, \lambda)=z_2^{-1}(p, \lambda).$$

From Th. (4) (Appendix), $z_2^{-1}(p, \lambda)=z_2(p, -\lambda)$. (4.2)

Hence $F(p)=-F(p)$. Thus

$$dpdq/F(p)F(q)$$
$$\equiv(dx_2^2-dx_1^2)/F(x_2-x_1)F(x_2+x_1) \tag{4.3}$$

is invariant.[7] With $G(z)=\int^z dz/F(z)$ this is at once

$$dG(p')dG(q')=dG(p)dG(q). \tag{4.31}$$

[7] The group theory thus gives a proper way of setting up the invariant quadratic form. Page has given the form $dx_1'^2-dx_2'^2/(1+\lambda x_1')^2-\lambda^2x_2'^2=dx_1^2-dx_2^2/(1+\lambda x_1)^2-(\lambda x_2)^2$ for motion with constant acceleration. The parameter of transformation occurs here and thus implies a particular transformation for just two observers. One may take advantage of the invariance of $1+\lambda x_1/\lambda x_2$ to write this also in the form $dx_1^2-dx_2^2/x_2^2$ or $dx_1^2-dx_2^2/(1+\lambda x_1)^2$ or a variety of equivalent forms. The canonical form, Eq. (4.3), is, in the Page case (*c*), $dx_1^2-dx_2^2/(x_1^2-x_2^2)^2$ and may be established also by using P. I, Eq. (29), in conjunction with his form. Moreover, the noninvariant quadratic given by Milne, p. 43, is also expressed invariantly by Eq. (4.3).

Other forms may be obtained by adjunction of invariant factors. The usual relativity theories introduce a universal time-like[8] quadratic form with an "interval significance." In the new relativity, the invariant quadratic for two particles, differing slightly in coordinates, is determined by the relative motions of observers contemplating them. In the practical dynamics of local systems for instance, all sorts of motion classes of observers enter under suitable force distributions and a different invariant form is to be associated with each class. There seems no compelling reason to impose a particular "interval significance"[9] on the quadratic. The invariant form of Eq. (4.3) is singled out by reason of simplicity and its interesting transformation theory[10] as well as for the value attaching to a study of non-interval forms in relativity.

It is important to observe that Eq. (4.3) is derived from the equivalence conditions and not conversely. Accordingly, the reader may, if he wishes, consider it merely an interesting concomitant. However, one may investigate the consequences of the attractive suggestion of using this quadratic form to determine consistent motion types and their combinations. This amounts to finding the transformations leaving Eq. (4.31)[11] unchanged. These are

$$G(q')=G(q)+\lambda, \quad G(p')=G(p)-\lambda, \tag{5}$$

$$G(q')=G(q)+\lambda, \quad G(p')=G(p)+\lambda, \tag{5.01}$$

$$G(q')=G(q)e^{\lambda}, \quad G(p')=G(p)e^{-\lambda}. \tag{5.02}$$

That all continuous transformations[12] are included follows from the well-known result that a quadratic form in two variables is left invariant by a three-parameter continuous group at most. From these the infinitesimal transformations are easily derived in the form

$$U_1=F(q)\partial/\partial q-F(p)\partial/\partial p, \tag{5.1}$$

$$U_2=F(q)\partial/\partial q+F(p)\partial/\partial p, \tag{5.11}$$

$$U_3=F(q)G(q)\partial/\partial q-F(p)G(p)\partial/\partial p. \tag{5.12}$$

Furthermore

$$(U_1U_2)=0, \tag{5.2}$$

$$(U_1U_3)=U_2, \tag{5.21}$$

$$(U_2U_3)=U_1, \tag{5.22}$$

i.e., U_1 and U_2 generate an Abelian 2-parameter group. Eqs. (5.21), (5.22) indicate that U_2, U_3 and U_1, U_3 do not generate 2-parameter groups though U_1, U_2 and U_3 generate a 3-parameter group of course.

We may make an important observation at this point. For general F no linear combination of the U's yields

$$q\frac{\partial}{\partial q}-p\frac{\partial}{\partial p} \quad \text{or} \quad x_2\frac{\partial}{\partial x_1}+x_1\frac{\partial}{\partial x_2},$$

i.e., the infinitesimal transformation of the Lorentz group. Thus if I and II are related by the transformations generated by U_1, it is not generally true that the transformations to an observer III's coordinates where II moves with constant velocity relative to II, for instance, can be obtained by subjecting x_1 and x_2 to a Lorentz transformation. However,[13] if $F(z)^{[14]}=(z+a)^n$ the Lorentz group is included for all real finite n where the presence of "a" indicates a translation along the x axis. For $n=1$, $a=0$ the Lorentz group is U_1; for all other n values it is U_3 (or rather generated by the infinitesimal transformation).

[8] The constant c (light velocity) may be introduced in such wise as to make the form time-like dimensionally. An "interval" definition requiring $ds^2\sim dt^2$ to follow as a consequence of $dx^2=0$ would not comprehend the quadratics of Eq. (4.3), in general.

[9] If the "cosmological principle" of Milne is postulated, only one motion type is present for the system, but this is not at all a necessary assumption. For this case Robertson, Phys. Rev. **49**, 755 (1936) (published after this work was submitted) has given a deep-lying treatment of the Page theory, utilizing his earlier papers in the Astrophys. J. His form represents the universal generalized "interval" since all observers are of the one motional type, and varies by a conformality factor from that given in Eq. (4.3). Though the writer must own himself anticipated by this work of Professor Robertson in perhaps the main novelty, namely the group theoretic approach, the "local" viewpoint and the generalizations introduced here are quite different.

[10] The only other available quadratic forms for which a 3-parameter group exists involve the invariant I_1 (Cf. Eq. 6.1) in the factor $(\alpha I_1+\beta)^{-2}$ or $(\alpha \sinh aI_1+\beta\cosh aI_1)^{-2}$.

[11] The first draft of this paper accomplished this objective by using Killing's equations in connection with the quadratic form of Eq. (4.3). The simpler derivation in the text was suggested, essentially, by the referee.

[12] The discontinuous reflection transformation $p'=q$, $q'=p$, which changes the indicatrix of the pq plane, has no physical significance.

[13] The fact that the developments using the quadratic form as a governing invariant admit transformations generalizing the Lorentz transformation in the general case has a high degree of interest in showing the new possibilities opened up by this view.

[14] There seems no obvious reason why $F((z)$ cannot be other than a simple power, though some cases will probably be barred on physical grounds. Cf. the restrictions on n later.

It is of interest to write the generating differential equations involving U_1 in the p's, q's and x's and t's. With $w=dp/dq$, $b=dx_1/dx_2$; $s=dw/dq$, $a=dv/dx_2$ it follows from Th. (6) (Appendix) that

$$d\lambda=\frac{dp}{-F(p)}=\frac{dq}{F(q)}=\frac{2dx_1}{F(q)+F(p)}=\frac{2dx_2}{F(q)-F(p)}$$

$$=\frac{-dw}{w(F'(p)+F'(q))}=\frac{2dv}{(F'(q)+F'(p))(1-v^2)}$$

$$=\frac{ds}{wF''(q)+w^2F''(p)+sF'(p)}$$

$$=\frac{2da}{\{F''(p)+F''(q))+v(F''(q)-F''(p))\}(1-v^2)}$$
$$-3av(F'(q)+F'(p))-a(F'(q)-F'(p)). \quad (6)$$

The following are invariant combinations:

$$G(q)+G(p)=I_1, \quad (6.1)$$

$$F(q)w/F(p)=I_2, \quad (6.11)$$

$$F'(q)F(q)w/F(p)+F^2(q)s/F(p)$$
$$-F^2(q)F'(p)w^2/F^2(p)=I_3,$$

$$\text{or } I_2F'(q)-I_2^2F'(p)+F(q)^2s/F(p)=I_3. \quad (6.111)$$

Eq. (6.111) provides the starting point for acceleration discussions.

Coincidence of observer at $x_2=x_2'=0$ is not demanded by the formulae. Neither is isochronism. Sufficient conditions for the latter are, for instance, the stipulation that G be an odd function for then setting $x_2=0$ in Eq. (6.1) gives $G(p')+G(q')=0$, which involves as a solution $p'=-q'$, i.e., $x_2'=0$.

Eq. (6.11) may be restated as

$$w/w'=F(q')F(p)/F(p')F(q). \quad (6.2)$$

Consider the two cases where the velocity of III relative to II is v_1' and $0=v_2'$, respectively, the space time coordinates being the same. Since the right side of Eq. (6.2) is independent of velocities, we have

$$\frac{v_1-1}{v_1+1}\Big/\frac{v_1'-1}{v_1'+1}=\frac{v_2-1}{v_2'+1}\Big/\frac{v_2'-1}{v_2'+1}; \quad (6.3)$$

$$\therefore \quad \frac{v_1-1}{v_1+1}=-\frac{v_1'-1}{v_1'+1}\cdot\frac{V-1}{V+1}, \quad (6.4)$$

where $V\equiv v_2$ is also the velocity of II relative to I if the III's coincide instantaneously with II. This is the Einstein-Lorentz addition law for velocities. However, it is clear that the velocities are not (in contradistinction to the Einstein theory) independent of time and position. That is to say particles stationary relative to II have velocities with respect to I which depend on their coordinates. In fact, setting $w'=1$ corresponding to $v_2'=0$ in Eq. (6.2) gives the formula

$$V=[F(q')F(p)+F(p')F(q)]/F(q')F(p)$$
$$-F(p')F(q). \quad (6.5)$$

On replacing p', q' in Eq. (6.5) by the values derived from Eq. (5), V becomes a generally non-constant function of p, q and λ. Cf. Eq. (8.1) with $v'=0$.

We have now to treat the significance of the two new transformations U_2 and U_3. Page-Milne equivalence implies transformations of type U_1. It may easily be shown that the converse is true. Evidently, U_3 is of U_1 type with FG replacing the customary F. U_2 implies, however, equivalences other than those of the Page-Milne scheme. A conservative view might, therefore, bar such transformations as extraneous and without physical significance. However, conceivably, the new relativity may be extended to include a dual type of equivalence involving U_2, at least in some cases. For instance, if F is an even function, the equivalences determined by U_2 amount to interchanging the meanings of x_1 and x_2 in the Page-Milne equivalence. Discussion of such possibilities would only divert the developments to speculations irrelevant to the purpose of this paper.

It is clear that Eq. (6.4) does not imply the existence of a Lorentz group. We have assumed there two observers I and II contemplating another, III, moving at not necessarily constant velocity relative to II and have found the relations between I and II's estimates of III's coordinates in Eqs. (6.2) and (6.4). In the cases where the Lorentz transformation enters, the physical situation is the following: three observers, I, II, and III contemplate a fourth, IV. III moves with constant velocity V relative to II. We are interested in the relation between the observations of I and III on IV. On writing double primes for III's coordinate assignments we need

merely use the Lorentz transformation

$$x_1''=(x_1'-vx_2')/(1-v^2)^{\frac{1}{2}};\qquad x_2''=(x_2'-vx_1')/(1-v^2)^{\frac{1}{2}} \tag{7}$$

and then employ the usual transformations of x_1', x_2' to x_1, x_2 as conditioned by the motion of II relative to I.

It is necessary to point out, however, that even when all II type observers are equivalent under the motion implied by U_1 no equivalence relations hold for the III's associated with their respective II's, since U_1 and U_3 do not form a group. This is somewhat disappointing. Stated otherwise, there is, in general, no transformation of the type obtained by compounding a Lorentz and a finite transformation of the sort generated by U_1 which will relate III_1 and III_2, where $III_1\sim_{V\text{constant}}II_1$ and $III_2\sim_{V\text{constant}}II_2$. (To maintain the group property it is necessary to take the three-parameter group generated by U_1, U_2 and U_3 for the connection.) This indicates the role of U_2 in the theory. If U_2 be barred, the relations involving it, just given, are to be considered physically unrealizable. Accordingly, the nature and utility of the Lorentz transformation in the general case (as well as the special instance of constant acceleration first treated by Page) is given a definite characterization.

For illustration and further development of the ideas of this article, let us fix our attention on the fairly general case $F(z)=z^n (n\neq 1$ for then U_1 is merely the Lorentz group).

$$p'=p/(1-\lambda p^{n-1})^{1/(n-1)},\qquad q'=q/(1+\lambda q^{n-1})^{1/(n-1)}. \tag{8}$$

For $n=2$ we have

$$p'=p/(1-\lambda p),\quad q'=q/(1+\lambda q),$$

agreeing with Page, P. I, p. 261.

The positive real roots in the denominators of Eq. (8) are implied by the condition $L_{\lambda\to 0}q'$, $p'=q$, p. If negative p (or p') be contemplated as is the case when, for instance, the observations for $x_2=0$ (or $x_2'=0$) are real, then the admissible n values are $n=s/2r+1$, $|r|$ and $|s|$ both integral. It is clear from Eq. (8) that only part of the x_1 axis is mapped continuously on the x_1' axis (and conversely), i.e., for $\lambda>0$ the condition $1-\lambda p^{n-1}>0$, or $x_1>x_2-(\lambda)^{1/(1-n)}$ must be satisfied.

The velocity relations are that $[(v-1)/(v+1)]\times(q/p)^n$ is invariant and

$$\frac{v-1}{v+1}\frac{v'+1}{v'-1}=\left(\frac{1-\lambda p^{n-1}}{1+\lambda q^{n-1}}\right)^{n/(n-1)}=\left(\frac{1-\lambda q'^{n-1}}{1+\lambda p'^{n-1}}\right)^{n/(n-1)}. \tag{8.1}$$

To obtain the equation of motion of II relative to I we remark that evidently II's x_1' coordinate for himself is 0. Hence setting $x_1'=0$ in Eq. (8) and eliminating x_2', the motional equation is given as

$$2\lambda[x_2^2-x_1^2]^{n-1}+(x_2-x_1)^{n-1}-(x_2+x_1)^{n-1}=0.$$

Appendix

The group axioms are (1). If $x^{i'}=f^i(x'\cdots x^n;\ a_1\cdots a_r)$ and $x^{i''}=f^i(x^{i'}\cdots x^{n'};\ b_1\cdots b_r)$ then $c_\sigma=\phi_\sigma(a_1\cdots a_r;\ b_1\cdots b_r)$ such that $x^{i''}=f^i(x'\cdots x^n;\ c_1\cdots c_r)$. (2) If $x^i\to x^{i'}\to x^{i''}\to x^{i'''}$ the associative law holds in combining to get the $x^i\to x^{i'''}$ transformation. (3) The identity transformation exists and the parameter values associated are the same for all transformations in the group. (4) A unique inverse exists for every transformation.

Th. (1) For group transformations

$$\partial x^{i'}/\partial a^j=\Sigma_{\sigma=1}^{r}X_\sigma{}^i(x^{i'}\cdots x^n)A_j{}^\sigma(a_1\cdots a_r).$$

Definition: The infinitesimal transformations of the group are given by $U_\rho=\Sigma_{i=1}^{n}X_\rho{}^i(x'\cdots\lambda^n)(\partial/\partial x^i)$, $X_\rho{}^i$ as in Th. (1).

Th. (2). The necessary and sufficient conditions that $U_1,\cdots U_r$ generate an r-parameter group are that

$$(U_iU_j)\equiv U_iU_j-U_jU_i=\Sigma_{\sigma=1}^{r}c_\sigma U_\sigma;$$

c_σ is a constant and $i,\ j=1,\ \cdots r$.

Th. (3). Canonical parameters exist such that the group transformations may be written symbolically

$$x^{i'}=e^{+\Sigma\rho\lambda_\rho U_\rho}x^i.$$

Th. (4). For the canonical parameters the inverse transformation replaces λ_m by $-\lambda_m$ and the identity transformation is given by $\lambda_m=0$.

Th. (5). The finite transformations are obtained from the infinitesimal transformations by integrating the systems $dp=dx^i/\Sigma_{\sigma=1}^{r}\lambda_\sigma X_\sigma{}^i(x'\cdots x^n)$ subject to the conditions $x^i|_{p=0}=x^i$; $x^i|_{p=p}=x^{i'}$. If $\lambda_\sigma p$ is replaced by T_σ the terms $\{T_\sigma\}$ may be taken as the r essential independent group parameters.

If $v=dx_1/dx_2$, $a=dx_1^2/dx_2^2$ etc., the extended infinitesimal transformation involving change in v, $a\cdots$ is Th. (6).

$$U=X^1\frac{\partial}{\partial x^1}+X^2\frac{\partial}{\partial x^2}+X^v\frac{\partial}{\partial x}+X^a\frac{\partial}{\partial a}+\cdots,$$

$$X^v=\left(\frac{\partial}{\partial x^2}+v\frac{\partial}{\partial x^1}\right)X^2-v\left(\frac{\partial}{\partial x^2}+v\frac{\partial}{\partial x^1}\right)X^1,$$

$$X^a=\left(\frac{\partial}{\partial x^2}+v\frac{\partial}{\partial x^1}+a\frac{\partial}{\partial v}\right)X^v-a\left(\frac{\partial}{\partial x^2}+v\frac{\partial}{\partial x^1}\right)X^1.$$

LETTERS TO THE EDITOR

Prompt publication of brief reports of important discoveries in physics may be secured by addressing them to this department. Closing dates for this department are, for the first issue of the month, the eighteenth of the preceding month, for the second issue, the third of the month. The Board of Editors does not hold itself responsible for the opinions expressed by the correspondents.

Communications should not in general exceed 600 words in length

Note on Diurnal Variation of Cosmic-Ray Intensity

It has been suggested[1] that one possible cause of the diurnal variation in the intensity of cosmic rays might be fluctuations in the earth's magnetic field. This note presents the results of calculations carried out in the attempt to determine what effect fluctuations of terrestrial magnetism may have upon cosmic-ray intensities. Latitude effect curves give the required connection between magnetic field and cosmic-ray intensity if some assumption is made as to the nature of the field-sensitive portion of the rays. Also there must be some cause postulated for the variations in the earth's field.

Following Compton[2] it has been assumed that the field-sensitive portion of the rays is composed of four equally ionizing groups of electrons having energies corresponding to the following values of Lemaitre and Vallarta's X: 0.30, 0.35, 0.40, 0.45. This has been shown to give a curve which very satisfactorily fits the sea-level latitude effect data. It has been further assumed that diurnal variations in the earth's field are due to a variation in the magnetic moment of the earth. While it is clear that this cannot be a correct physical picture since the sign of this diurnal variation is not the same at all latitudes, it seems also clear that any of the mechanisms which have been considered possible, such as circulating currents in the earth and air and diamagnetism in the high atmosphere, would have less effect on cosmic rays. Any of these disturbing factors can affect only a limited portion of the earth's field and might give rise to quite different effects at a distance of a few hundred kilometers above the earth's surface. The results obtained on this simple assumption of a varying magnetic moment may thus be considered to represent the maximum effect which variations of terrestrial magnetism may have on cosmic-ray intensity.

Lemaitre and Vallarta's original curves[3] give intensity as a function of latitude, with separate curves for each value of X. From these can be obtained data for the drawing of curves showing intensity as a function of X, with separate curves for each latitude. The slope at any point on one of these curves is proportional to the rate of change of intensity with X for the particular latitude and value of X represented. Since X is a number which represents the relation between the energy in electron volts of the rays and the magnetic moment of the earth, it is possible to find the value of dX/dM for any value of X, and hence the manner in which a variation of M affects the intensity. The following relations are used:

$$\delta I_{la} = (dI_{la}/dX)(dX/dM)\delta M,$$
$$\delta I/I = \Sigma \delta I_{la}/\Sigma I_{la},$$
$$X = [Er^2/300M]^{\frac{1}{2}}.$$

I_{la} is the intensity at a given latitude l of the component of energy a. M is taken as 8×10^{25} gauss cm^3, and since the calculations are for sea level r is the radius of the earth, 6.4×10^8 cm.

What is actually calculated is the percent variation in total intensity of the cosmic rays produced by the observed average diurnal variation in H, the horizontal component of the earth's field,[4] interpreted of course as a variation in M. This has been carried out for latitudes 25°, 30°, 35°, 40°, and 45°, since these cover the region of large latitude effect. The resulting intensity variations are, respectively, 0.0048 percent, 0.0012 percent, 0.0042 percent, 0.0086 percent and 0.0068 percent.

R. L. Doan[5] from the simultaneous records of five ionization meters over a period of ten days of exceptionally constant barometric pressure, derives a diurnal variation with a maximum about 0.19 percent greater than the average, with a probable error of 0.035 percent. This was at geomagnetic latitude 52°, beyond the region of latitude effect variation. Since the maximum intensity change calculated above is only about one-fourth of the probable error of Doan's result, it appears improbable that fluctuations in the earth's field are responsible for any significant part of this variation.

Thanks are due Professor A. H. Compton for a helpful discussion of the problem.

JULIAN L. THOMPSON

Ryerson Physical Laboratory,
University of Chicago,
October 14, 1936.

[1] R. Gunn, Phys. Rev. **41**, 111 (1932).
[2] A. H. Compton, Phys. Rev. **43**, 399, note 20 (1933).
[3] G. Lemaitre and M. L. Vallarta, Phys. Rev. **43**, 87 (1933).
[4] R. Gunn, Phys. Rev. **32**, 139, Fig. 3 (1928).
[5] R. L. Doan, Phys. Rev. **49**, 107 (1936).

Nuclear Forces

In connection with the two papers which appear in this issue on proton scattering as measuring the attractive forces inside atomic nuclei, it may be of interest to remark that in contrast to the force of gravity and alluding to the correspondingly universal role played by this attraction in giving rise to mass defect or lightness, it has been referred to in our laboratory as the force of levity. The term has previously been used by Boyle, Clerke and others (refer to Century Dictionary). Although as general a property of matter as the force of gravity it is of course not an exact opposite; both are attractions.

M. A. TUVE

Department of Terrestrial Magnetism,
Carnegie Institution of Washington,
Washington, D. C.,
October 16, 1936.

Photoelectric Sensitization of Potassium by Means of Hydrogen

A glow discharge in hydrogen has long been known to increase the sensitivity of a potassium photoelectric cell. The effect of the discharge is to produce a spectral maximum in the visible region of the spectrum (at 4360A). This is referred to as the selective photoelectric effect. Pure potassium shows no selective maximum in the visible part of the spectrum. All of the earlier work was done on relatively thick layers of potassium. Campbell[1] reported, in 1928, that a glow discharge in hydrogen in a "thin film cell" produced a greater red sensitivity than in a cell with a thick layer of potassium. Fleischer and Teichmann[2] were able to produce the selective photoelectric effect by depositing a film of potassium on a potassium hydride surface without the hydrogen discharge. Neither of these experimenters made any attempt to study the sensitization as a function of the thickness of the potassium film.

In the present experiment an "atom gun," like that used by Brady,[3] was used to control and to determine the thickness of the potassium film. The potassium was thoroughly outgassed and was deposited on a freshly evaporated silver surface. The hydrogen was admitted to the cell by flaming a palladium tube attached to the cell. In each case the film was tested for photoelectric sensitivity after the hydrogen was pumped from the cell. The results here given are for light from a monochromator set to transmit a narrow band of light at approximately 4400A. For a potassium film of 0.5 molecular layer, hydrogen admitted to the cell destroyed the photoelectric effect completely. This was found to be true even though the hydrogen was admitted at a pressure as low as 5×10^{-5} mm. A discharge passed at pressures ranging from 10^{-3} to 1 mm failed to restore the photoelectric effect even though a strong white light source was used for illumination. The disappearance of the effect is undoubtedly due to the formation of potassium hydride which is known to be photoelectrically insensitive. For a monomolecular layer film, the admission of hydrogen destroyed the photoelectric effect as before. A discharge in hydrogen at various pressures, as before, failed to restore the effect. The most striking effect was the appearance of a strong selective photoelectric effect if a very small deposit of potassium was made on top of the potassium hydride layer. A deposit of only 0.1 molecular layer was sufficient to give a pronounced selective photoelectric effect. This result indicates that isolated atoms of potassium held away from the underlying metal surface by a layer of potassium hydride are responsible for the selective effect. This is in accordance with the model proposed by Zener[4] to explain the high efficiency encountered in the selective photoelectric effect. It also agrees with the views set forth by de Boer.[5] A film of 5 molecular layers was tested also and here the admission of hydrogen did not destroy the photoelectric effect completely, but reduced it to approximately 0.05 of its value before the hydrogen was admitted. Passing a discharge through the hydrogen had no appreciable effect in this case either.

The fact that Campbell was able to sensitize the thin film by means of the hydrogen discharge may have been due to the fact that he was working with films thicker than those reported on in this experiment, since he had no means for ascertaining the thickness of his films. The results of the present experiment indicate that the sensitization of a potassium photoelectric cell by means of a hydrogen discharge is only effective for thick layers of potassium.

The senior author (J. J. B.) wishes to take this opportunity to thank the committee on the Joseph Henry Fund of the National Academy of Sciences for the aid of a grant used in the purchase of part of the research apparatus. He wishes, also, to thank the physics department of the University of California for the loan of the monochromator.

JAMES J. BRADY
JOSEPH H. ROCHEL, S.J.

St. Louis University,
St. Louis, Missouri,
October 16, 1936.

[1] N. R. Campbell, Phil. Mag. **6**, 633 (1928).
[2] Fleischer and Teichmann, Zeits. f. Physik **61**, 227 (1930).
[3] J. J. Brady, Phys. Rev. **41**, 613 (1932).
[4] C. Zener, Phys. Rev. **47**, 15 (1935).
[5] J. H. de Boer, *Electron Emission and Adsorption Phenomena* (1935), p. 210.

Second-Order Spin Effects in H^3

The Majorana-Heisenberg mixed operator $(1-g)P^M+gP^H$ for neutron-proton interaction causes a mixing of states with different spin symmetries. If the ground states of H^3 and He^4 are assigned a definite multiplicity the mixed operator reduces to $(1-g/2)P^M$. When g is not small the mixing effect will be appreciable and the equivalent Majorana operator valid only in first approximation. Since g probably lies somewhere in the range 0.20 to 0.25, it would seem desirable to estimate the second-order effects.

The ground state of H^3 with spin function $2^{-\frac{1}{2}}\alpha_1\times(\alpha_2\beta_3-\alpha_3\beta_2)$ combines through the mixed operator with states of parallel neutron spin $2^{-\frac{1}{2}}\alpha_1(\alpha_2\beta_3+\alpha_3\beta_2)$ and $\beta_1\alpha_2\alpha_3$ (the subscript 1 refers to the proton). The energy will be lowered by ΔE where

$$\Delta E=\sum_{n>0}\frac{|(0|H|n)|^2}{E_n-E_0}=\frac{1}{E_{av}-E_0}\sum_{n>0}|(0|H|n)|^2=\frac{(0|H^2|0)}{E_{av}-E_0}.$$

The subscript 0 refers to the ground state and n to excited states (in the continuum) of parallel neutron spin. E_{av} represents a "mean value" state in the continuum. The perturbation energy

$$H=V_{12}\{gP_{12}^H-(g/2)P_{12}^M\}+V_{13}\{gP_{13}^H-(g/2)P_{13}^M\}$$

and

$$(0|H|0)=0.$$

Squaring H and summing over spins we find

$$(0|H^2|0)=\tfrac{3}{2}g^2\int\psi_0\{V_{12}^2-V_{12}V_{23}P_{12}^MP_{13}^M\}\psi_0 d\tau.$$

Setting

$$\psi_0=N\exp\,-\tfrac{1}{2}\nu(r_{12}^2+r_{13}^2)-\tfrac{1}{2}\mu r_{23}^2 \quad\text{and}\quad V_{ij}=Ae^{-(r_{ij}/a)^2}$$

we obtain

$$(0|H^2|0)=\tfrac{3}{2}g^2A^2\left\{\left(\frac{\sigma}{\sigma+2}\right)^{\frac{1}{2}}-\left(\frac{4\sigma^2}{(3+2\sigma)(1+2\sigma)}\right)^{\frac{1}{2}}\right\},$$

where $\sigma=\frac{1}{2}\nu a^2=0.934$ from calculations on H^3 including neutron-neutron forces and $\mu=\nu$ to sufficient accuracy.[1] Using Feenberg and Knipp's[2] estimate of 75 mc^2 for A and $g\leqq0.21$ one obtains 20 $(mc^2)^2$ for $(0|H^2|0)$.

The energy denominator $E_{av}-E_0$ may be approximately evaluated from the sum rules for oscillator strengths. In Feenberg units the kinetic energy is given by $-\frac{1}{2}(\Delta_1+\Delta_2+\Delta_3)$, which becomes $-\frac{3}{4}\Delta_x-\Delta_{x'}$ upon transforming to the coordinates $\mathbf{r}=\mathbf{r}_1-(\mathbf{r}_2+\mathbf{r}_3)/2$, $\mathbf{r}'=\mathbf{r}_2-\mathbf{r}_3$. In terms of these coordinates the sum rules for non-Majorana potentials are:

$$\sum_n (E_n-E_m)\,|(n|x|m)|^2=\tfrac{3}{4}, \quad \sum_n (E_n-E_m)\,|(n|x'|m)|^2=1.$$

The latter sum rule connects the ground state with excited states having parallel neutron spins.

$$(E_{av}'-E_0)\sum_n |(n|x'|0)|^2=(E_{av}'-E_0)(0|x'^2|0)=1.$$

We identify E_{av}' with E_{av} since they both represent the "center of gravity" of the continuum for the same excited states. This is of course only a very rough approximation. Using the wave function ψ_0 above, one finds that

$$(0|x'^2|0)=1/(2\mu+\nu)=a^2/2\sigma \leqq 1/(30\,mc^2).$$

This would lead to an estimate of $\frac{3}{4}\,mc^2$ for ΔE. However, one may expect a greater energy denominator because of the fact that Majorana forces will introduce an additional positive term, on the right side of the sum rule equations, which represents the noncommutability of P^M with the coordinate.[3] Upon evaluation of this term ΔE appears finally to be of the order of magnitude $0.5\,mc^2$. A more careful estimate of this effect will be made in a later paper.[4]

The writer is obliged to Dr. L. W. Nordheim and Dr. Eugene Feenberg for conversations on this subject.

R. D. PRESENT

Purdue University,
Lafayette, Indiana,
October 19, 1936

[1] Bethe and Bacher, Rev. Mod. Phys. **8**, 82 (1936); cf. pp. 146–7.
[2] Feenberg and Knipp, Phys. Rev. **48**, 906 (1935).
[3] Cf. Feenberg, Phys. Rev. **49**, 328 (1936).
[4] R. D. Present and W. Rarita, not yet published.

Reflectivity of Evaporated Silver Films

Pure silver films, deposited upon glass by evaporation in a vacuum, have recently been made by us which show appreciably higher coefficients of reflection than those from silver deposited by any other method. We have made an intensive investigation of the influence of the several variables in the evaporation process upon the properties of the deposited metal films and have applied the results of this study particularly to the evaporation of silver. Pure aluminum films were made by the same technique, and for comparison purposes were subjected to the same reflection coefficient measurements with conditions of measurement identical to those used for the silver film. The results are presented in Table I.

The influence of the infrared radiation is clearly indicated. The sodium arc, however, was used with a monochromator which completely eliminated the infrared. The Wratten filters were found to transmit some infrared. Hence, for comparison purposes the value found for the yellow light is the most reliable. This value is approximately 5.5 percent higher than that ordinarily given for silver.

TABLE I. *Reflection coefficients of silver and aluminum.*

Source of Light	Filter	Reflection Coefficients Silver	Reflection Coefficients Aluminum
White light from a 6-volt tungsten lamp	None	99.4%	89.5%
Same	One-inch water cell	99.0%	89.5%
Same	Water cell and Wratten Red No. A25	98.5%	89.2%
Same	Water cell and Wratten Green No. B58	98.5	89.6
Same	Water cell and Wratten Blue No. C5–47	98.0	88.6
Sodium Arc	None	98.5	89.5

The silver used was chemically pure and was carefully cleaned to remove surface impurities. In the vacuum chamber, before evaporation, the metal was carefully heated in a tantalum or molybdenum trough to remove all foreign matter volatile at temperatures less than that needed to vaporize the silver. This preliminary treatment is done under shields in the vacuum chamber in order to prevent contamination of the cleaned glass surface upon which the silver is later deposited. The shields are operated by an external lever mechanism through greased, ground joints.

We have noticed also that silver mirrors made by this improved technique do not seem to tarnish as readily as ordinary silver mirrors do. After standing in the laboratory for six weeks with no protection from the gases present, a decrease of less than one percent was found.

We have not made any attempt as yet to detect differences in the nature of silver films deposited by evaporation or by chemical methods, but believe the evidence here presented is indicative of some inherently dissimilar structures.

HIRAM W. EDWARDS
ROBERT P. PETERSEN

University of California
at Los Angeles,
October 3, 1936.

A Correction to Note on "The Electric Moment of the $^1\Sigma_+$ to O^+ Transition in the Continuum of Cl_2"[1]

In the formula in the first paragraph, C should be c.

The fourth line of the second paragraph, "to $\Sigma^2_{E'FE'J''J'}=1$" should read "to $\Sigma_{E'}F^2_{0E'J''J'}=1$".

G. E. GIBSON
O. K. RICE

Department of Chemistry,
University of North Carolina,
Chapel Hill, North Carolina,
September 30, 1936.

[1] Gibson and Rice, Phys. Rev. **50**, 380 (1936).

Proceedings of The New England Section of the American Physical Society

Minutes of the Brunswick Meeting, October 10, 1936

THE ninth regular meeting of the New England Section was held in Brunswick, Maine, on Saturday, October 10, at Bowdoin College. The presiding officer for the morning session for contributed papers was Professor R. B. Lindsay, Chairman of the Section. Professor Lindsay was also the presiding officer at the business meeting of the afternoon session. At the business meeting, the following officers were elected for the ensuing year:

Professor F. A. Saunders, *Chairman*
Professor P. M. Morse, *Vice Chairman*
Professor J. C. Boyce, *Secretary-Treasurer*
Professors Gladys A. Anslow and L. W. McKeehan, *Program Committee.*

A vote of thanks was extended to the members of the physics department at Bowdoin College for their generous hospitality. After the business meeting, the Bowdoin Physics Laboratories were open for inspection.

The first part of the afternoon session was a colloquium on "The Teaching of Intermediate Physics" led by Professors Hull, Little and Margenau. After the three talks, there was considerable general discussion. The second half of the afternoon session was an invited paper by Dr. Karl K. Darrow on "The Concept of Spin."

Thirty-one members attended the morning session and forty-five the afternoon session.

The program of the Section consisted of seven papers, the abstracts of which are given below.

Philip M. Morse, *Secretary-Treasurer, New England Section*

Abstracts

1. The Structure of Crystalline Bromine. B. Vonnegut and B. Warren, *Massachusetts Institute of Technology.*—Bromine is one of the very few elements for which the crystal structure has not previously been determined. The material melts at $-7.3°C$, and single crystals are readily obtained from the vapor. X-ray oscillation patterns were made, oscillating about the c axis. The crystals were maintained during a 12 hour exposure by being cemented on a glass fiber, and placed in the exhaust from a liquid-air container. The crystal system is orthorhombic with axes $a=4.48A$, $b=6.67A$, $c=8.72A$. The space group is *Ccma* (V_h^{18}). Density values in the literature differ considerably, the final structure requires 8 atoms in the unit cell, and from this the density can be calculated to be 4.05 ($-150°C$). The value 3.4 given in I.C.T. is badly in error. The 8 atoms are in the position $8f$, with $x=0.135$ and $z=0.110$. The structure is definitely one of diatomic molecules, each atom having one nearest neighbor at 2.27A, and no other neighbors closer than 3.30A. The Br–Br distance 2.27A is in good agreement with the band spectrum value 2.28A, and the electron diffraction value from Br_2 vapor 2.28A. The structure of bromine is isomorphous with that of iodine, but from preliminary reports apparently different from chlorine. The structure is one more example of the application of the 8-N law to the structures of the elements in columns IV–VII.

2. Young's Modulus in Bismuth Crystals. A. B. Focke, R. B. Lindsay and C. R. Wilks, *Brown University.*—The Young's modulus of bismuth single crystals has been measured in the two principal crystallographic directions The measurements were made by determining the velocity of sound in a short, single crystalline rod soldered between two longer steel rods. One end of this system was driven by the familiar type of moving coil used in loudspeakers. The other end was free. The sound velocity was computed from the observed distance between two nodes when all or part of the crystal was included between them. Considering one of the nodes to be at a distance l_1 from the nearest steel-crystal junction, the length of the crystal to be l_2 and the distance from the crystal to the second node to be l_3, the expression

$$k_2 l_2 = n\pi - (\eta_1 k_1 l_1 + \eta_3 k_1 l_3)$$

has been derived where n is integral. $k_1=2\pi\nu/C_1$, $k_2=2\pi\nu/C_2$, $\rho_1 C_1 S_1/\rho_2 C_2 S_2$. $\tan k_1 l_1 = \tan \eta_1 k_1 l_1$, $(\rho_1 C_1 S_1/\rho_2 C_2 S_2)\tan k_1 l_3 = \tan \eta_3 k_1 l_3$, ν is the frequency, C_1 the velocity of sound in steel, C_2 the velocity in the sample under test, ρ the density and S the cross section of the material (indicated by the subscript). Measurements were made on four crystals in which the principal axis was perpendicular to the length of the rod and three crystals in which the principal axis was parallel to the rod. The velocities obtained for these crystals were $C_\perp=2026$ meters per sec., and $C_\parallel=1541$ meters per sec. These give for the Young's moduli $Y_\perp=4.04\times10^{11}$ dynes per cm², and $Y_\parallel=2.25\times10^{11}$ dynes per cm².

3. The Automatic Spectrographs of the Harvard-M. I. T. Eclipse Expedition. D. H. Menzel, H. Hemmendinger,

Harvard University Observatory, R. d'E. ATKINSON, *Rutgers University*, AND J. C. BOYCE, *Massachusetts Institute of Technology*.—The use of Dow metal made possible the construction of three rigid but portable eclipse spectrographs. Four plane gratings with lenses and cameras were mounted in a single box. The box was pivoted in a cradle so that it could be adjusted to the sun's declination. The cradle was mounted on a polar axis fitted with a clock drive. Three of the cameras provided automatic exposure of one second duration every two seconds, while the fourth, covering the infrared range, was manually operated. The second spectrograph, consisting of three prisms, lens and moving film camera, was mounted on top of the box containing the quadruple spectrograph. The third instrument contained two concave gratings and six moving film cameras. The eclipse was observed at Ak Bulak in Soviet Central Asia on June 19, 1936. Observing conditions were excellent, and the instruments operated satisfactorily. Typical spectra will be shown.

4. Statistical Analysis of the Counting Rate Meter. L. I. SCHIFF AND ROBLEY D. EVANS, *Massachusetts Institute of Technology*.—The counting rate meter, or vacuum tube speedometer, is an integrating and averaging instrument with an electrical, exponentially decaying memory. It is designed to replace message-register equipment in all particle counting apparatus, and is ideally suited to continuous photographic recording. The average current to the output meter is proportional to the counting rate for constant sources or for decaying sources whose mean life is significantly greater than the time constant RC of the output tank circuit. This RC is analogous to a radioactive mean life, and may be regarded as a mean memory time. While the output current depends only on the output resistance R, and not on the output capacitance C (except for very rapidly decaying sources), the statistical fluctuations in the output current depend upon RC, and are equivalent to the fluctuations expected in a time interval of $2RC$. Expressions are derived for the condenser charge Q, or output current Q/RC, for constant and decaying sources of radiation, as well as for the expected *fractional* statistical fluctuations in these cases. Details of this work will appear shortly in the *Review of Scientific Instruments*.

5. A Mass-Spectrographic Study of the Isotopes of Argon, Potassium, Rubidium, Zinc and Cadmium. ALFRED O. NIER, *University of Minnesota*. (*Now National Research Fellow, Harvard University*.)—A magnetic mass spectrograph is described which is suitable for the measurement of relative abundance of isotopes in those elements which may be put in a volatile form. In argon the presence of A^{38} was verified. In potassium a new isotope, K^{40}, was found. No isotopes other than Rb^{85} and Rb^{87} could be found in rubidium. Zinc is shown to consist of the isotopes 64, 66, 67, 68 and 70 present in abundances proportional to the numbers: 100, 53.8, 7.59, 34.3 and 1.00, respectively. The chemical weight calculated from these figures is 65.31 as compared to the international value, 65.38. Cadmium is shown to consist of the isotopes, 106, 108, 110, 111, 112, 113, 114, and 116 present in amounts proportional to the numbers: 4.79, 3.71, 45.6, 46.6, 86.5, 43.9, 100, and 26.1, respectively. Cd^{115} and Cd^{113}, if present, are present to less than 1 part in 800 and 14,700 in cadmium, respectively. The chemical weight calculated from the figures given above is 112.37 as compared to the international value, 112.41.

6. Colloquium on the Teaching of Intermediate Physics. G. F. HULL, *Dartmouth College*, N. C. LITTLE, *Bowdoin College* AND H. MARGENAU, *Yale University*.

7. The Concept of Spin. KARL K. DARROW, *Bell Telephone Laboratories*.